WATEREUSE

Formation of Nitrosamines and Perfluoroalkyl Acids During Ozonation in Water Reuse Applications

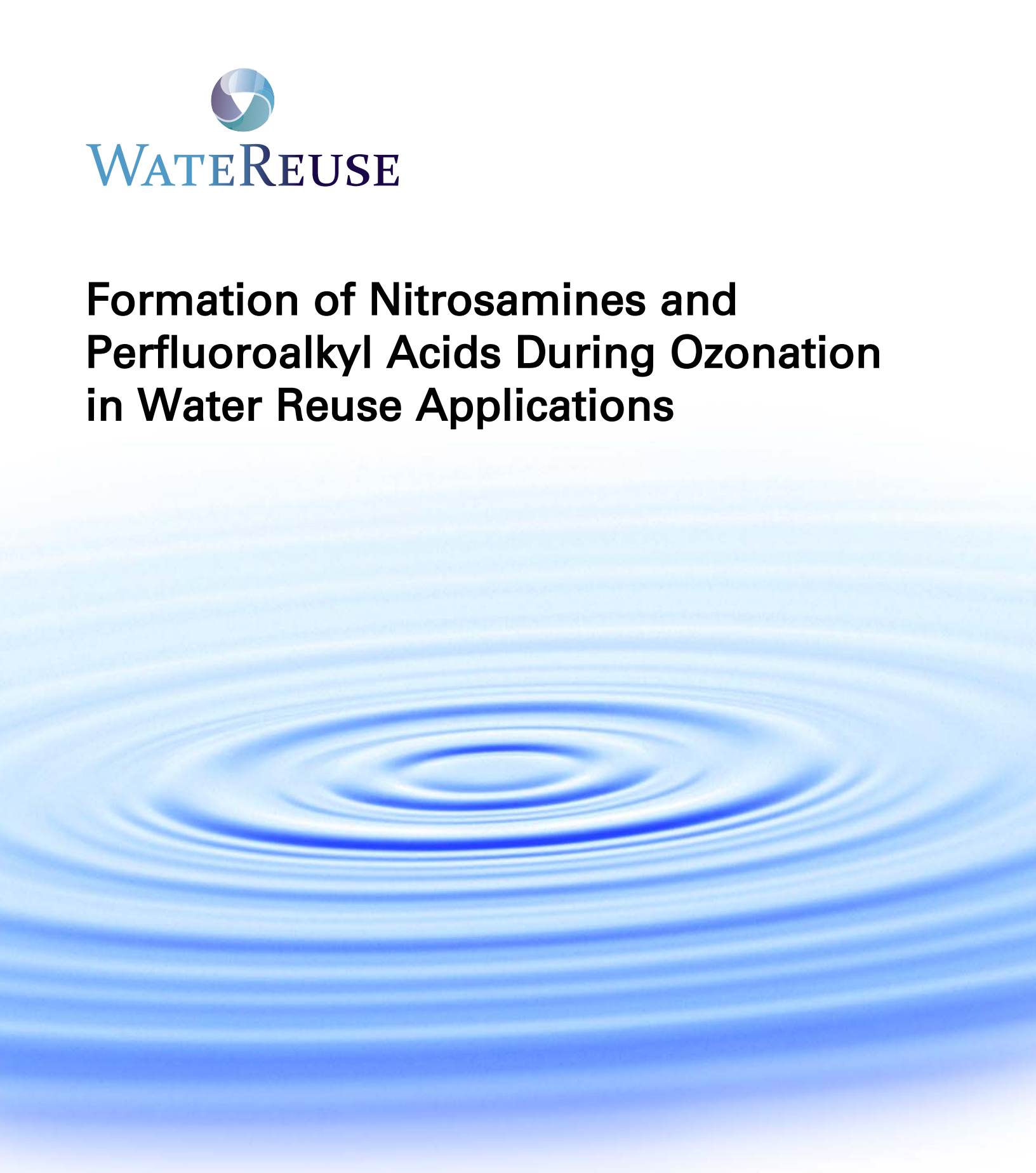

WateReuse Research Foundation

Formation of Nitrosamines and Perfluoroalkyl Acids During Ozonation in Water Reuse Applications

About the WateReuse Research Foundation

The mission of the WateReuse Research Foundation is to conduct and promote applied research on the reclamation, recycling, reuse, and desalination of water. The Foundation's research advances the science of water reuse and supports communities across the United States and abroad in their efforts to create new sources of high quality water for various uses through reclamation, recycling, reuse, and desalination while protecting public health and the environment.

The Foundation sponsors research on all aspects of water reuse, including emerging chemical contaminants, microbiological agents, treatment technologies, reduction of energy requirements, concentrate management and desalination, public perception and acceptance, economics, and marketing. The Foundation's research informs the public of the safety of reclaimed water and provides water professionals with the tools and knowledge to meet their commitment of providing a reliable, safe product for its intended use.

The Foundation's funding partners include the supporters of the California Direct Potable Reuse Initiative, Water Services Association of Australia, Pentair Foundation, and Bureau of Reclamation. Funding is also provided by the Foundation's Subscribers, water and wastewater agencies, and other interested organizations.

Formation of Nitrosamines and Perfluoroalkyl Acids During Ozonation in Water Reuse Applications

Eric R. V. Dickenson, Ph.D.,
Southern Nevada Water Authority

Aleksey N. Pisarenko, Ph.D.,
Southern Nevada Water Authority, currently *Trussell Technologies, Inc.*

Erica J. Marti, M.S.,
Southern Nevada Water Authority

Daniel Gerrity, Ph.D.,
Southern Nevada Water Authority, currently *University of Nevada, Las Vegas*

Brett J. Vanderford,
Southern Nevada Water Authority

WateReuse Research Foundation
Alexandria, VA

Disclaimer

This report was sponsored by the WateReuse Research Foundation. The Foundation and its Board Members assume no responsibility for the content reported in this publication or for the opinions or statements of facts expressed in the report. The mention of trade names of commercial products does not represent or imply the approval or endorsement of the WateReuse Research Foundation. This report is published solely for informational purposes.

For more information, contact:
WateReuse Research Foundation
1199 North Fairfax Street, Suite 410
Alexandria, VA 22314
703-548-0880
703-548-5085 (fax)
www.WateReuse.org/Foundation

WateReuse Research Foundation Project Number: WRRF-11-08
WateReuse Research Foundation Product Number: 11-08-1

ISBN: 978-1-941242-23-0

Contents

Figures

Tables

Acronyms

2-F-DMH	2-furaldehyde 2,2-dimethylhydrazone
4-M-3-TSC	4-methyl-3-thiosemicarbazide
4:2FTS	4:2 fluorotelomer sulfonate
5:2 FTCA	5:2 fluorotelomer acid
6:2 FTCA	6:2 fluorotelomer acid
6:2 FTOH	6:2 fluorotelomer alcohol
6:2 FTS	6:2 fluorotelomer sulfonate
6:2 FTUCA	6:2 fluorotelomer unsaturated acid
7:2 FTOH	7:2 fluorotelomer alcohol
7:3 FTCA	7:3 fluorotelomer acid
7:3 FTUA	7:3 fluorotelomer unsaturated amide
7:3 FTUCA	7:3 fluorotelomer unsaturated acid
8:2 diPAP	sodium bis-perfluorodecyl phosphonate
8:2 FTAL	8:2 fluorotelomer aldehyde
8:2 FTCA	8:2 fluorotelomer acid
8:2 FTOH	8:2 fluorotelomer alcohol
8:2 FTS	8:2 fluorotelomer sulfonate
8:2 FTUCA	8:2 fluorotelomer unsaturated acid
8:2 PAP	sodium perfluorodecyl phosphonate
10:2 FTOH	10: fluorotelomer alcohol
•OH	hydroxyl radical
$[•OH]_{ss}$	hydroxyl radical exposure
ACR	accurate radioisotope counting
Acetone DMH	acetone dimethylhydrazone
AOP	advanced oxidation process
ASPE	automated solid-phase extraction
BAC	biological activated carbon
BNR	biological nutrient removal
BOD	biological oxygen demand
CAS	conventional activared sludge
CAS	Chemical Abstract Services
CL-UDMH	chlorinated unsymmetrical dimethylhydrazine
COAG	coagulation
COD	chemical oxygen demand
CT	contact time
DAFF	coagulation and dissolved air flotation filtration
DCM	dichloromethane
DI	deionized (water)
DMA	dimethylamine
DMC-phenyl	*N*-{[(dimethylamino)carbonyl]oxy}-2-phenylacetamide
DMC-dithio	*N′*-{[(dimethyl- amino)carbonyl]oxy}-4-(1,3-dithiolan-2-yl)benzenecarboximidamide
DMDTC	dimethyl-dithiocarbamate

DMS	dimethylsulfamide
DMSC	*N*-1-(3-{[(2,2-dimethylhydrazino) carbonyl]amino} -4-methylphenyl)-2 ,2-dimethyl-hydrazine-1- carboxamide
DOC	dissolved organic carbon
DON	dissolved organic nitrogen
DBP	disinfection byproduct
EEM	excitation-emission matrix (fluorescence spectroscopy)
EfOM	effluent organic matter
EPA	Environmental Protection Agency (U.S.)
ESI	electro-spray ionization
F:M	food to microorganism ratio
FASA	perfluoroalkyl sulfonamide
FASAA	perfluoroa;ky; sulfonamide-acetic acid
FASE	perfluoroa;ky; sulfonamide-ethanol
FI	fluorescence index
FOSA	perfluoro-octane sulfonamide
FP	formation potential
FRI	fluorescence regional integration
FTAL	fluorotelomer aldehyde
FTCA	fluorotelomer carboxylate
FTOH	fluorotelomer alcohol
FTS	fluorotelomer sulfonate
FTUCA	fluorotelomer unsaturated carboxylic acid
GAC	granular activated carbon
GC	gas chromatography
GF	gravity filtration
GF/F	glass fiber filter
HLB	hydrophobic-lipophilic balance
HRT	hydraulic retention time
IPR	indirect potable reuse
Kd	partitioning coefficient
LC	liquid chromatography
M	molar, unit of concentration (mol/L)
MBR	membrane bioreactor
MDL	method detection limit
MF	microfiltration
MLSS	mixed liquor suspended solids
MRL	method reporting limit
MRM	multiple reaction monitoring
MS	mass spectrometry
NDBA	*N*-nitrosodibutylamine
NDMA	*N*-nitrosodimethylamine
NDEA	*N*-nitrosodiethylamine
NDELA	*N*-nitrosodiethylamine
NDPA	*N*-nitroso-di-n-propylamine
NDPh	*N*-nitroso-diphenylamine

N-EtFOSA	n-ethyl perfluorooctane sulfonamide
N-EtFOSAA	n-ethyl perfluorooctane sulfonamidoacetic acid
N-EtFOSE	n-ethyl perfluorooctane sulfonamidoethanol
N-MeFOSA	n-methyl perfluorooctane sulfonamide
N-MeFOSAA	n-methyl perfluorooctane sulfonamidoacetic acid
N-MeFOSE	n-methyl perfluorooctane sulfonamidoethanol
NF	nanofiltration
NMEA	*N*-nitrosomethyl-ethylamine
NMOR	*N*-nitrosomorpholine
NOM	natural organic matter
NPYR	*N*-nitrosopyrrolidine
NTU	nephelometric turbidity unit
O_3:TOC	ozone to TOC ratio
PAC	powdered activated carbon
PACT	powedered activated carbon treatment
PAP	perfluoroalkyl phosphonates
pCBA	parachlorobenzoic acid
PFAA	perfluoroalkyl acid
PFAS	perfluoroalkyl and polyfluoroalkyl substance
PFBA	perfluorobutanoic acid
PFBS	perfluorobutane sulfonic acid
PFC	perfluorinated chemical
PFCA	perfluoroalkyl carboxylic acid
PFDA	perfluorodecanoic acid
PFDoDA	perfluorododecanoic acid
PFDS	perfluorodecane sulfonic acid
PFHp	perfluoro-heptane sulfinate
PFHpA	perfluoroheptanoic acid
PFHpS	perfluoroheptane sulfonic acid
PFHxA	perfluorohexanoic acid
PFHxS	perfluorohexane sulfonic acid
PFNA	perfluorononanoic acid
PFNS	perfluorononane sulfonic acid
PFN sulfinate	perfluoro-nonane sulfinate
PFOA	perfluorooctanoic acid
PFOS	perfluorooctane sulfonic acid
PFO sulfinate	perfluoro-octane sulfinate
PFPn	perfluoro-pentane sulfinate
PFPnA	perfluoropentanoic acid
PFPnS	perfluoropentane sulfonic acid
PFSA	perfluoroalkyl sulfonic acid
PFSiA	perfluoroalkyl sulfinate
PFUnDA	perfluoroundecanoic acid
PLC	programmable logic controller
polyDADMAC	poly(diallyldimethylammonium chloride) (polymer)
PVDF	polyvynilidene fluoride

RAC	Research Advisory Committee
RO	reverse osmosis
RSD	relative standard deviation
SNWA	Southern Nevada Water Authority
SPE	solid phase extraction
SRT	sludge retention time
SUVA	specific UV absorbance
tBA	t-butyl alcohol
TDS	total dissolved solids
TF	trickling filter
TMA	trimethylamine
TMDS	1,1,1',1'-tetramethyl-4,4'-(methylene-di-phenylene) disemicarbazide
TMP	transmemrane pressure
TOC	total organic carbon
TONO	total *N*-nitrosamine method
TOrC	trace organic contaminant
TSS	total suspended solids
UDMH	unsymmetrical dimethylhydrazine
UF	ultrafiltration
UV	ultraviolet light
UVT	UV transmittance at 254 nm
ZVI	zero valent iron

Foreword

The WateReuse Research Foundation, a nonprofit corporation, sponsors research that advances the science of water reclamation, recycling, reuse, and desalination. The Foundation funds projects that meet the water reuse and desalination research needs of water and wastewater agencies and the public. The goal of the Foundation's research is to ensure that water reuse and desalination projects provide sustainable sources of high-quality water, protect public health, and improve the environment.
An Operating Plan guides the Foundation's research program. Under the plan, a research agenda of high-priority topics is maintained. The agenda is developed in cooperation with the water reuse and desalination communities including water professionals, academics, and Foundation subscribers. The Foundation's research focuses on a broad range of water reuse and desalination research topics including:

- Defining and addressing emerging contaminants, including chemicals and pathogens
- Determining effective and efficient treatment technologies to create 'fit for purpose' water
- Understanding public perceptions and increasing acceptance of water reuse
- Enhancing management practices related to direct and indirect potable reuse
- Managing concentrate resulting from desalination and potable reuse operations
- Demonstrating the feasibility and safety of direct potable reuse

The Operating Plan outlines the role of the Foundation's Research Advisory Committee (RAC), Project Advisory Committees (PACs), and Foundation staff. The RAC sets priorities, recommends projects for funding, and provides advice and recommendations on the Foundation's research agenda and other related efforts. PACs are convened for each project to provide technical review and oversight. The Foundation's RAC and PACs consist of experts in their fields and provide the Foundation with an independent review, which ensures the credibility of the Foundation's research results. The Foundation's Project Managers facilitate the efforts of the RAC and PACs and provide overall management of projects.

The ability of ozone treatment to mitigate human and environmental impacts associated with pathogens and trace organic contaminants is making it a promising and trending treatment alternative in water reuse applications. However, the formation of ozone byproducts could be a barrier to the use of ozone in potable water reuse applications, particularly; several high priority nitrosamines and perfluoroalkyl acids (PFAAs) have the potential to form during chemical oxidation processes. This may force utilities to rely exclusively on energy-intensive alternatives, such as reverse osmosis and ultraviolet advanced oxidation. As a result of significant improvements over the last two decades, ozone technology has matured and is a more competitive treatment option. Ozone's effectiveness in mitigating the potential human and environmental impacts associated with trace organic contaminants and pathogens has made ozonation a popular treatment alternative in water reuse applications; however, the drawbacks of ozone, particularly the potential for nitrosamine and PFAA formation, must be addressed.

Doug Owen
Chair
WateReuse Research Foundation

Melissa L. Meeker
Executive Director
WateReuse Research Foundation

Acknowledgements

This study would not have been possible without the insights, efforts, and dedication of many individuals and organizations. These include the members of the research team and the Project Advisory Committee (members identified below); the WateReuse Research Foundation Project Manager, Stefani McGregor; and the following research team members. Dr. Eric Wert, SNWA Project Manager, provided guidance to the project. Dr. Yue Wang and Michael Strileski, SNWA graduate interns, and Dr. Riley Flowers, SNWA postdoctoral researcher, contributed to the operation of the pilot systems. Rebecca Trenholm, Oscar Quiñones, Janie Zeigler-Holady and Josephine Chu from the SNWA, contributed to nitrosamine and perfluoroalkyl and polyfluoroalkyl substances analysis. Dave Rexing and Jennifer Fuel from SNWA provided administrative support for the project. The team would like to express thanks to Dr. Julie Peller at Indiana University Northwest for performing radiolysis experiments. The team also would like to thank anonymous utilities that provided water quality data pertaining to their treatment systems and collected samples that were used by the Project Team during the course of the project. We thank Hydranautics, a Nitto Denko Corporation, and APTwater® for their in-kind contribution of supplying their Hydrasub® Membrane Bioreactor and HiPOx® O_3 pilot systems, respectively, and associated equipment support, and the City of Las Vegas Water Pollution Control Facility for allowing the project team to employ the pilot skids on-site, operational support of the skids, and water quality analyses for samples collected from the pilot system. We thank Dr. Julien Reungoat and Dr. Maria Farré at the University of Queensland for their support in collecting samples from an Australian water recycling plant.

Since the start of the project, principal investigators Dr. Aleksey Pisarenko and Dr. Daniel Gerrity have changed their places of employment. Dr. Pisarenko is now employed by Trussell Technologies Inc., and Dr. Gerrity is employed by the University of Nevada, Las Vegas.

Project Advisory Committee
Dr. Julie Peller, *Indiana University Northwest*
Andy Salveson, *Carollo Engineers*
Rajen Budhia, *West Basin Municipal Water District*
Pankaj Kulshrestha, *University at Buffalo, The State University of New York*

Project Manager
Stefani McGregor, *WateReuse Research Foundation*

Executive Summary

The ability of ozone treatment to mitigate human and environmental impacts associated with pathogens and trace organic contaminants is making it a promising and trending treatment alternative in water reuse applications, particularly potable reuse. The ability to employ ozone treatment within potable reuse scenarios that do not rely on reverse osmosis/ultraviolet–advanced oxidation processes (RO/UV–AOP) will allow more U.S. communities to adopt and implement alternative treatment strategies for potable reuse; however, the formation of ozone byproducts could be a barrier to the use of ozone. Particularly, several nitrosamines and perfluoroalkyl acids (PFAAs), that have the potential to form during chemical oxidation processes, are high priority contaminants listed on the current U.S. Environmental Protection Agency's Contaminant Candidate List. The objectives of this study were to assess whether nitrosamines or PFAAs form upon ozonation of various treated wastewaters, evaluate the factors responsible for their formation, and recommend mitigation strategies.

The research approach for this study included the following major tasks: (1) perform a literature review on nitrosamines and perfluoroalkyl acids occurrence, relevant precursors and formation pathways, factors that affect formation, and proven and potential mitigation strategies (Chapters 2 and 3); (2) evaluate their occurrence and formation at full- and pilot-scale treatment systems (Chapter 4); (3) perform bench-scale studies to determine critical factors affecting their formation (Chapters 5 through 7); and (4) evaluate and identify useful mitigation strategies (Chapter 8).

On the basis of monitoring for various nitrosamines at full- and pilot-scale systems and bench-top studies, *N*-nitrosodimethylamine (NDMA) was the dominant nitrosamine formed during ozonation; therefore, it became the focus of this study. Formation was isolated or did not occur for the other targeted nitrosamines; however, unknown nitrosamines were formed, and NDMA accounted for about half of the total nitrosamines after ozone treatment. *N*-nitrosomorpholine (NMOR) was the second most frequently detected nitrosamine in studied wastewaters before ozone treatment, but NMOR levels did not change during ozone treatment, suggesting it is neither formed nor transformed during ozone treatment.

In previous studies, several precursors containing hydrazine (e.g., unsymmetrical dimethylhydrazine, semicarbazides) and sulfamide moieties that have a relatively high molar NDMA yield (10–80%) were identified upon ozonation. The hydrazine compounds have a dimethylamino group that is connected to a nitrogen atom, and the sulfamides have a dimethylamino group and a nitrogen atom that are separated by a $-SO_2$ group. During reactions with an oxidant, the $-SO_2$ group leaves. This allows for a recombination of the dimethylamino group with a nitrogen atom and leads to NDMA formation. Thus, compounds with a similar leaving group (like $-SO_2$) can be potential precursors.

This study identified six new organic compounds as significant NDMA precursors: two hydrazones (22–66%), another semicarbazide (64–90%), a thiosemicarbazide (12–14%), and two carbamates (2–15%). For compounds with similar structures, NDMA molar conversion was higher for compounds with an electron donating group and lower for compounds with a greater electron withdrawing effect; this is due to lower reactivity with molecular ozone. These same precursor compounds had considerably lower NDMA yields (<1.5%) when they were allowed to react with monochloramine alone. Similarly, well-known chloramine-reactive precursors, such as some secondary and tertiary amine compounds that contain a dimethylamino group only (no additional nitrogen atoms) can also form NDMA upon

ozonation, however at molar yields that are typically low (i.e., <0.1%). These findings suggest the ozone-reacting precursors are distinctly different than other dimethylamino-containing compounds that are more reactive towards chloramines. However, occurrence of these new ozone-reacting precursor compounds identified in this study has not been reported in U.S. wastewaters; therefore, their potential contribution to NDMA formation during ozonation needs to be further addressed in future studies.

On the basis of full-scale system data and bench-top studies, some PFAAs were formed after ozonation of secondary treated wastewaters. The extent of formation and the PFAAs that formed varied among wastewaters but commonly included perfluoropentanoic acid (PFPnA), perfluorohexanoic acid (PFHxA), perfluorooctanoic acid (PFOA), and perfluorobutane sulfonic acid (PFBS). The most consistently formed PFAA was PFHxA, with an increase in concentration up to 11 ng/L, thus it was used as an indicator of perfluoroalkyl acid formation in the follow-up discussions in this report.

NDMA and PFHxA formation during ozonation of wastewater was dependent on the applied ozone concentration. For a majority of the treated wastewaters that were evaluated, the NDMA formation was near its maximum at ozone to total organic carbon ratio (O_3:TOC) >0.5. For half of the treated wastewaters, PFHxA reached its maximum formation at O_3:TOC>1.0, whereas for the other wastewaters the maximum was achieved at O_3:TOC ratios between 0 and 0.5. As demonstrated in bench-scale wastewater and model compound testing, the hydroxyl radical exposure did not result in NDMA formation, which confirms that NDMA formation is due to reactions of precursors with molecular ozone. Results are inconclusive in determining the relative role of hydroxyl radical and molecular ozone towards PFAA formation because of relatively low formation and uncertainty of the measured concentrations. The effect of pH in the 6 to 8 range had little impact on either NDMA or PFAA formation with ozonation. Similar to the previously reported NDMA formation from dimethylsulfamide, bromide catalyzed NDMA formation in ultrapure water solutions of a few model precursor compounds; however, the majority of precursor compounds showed no enhancing effect of bromide on NDMA formation. It is interesting that higher NDMA formation was observed in ozonated wastewater than in ozonated ultrapure water spiked with certain precursor compounds. More work is needed to assess the effects of ionic strength and common wastewater constituents (e.g., bromide, metals, bicarbonate, phosphate, nitrate, chloride, and sulfate ions) on catalyzing NDMA formation.

Adding a biological secondary pretreatment rather than relying on primary clarification is effective at reducing NDMA precursors (and NDMA itself), and secondary treatment systems that employ partial or full nitrification are more able to reduce their levels than nonnitrified wastewaters. Other possible NDMA precursor pretreatment strategies that need to be explored further include biofiltration, granular activated carbon adsorption (GAC), and preoxidation (other than ozone) strategies. Biological pretreatment was less effective at reducing PFAA precursors. In fact, several PFAAs, such as PFHxA, increased (by 5–26 ng/L), possibly because of biological transformation of perfluoroalkyl compounds with a higher molecular weight.

In general, differing conventional activated sludge pretreatments (partially nitrifying to fully nitrifying and partially denitrifying treatments) did not impact resulting PFHxA precursor levels in secondary effluent or the PFHxA formation resulting from posttreatment ozonation. The results demonstrate that PFAA levels can increase during both secondary biological treatment and subsequent ozone treatment, but final PFAA levels were generally lower than 40 ng/L, with the exception of one plant. The

determination of which PFAAs and their regulatory levels are pursued will bring into context the importance of these occurrence levels and establish whether PFAAs will be an issue.
The posttreatment options for NDMA and PFAA removal vary. UV photolysis and biological activated carbon (BAC) treatment options have shown to be the most effective for NDMA removal. UV photolysis has been selected for full-scale reuse applications and proven to be an effective NDMA reduction strategy; however, UV treatment relies on an energy-intensive operation in which high UV dose and high water quality pretreatment (e.g., RO) are required. BAC treatment, a less energy-intensive option, appears to be an effective alternative postmitigation strategy for NDMA removal, but more research on the factors that govern its removal is necessary. Because of the recalcitrant nature of PFAAs, posttreatment options for their removal rely on physical separation processes, such as GAC, anion exchange, nanofiltration (NF), and RO treatment technologies. The NF and RO membrane technologies are currently the most effective for the removal of the shortest chain PFAAs.

As indicated by this study, NDMA and some PFAAs have a significant formation potential during the ozonation of treated wastewaters and thus are contaminants of concern for potable reuse treatment systems that employ ozone. However, control strategies, such as sufficient biological (e.g., nitrifying conditions), physical, or chemical pretreatment of precursors, optimized ozone dosing, or a combination of alternative posttreatment technologies (e.g., BAC and NF), can be applied to mitigate the formation of these contaminants.

Chapter 1

Introduction

Nitrosamines are disinfection byproducts commonly associated with chloramination (Choi and Valentine, 2002; Mitch et al., 2002, 2003a, 2003b), but recent studies indicate that direct formation during ozonation is also a common pathway (Andrzejewski et al., 2008; von Gunten et al., 2010; Oya et al., 2008; Schmidt and Brauch, 2008; Nawrocki and Andrzejewski, 2011; Pisarenko et al., 2012; Hollender et al., 2009). Nitrosamines are priority contaminants; the U.S. Environmental Protection Agency (EPA)'s Integrated Risk Information System database indicates that low ng/L level concentrations for six nitrosamines are associated with a 10^{-6} lifetime excess cancer risk. California's Department of Public Health has set 10 ng/L drinking water notification levels for three nitrosamines, and its Office of Environmental Health Hazard Assessment has established a 3 ng/L nonregulatory public health goal for *N*-nitrosodimethylamine (NDMA). Perfluoroalkyl acids (PFAAs) are another group of high priority contaminants with the potential for formation during chemical oxidation processes (Gauthier and Mabury, 2005; Plumlee et al., 2009). Human epidemiological studies have suggested some adverse health impacts resulting from exposure, including a recent report from the C8 Science Panel that linked perfluorooctanoic acid (PFOA) to testicular and kidney cancer and another study that found an association between PFOA and perfluorooctane sulfonic acid (PFOS) exposure and a reduced humoral immune response to routine childhood immunizations in children ages 5 to 7 years. In 2009, the EPA established Provisionary Health Advisory values for PFOA and PFOS of 0.4 and 0.2 µg/L, respectively, in response to an emergency situation in Decatur, AL, to protect residents from short-term exposure. Several nitrosamines and PFAAs are included on the most recent U.S. EPA Contaminant Candidate List. Six nitrosamines and six PFAAs are also listed in U.S. EPA's Unregulated Contaminant Monitoring Rules 2 and 3, respectively, which require nationwide monitoring by public water suppliers to provide occurrence data needed for regulatory decision making.

The formation of nitrosamines and PFAAs may be a significant barrier to the use of ozonation in water reuse applications, particularly for potable reuse. This may force utilities to rely exclusively on energy-intensive alternatives, such as reverse osmosis (RO), and ultraviolet (UV) advanced oxidation. As a result of significant improvements over the last two decades, ozone technology has matured and is a more competitive treatment option. Ozone's effectiveness in mitigating the potential human and environmental impacts associated with trace organic contaminants and pathogens has made ozonation a popular treatment alternative in water reuse applications; however, the drawbacks of ozone, particularly the potential for nitrosamine and PFAA formation, must be addressed. The objectives of this study were to assess whether nitrosamines or PFAAs form upon ozonation of various treated wastewaters, evaluate the factors responsible for their formation, and recommend mitigation strategies.

Chapter 2

Background

This chapter provides detailed background information on nitrosamines and perfluoroalkyl and polyfluoroalkyl substances (PFASs) related to water and wastewater treatment. The nitrosamines section covers precursors, three major formation pathways, and mitigation strategies. The main focus is on NDMA because this compound has been studied more frequently. The PFAS section covers the categories of PFASs, precursors and their degradation, possible formation with ozonation, fate in water and wastewater treatment, and mitigation strategies. More than 100 peer-reviewed articles were read to compile this literature review.

2.1 Nitrosamines

Nitrosamines, particularly NDMA, have received a great deal of attention as emerging water contaminants. NDMA is classified as a B2 carcinogen by the U.S. EPA, which means it is a probable human carcinogen (US EPA, 2012). It is listed on the third Contaminant Candidates List (CCL 3), along with several other nitrosamines (*N*-Nitrosodiethylamine [NDEA], *N*-Nitrosodiphenylamine [NDPhA], *N*-Nitroso-di-n-propylamine [NDPA], and *N*-Nitrosopyrrolidine [NPYR]). The California Department of Public Health has established 10 ng/L as a drinking water notification level for NDMA, NDPA, and NDEA. The characteristics of NDMA cause it to be an extensive environmental concern. It is miscible with water and has low sorption potential (Kommineni et al., 2003), making it very mobile in the environment. Although no longer produced deliberately, NDMA sources include the rubber, dye, tanning, and pesticide industries. NDMA has been found in groundwater near sites that produce rocket fuel containing unsymmetrical dimethylhydrazine (UDMH; Mitch et al., 2003b). In addition, NDMA and other nitrosamines are formed as disinfection byproducts (DBPs) in drinking water and wastewater treatment.

2.1.1 Potential Precursors

In order for nitrosamines to form as DBPs, the right starting material must be present in the water or wastewater. Because the majority of nitrosamine research has focused on NDMA, the precursors identified in literature are for this compound.

2.1.1.1 Chloramination

The main NDMA precursors for chloramination are dimethylamine (DMA), trimethylamine (TMA), and other tertiary amines with a dimethylamino group, such as the pesticide diuron, the pharmaceutical ranitidine, and an industrial chemical called dimethyl-dithiocarbamate (Table 2.1). One research group looked at 20 pharmaceutical compounds and found 8 with >1% NDMA molar yield (Shen and Andrews, 2011). Some quaternary amines, such as the coagulant polymer poly(diallyldimethylammonium chloride) (polyDADMAC) and the consumer product ingredient benzalkonium chloride, are also chloramination precursors for NDMA (Kemper et al., 2010; Padhye et al., 2011; Park et al., 2009).

Natural organic matter (NOM) includes nitrogen-containing compounds that may form NDMA. Chen and Valentine (2007) concentrated NOM and analyzed various fractions to determine NDMA formation potential (NDMA-FP). The hydrophilic and basic fractions showed the strongest NDMA-FP per mass, but the hydrophobic acidic fraction had a much greater total mass and contributed the largest portion (71%) of the NDMA-FP. Neutral compounds provided only 1.6% of the total NDMA-FP, which indicates that the precursors tend to be charged compounds (Chen and Valentine, 2007). In another fractionation experiment, researchers found that half of the NMDA precursors in wastewater influent were sorbed to particles, suggesting that many precursors are hydrophobic and sorb readily (Krauss et al., 2010). A study on dissolved organic nitrogen (DON) in wastewater indicated that NDMA precursors are low molecular weight compounds (<1 kDa) but not amino acids (Pehlivanoglu-Mantas and Sedlak, 2008).

2.1.1.2 Ozonation

A few precursors have been identified for NDMA formation caused by ozonation. These compounds have the dimethylamino group and an additional nitrogen atom. The precursors UDMH, daminozide, and 1,1,1′,1′-tetramethyl-4,4′-(methylene-di-p-phenylene) disemicarbazide (TMDS) all have the dimethylamino group attached to another nitrogen (Table 2.2). Another precursor, dimethylsulfamide (DMS), has the dimethylamino group separated from the nitrogen by SO_2. Schmidt and Brauch (2008) suggest that similar compounds with a good leaving group like -SO_2 could be potential precursors.

Compounds with a dimethylamino group only and no additional nitrogen are not significant precursors for NDMA with ozonation, unlike chloramination precursors. Various organic dyes with tertiary amines were shown to have NDMA molar yields less than 0.001% (Oya et al., 2008). Dimethyl-dithiocarbamate (DMDTC) has been shown to form NDMA through oxidation with monochloramine and ozone at the same yield (Padhye et al., 2013); however, the molar yield is 0.008%. All compounds in Table 2.2 have molar yields greater than 10%.

Much less is known about the precursors forming NDMA through ozonation. There are no fractionation studies to identify precursor characteristics, such as whether they are hydrophobic or hydrophilic. Chemical structure appears to be the most relevant characteristic in predicting NDMA formation.

Table 2.1. Selected Precursors Forming NDMA through Chloramination

Compound Name	Structure	Description	Reference
Dimethylamine	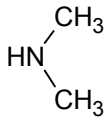	Commonly found in wastewater, feces, urine, algae, and plants; can be found in herbicides	(Mitch et al., 2003b)
Ranitidine	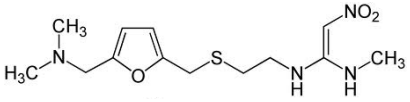	Stomach acid inhibitor; pharmaceutical	(Shen and Andrews, 2011)
Trimethylamine	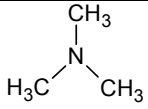	Commonly found in wastewater, feces, and urine	(Mitch et al., 2003b)
Diuron	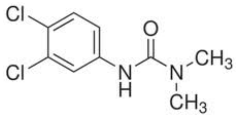	Herbicide	(Chen and Young, 2008)
Benzalkonium chloride	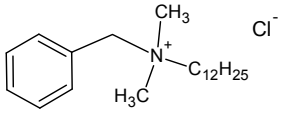	Quaternary amine used in personal and consumer products	(Kemper et al., 2010)
PolyDADMAC	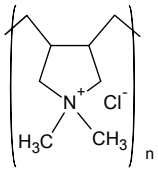	Coagulation polymer	(Park et al., 2009)
Dimethyl-dithiocarbamate	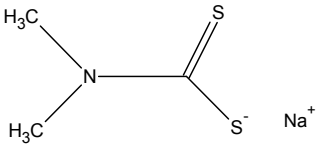	Used in manufacturing to remove metals and for root control in sewers	(Padhye et al., 2013)

Note: polyDADMAC=Polydiallyldimethylammonium chloride

Table 2.2. Selected Precursors Forming NDMA through Ozonation

Compound Name	Structure	Description	Reference
Unsymmetrical dimethylhydrazine	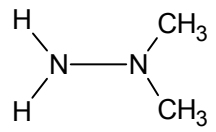	Rocket fuel component; intermediate in NDMA formation	(Schmidt and Brauch, 2008)
Tolylfluanid	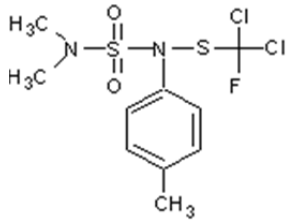	Fungicide	(Schmidt and Brauch, 2008)
Dimethylsulfamide	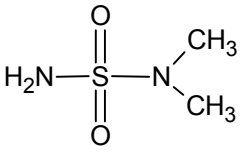	Decomposition product of tolylfluanid	(Schmidt and Brauch, 2008; von Gunten et al., 2010)
N,N-dimethyl-*N*'-(4-methylphenyl)-sulfamide	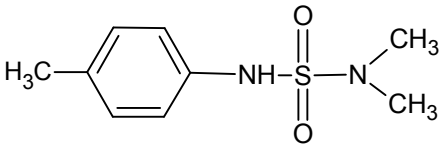	Tolylfluanid metabolite	(Schmidt and Brauch, 2008)
Daminozide	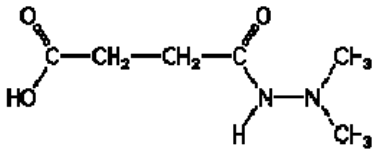	Plant growth additive	(Schmidt and Brauch, 2008)
1,1,1′,1′-tetramethyl-4,4′-(methylene-di-*p*-phenylene) disemicarbazide	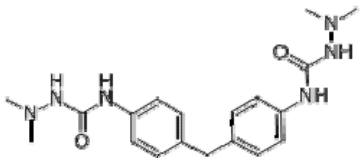	Anti-yellowing agent	(Kosaka et al., 2009)

Note: NDMA=N-Nitrosodimethylamine

2.1.2 Formation Pathways

Many different reactions are responsible for nitrosamine formation during drinking water and wastewater treatment. Several formation mechanisms have been identified, but many others require more investigation. Three main formation pathways include chloramination, nitrosation, and ozonation.

2.1.2.1 Chloramination

Previous research has focused on chloramination as the main disinfection process that forms NDMA. The reaction was originally thought to be a nucleophilic substitution between monochloramine and a secondary amine (Figure 2.1a). This reaction resulted in formation of UDMH, which was subsequently oxidized by chloramines to form NDMA (Choi and Valentine, 2002; Mitch and Sedlak, 2002). Continued research into the pathway provided evidence on reaction rates and intermediates, which caused the mechanism to be revised (Figure 2.1b). The modified pathway involves the reaction of dichloramine and a model secondary amine, dimethylamine (DMA), which forms chlorinated unsymmetrical dimethylhydrazine (Cl-UDMH) as an intermediate. Dissolved oxygen oxidizes Cl-UDMH to NDMA (Schreiber and Mitch, 2006). Consequently, NDMA formation may be greater in aerated processes for water and wastewater treatment. The conversion yield of DMA to NDMA varies in the literature, but it is greater than 3% molar yield controlling the order of ammonia and chlorine addition (Mitch et al., 2005). Although DMA appears to be an intermediate for precursors such as polyDADMAC (Padhye et al., 2011), the high molar yields for other tertiary amines (e.g., 90% for ranitidine) indicate there may be other mechanisms leading to NDMA formation that do not have a DMA intermediate.

2.1.2.2 Nitrosation

Nitrosation involves the reaction of nitrite and chlorine. At a low pH, hypochlorous acid and nitrite form one of two dinitrogen tetroxide (N_2O_4) tautomers (Figure 2.1c). One tautomer reacts with DMA to form NDMA, and the other tautomer results in the nitrated amine. The impact of this reaction is minor because of the very low molar yield (<0.0007%), and this formation pathway is more likely to occur in wastewater than drinking water because of the availability of nitrite (Shah and Mitch, 2012).

2.1.2.3 Ozonation

More recently, oxidation by ozone has been shown to directly form NDMA when precursors are present (Andrzejewski et al., 2008; Hollender et al., 2009; Oya et al., 2008; Pisarenko et al., 2012; Schmidt and Brauch, 2008). Very little is known about the formation pathway and any intermediates that are formed; however, it is unlikely that DMA is an intermediate because the molar yield for DMA and ozone is less than 0.4% (Andrzejewski et al., 2008), and some of the known precursors (e.g., UDMH, daminozide, and dimethylsulfamide) have molar yields greater than 50%. Von Gunten et al. (2010) proposed a mechanism for NDMA formation from DMS (Figure 2.1d). The mechanism is bromide-catalyzed and results in the loss of $-SO_2$ as a leaving group, after which the two nitrogen atoms are joined. UDMH conversion to NDMA is likely simple oxidation, but formation pathways for other precursors have not been identified.

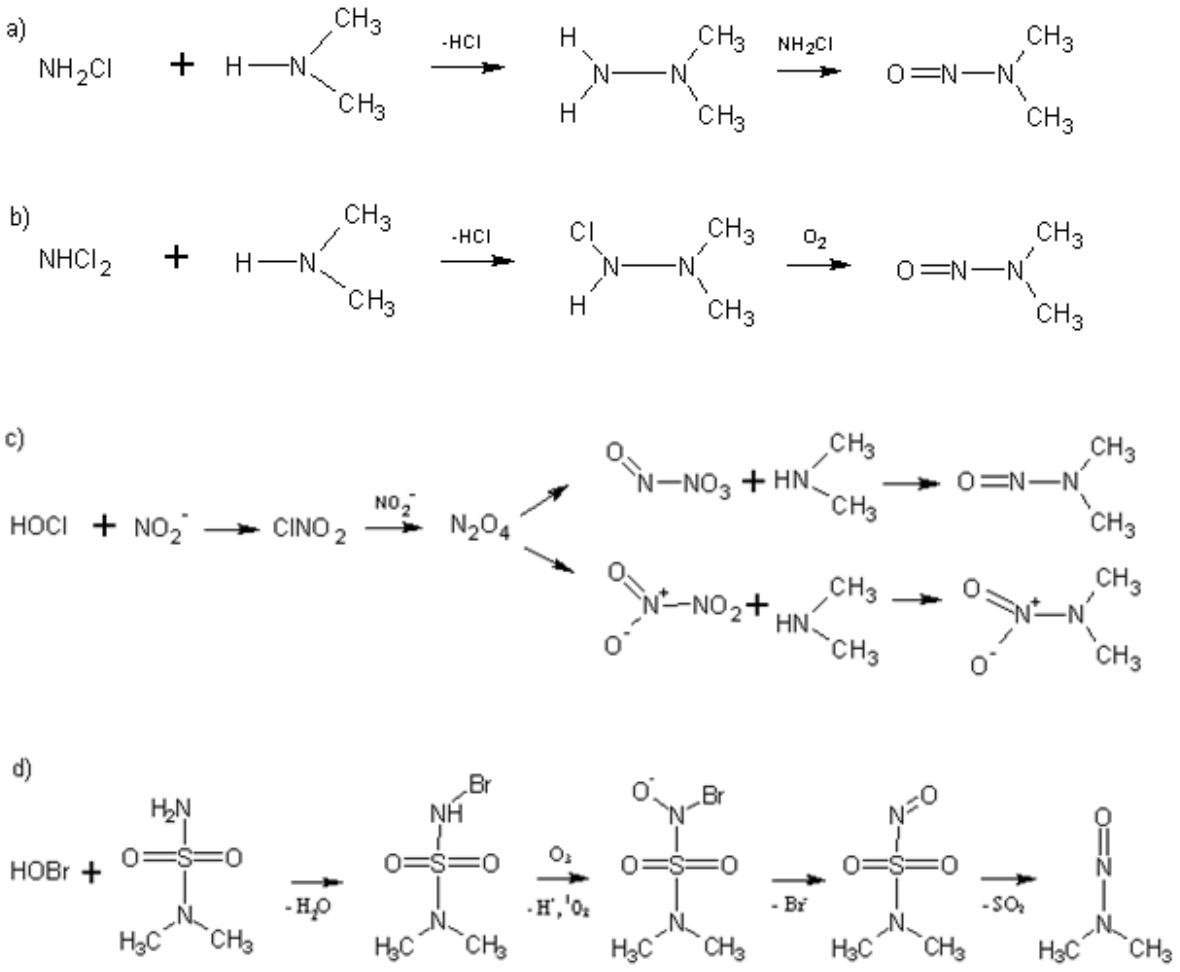

Figure 2.1. Proposed mechanisms for NDMA formation via (a) chloramination of dimethylamine; (b) revised chloramination of dimethylamine; (c) nitrosation of dimethylamine; and (d) ozonation of dimethylsulfamide.

Source: Shah and Mitch, 2012

2.1.3 Mitigation Strategies

Several techniques have been attempted to remove NDMA or prevent its formation. Strategies include membranes, photolysis, sorption, biodegradation, and advanced oxidation processes (AOP). Because nitrosamine compounds vary in size and polarity, mitigation strategies may be effective for some compounds but not for all nitrosamines or precursors.

2.1.3.1 Membranes

Membranes will effectively remove some nitrosamines and precursors. Microfiltration (MF) and ultrafiltration (UF) do not remove NDMA precursors (Farré et al., 2011a). In fact, NDMA may increase in wastewater treated with MF–RO because chloramination is used to prevent membrane biofouling

(Plumlee et al., 2008b). The need to use chloramines for biofouling prevention may limit the overall effectiveness of NDMA removal in wastewater by membranes. RO will remove many NDMA precursors (Farré et al., 2011a) but only about 50% of NDMA because of its small size (Plumlee et al., 2008b). Nitrosamines with greater molecular weight, than NDMA are removed by over 89% with RO membranes. Rejection for nitrosamines is based on size exclusion and not absorption into the membrane (Steinle-Darling et al., 2007).

Many factors affect membrane performance. In one study, ionic strength and pH did not influence RO rejection, but artificial fouling with alginate significantly decreased rejection (Steinle-Darling et al., 2007). Changes in the feed water may cause fouling, and this will in turn affect RO rejection (Plumlee et al., 2008b). Rejection of NDMA by RO and nanofiltration (NF) is challenging because of NDMA's low molecular weight and hydrophilic properties; therefore, other treatment strategies have to be considered for NDMA removal (Yangali-Quintanilla et al., 2010).

2.1.3.2 Photolysis

UV photolysis is effective at eliminating NDMA (Sharpless and Linden, 2005). NDMA has a strong UV absorption band at 230 nm and a weaker band at 330 nm (Plumlee, 2008). UV irradiation at 254 nm will degrade NDMA but only at around tenfold the dose to inactivate viruses (Mitch et al., 2003b). A pilot-plant study determined that a UV fluence of 540 mJ/cm^2 was needed to reduce organic contaminants, including NDMA, by 80%. This was 5 times greater than the disinfection dose needed to inactivate spores (Kruithof et al., 2007). A higher UV dose makes this type of treatment costly. Natural photochemical attenuation by sunlight is possible because of NDMA's weak absorption band at 330 nm. In a previous study, NDMA was degraded by 42% in 83 min under solar light exposure. Photolysis was hindered by dissolved organic matter (DOM) because of light screening (Plumlee, 2008).

Although UV irradiation reduces NDMA effectively, there are a few issues in implementing this treatment. A potential problem with UV treatment is that NDMA is degraded to DMA, and subsequent chloramination could reform NDMA (Zhao et al., 2008). The water quality influences the UV fluence needed and therefore the treatment cost. Pretreatment with UF and ion exchange to remove hydroxyl scavengers, such as nitrate and NOM, may be needed to reduce energy costs and eliminate NDMA precursors (Martijn et al., 2010). In addition, the presence of hypochlorite, chloramines, aqueous ferric iron, and ozone decrease UV transmittance, which negatively impacts the UV dose delivered (Cushing et al., 2001).

Xu et al. (2009a) investigated factors affecting UV destruction of NDMA. Complete degradation occurred at any initial concentration, but the reaction rate decreased with increasing initial concentration. Lower pH resulted in greater photodegradation, which was attributed to higher quantum yields. NDMA destruction was greater for solutions saturated with oxygen, as compared to nitrogen, and hindered by humic acid (Xu et al., 2009b), which may be the result of decreased UV transmittance.

2.1.3.3 Sorption

Activated carbon is moderately beneficial for removing nitrosamines. NDMA does not adsorb as strongly as other organic compounds, which is seen by its Freundlich isotherm constants (K=1.07–9.08 μg/g and 1/n=0.744–1.11; Kommineni et al., 2003). Groundwater at Rocky Mountain Arsenal, a rocket fuel production site, was remediated with granular activated carbon (GAC), carbonaceous resins, zeolite, silica, acidic hydrolysis, and metal complexation. GAC and the carbonaceous resins removed 99% of NDMA after equilibrium was achieved, whereas zeolite and silica removed 15 to 20%. Metal complexation and hydrolysis were not effective (Fleming et al., 1996). At the same site, another study found that NDMA adsorbed to the soil very little and was quickly desorbed in the presence of water (Gunnison et al., 2000). One group reported that activated carbon can act as a catalyst to form trace levels of NDMA from secondary amines (Padhye et al., 2010). This is important to consider because many analytical methods used activated carbon cartridges during solid-phase extraction.

A typical problem with activated carbon is disposal or regeneration after breakthrough. If GAC is not regenerated, it must be replaced, and this increases the treatment cost. On the other hand, regeneration may lead to deterioration of the carbon. Kommineni et al. (2003) used Fenton's reagent to destroy adsorbed NDMA (99% destruction) and regenerate GAC at pH 2 to 3. The regeneration cost was low ($0.10/lb GAC), and very little capacity was lost (<3.8%; Kommineni et al., 2003).

2.1.3.4 Biodegradation and Biofiltration

Biodegradation will eliminate NDMA (Sharp et al., 2005) and some of the polar or charged precursors (Krauss et al., 2010). For biological secondary treatment, NDMA removal is highly variable (0–75%), and there is no clear relationship between NDMA-FP and wastewater characteristics (e.g., biological oxygen demand [BOD], chemical oxygen demand [COD], suspended solids, nitrate, $NH4^+$, total N; Sedlak et al., 2005; Yoon et al., 2011). Groundwater contaminated with NDMA from rocket fuel production was remediated with an intercept-and-treat system. In 30 days, as much as 60% was biodegraded with facultative bacteria but only after the groundwater was treated with GAC (Gunnison et al., 2000). NDMA biodegradation is a co-metabolic process, and no microorganisms have been found that can use nitrosamines as the sole carbon source (Krauss et al., 2010). Initial concentration is an important factor. If the concentration is very low, removal does not occur (Gunnison et al., 2000).

Biofiltration is effective at decreasing NDMA precursors. In one study using a common influent (following dissolved air flotation and sand filtration), biofiltration alone reduced NDMA-FP by 85%, whereas ozonation alone reduced it by 66%. Consequently, biofiltration may be more effective at eliminating NDMA precursors than ozonation (Farré et al., 2011b). An advantage of biological activated carbon (BAC) is the possibility of bio-regeneration. In one study, the removal rates for trace organic compounds were constant over a 2-year period (Reungoat et al., 2011). Another biofiltration study used GAC and immobilized bacteria species to remove several amines (e.g., TMA, DMA, methylamine) from an air stream (Ho et al., 2008). The bacteria species *Arthrobacter* and *Paracoccus* could be useful for eliminating NDMA precursors. Other studies showed a decrease in NDMA in wastewater as a result of biodegradation through biological sand filtration (Hollender et al., 2009; Zimmermann et al., 2011).

2.1.3.5 Advanced Oxidation Processes

AOPs include ozone, ozone with hydrogen peroxide (O_3/H_2O_2), UV with hydrogen peroxide (UV/H_2O_2), and UV with ozone (UV/O_3). Most of these treatments hinge on the hydroxyl radical as a nonselective oxidant that will react with more constituents than UV or ozone alone.

As previously mentioned, ozonation of wastewater can result in NDMA formation; however, there may be a net reduction in NDMA formation potential with chloramination caused by the destruction of precursors with ozone (Lee et al., 2007a; Pisarenko et al., 2012). Adding hydrogen peroxide does not appear to improve NDMA removal. In a pilot-scale study by Pisarenko et al. (2012), O_3/H_2O_2 had little effect on direct NDMA formation or formation potential compared to ozone alone. Another study showed no significant difference between ozone and O_3/H_2O_2 for NDMA oxidation (Lee et al., 2007b). On the other hand, Yang et al. (2009) observed a large decrease in NDMA formation potential after treating DMA in deionized water with O_3/H_2O_2. It is not clear if the hydroxyl radical plays a role in NDMA formation, although it does increase DMA removal by oxidation, and this route could result in NDMA (Andrzejewski et al., 2008; Yang et al., 2009).

AOPs are influenced by operational factors such as initial concentration and pH. Removal rate decreased with increasing initial concentration (Xu et al., 2010). Species may be protonated, and hydroxyl radical reactions are pH dependent. In a study on the destruction of NDEA, UV alone showed a high removal rate with acidic and neutral pH, whereas UV/O_3 worked well at any pH.

Degradation products may differ with AOP treatments. Increasing the ozone dose resulted in higher concentrations of nitrate and lower DMA, but it did not affect the reaction rate. Hydroxyl radical reactions favored methylamine (MA) formation over DMA, which is useful in preventing regeneration of NDMA (Xu et al., 2009a). Adding 1 mM H_2O_2 to ozone increased DMA removal by 30% and decreased NDMA-FP by 88% (Yang et al., 2009). The authors hypothesize that the drop in NDMA-FP is because the hydroxyl radical eliminates hydroxylamine, which inhibits an NDMA formation pathway. A comparison of UV and UV/H_2O_2 revealed that hydrogen peroxide does not enhance NDMA degradation because of light screening (Sharpless and Linden, 2003); however, there is a difference in the transformation products formed. Chen et al. (2011) investigated DMA formation and NDMA-FP with UV and UV/H_2O_2. The authors found that increasing the H_2O_2 dosage and the contact time resulted in less DMA formation and consequently lower NDMA-FP.

The water quality prior to AOP treatment will influence NDMA formation. Zhao et al. (2008) investigated 11 parallel disinfection treatment trains with 7 surface waters. NDMA formation varied for waters with the same treatment; this was attributed to a difference in precursors (Zhao et al., 2008). In comparing secondary effluents after activated sludge and membrane bioreactor (MBR) treatments, the ozonated MBR effluent had a much lower NDMA concentration (Pisarenko et al., 2012). This suggests that more extensive treatment may remove NDMA precursors.

2.2 Perfluoroalkyl and Polyfluoroalkyl Substances

PFASs are environmentally persistent, anthropogenic chemicals found throughout the world, including remote regions such as the Arctic (Martin et al., 2004). PFASs and their precursors have been found in the atmosphere (Shoeib et al., 2006), rain (Loewen et al., 2005), oceans (Yamashita et al., 2005), surface water (Simcik and Dorweiler, 2005; Sinclair and Kannan, 2006), groundwater (Moody and Field, 1999; Schultz et al., 2004), tap water (Quiñones and Snyder, 2009; Takagi et al., 2008), bottled water (Kunacheva et al., 2010), municipal and industrial wastewater (Boulanger et al., 2005; Plumlee et al., 2008a; Quiñones and Snyder, 2009; Sinclair and Kannan, 2006), biosolids (Lindstrom et al., 2011), sediment (Becker et al., 2008; Hoehn et al., 2007), landfill leachate (Eggen et al., 2010), and street runoff (Kim and Kannan, 2007; Murakami et al., 2009). PFASs have also been detected in various biota and human serum (Giesy and Kannan, 2001; Toms et al., 2009). Major uses for PFASs are as surfactants, processing additives during fluoropolymer production, surface coatings for carpet and paper products, fire-fighting foam and electronic etching baths. Well-known brands include ScotchGard™, Teflon®, and Gore-Tex®.

Over the past 60 years, PFASs have been described by multiple terms, including perfluorochemicals, fluoropolymers, fluorinated polymers, fluorocarbons, and perfluorocarbons (Buck et al., 2011). The abbreviation "PFC" is frequently used in publications; however, it is defined differently depending on the author, and therefore the meaning is unclear. In addition, Kyoto Protocol documents use PFC to refer to the greenhouse gas family perfluorocarbons, which are distinctly different from the PFASs in commercial products. Buck et al. (2011) recommends the use of "perfluoroalkyl and polyfluoroalkyl substance" and the corresponding acronym PFAS (plural PFASs). This comprehensive term includes completely fluorinated aliphatic compounds (perfluoroalkyl substances) and partially fluorinated aliphatic compounds (polyfluoroalkyl substances). One major division within PFASs is the perfluoroalkyl acids (PFAAs), which have a carbon backbone with fluorine replacing the hydrogen atoms and an acid on the end. Examples include perfluorooctanoic acid (PFOA) and perfluorooctane sulfonic acid (PFOS).

PFASs are categorized into several groups, as shown in Table 2.3. Compared to ionic PFASs, neutral PFASs are more volatile, more biodegradable, and less water soluble. Ionic PFASs are persistent, bioaccumulative (Shaw et al., 2009), and very mobile in water systems, as shown by the transfer of PFASs from biosolids-amended soil to surface and well water (Lindstrom et al., 2011). PFASs may also transfer from soil to plants (Stahl et al., 2009) and possibly further to livestock, milk, and fish (ATSDR, 2013), which are additional human exposure routes.

Concern over possible adverse health effects has resulted in guidelines for selected PFASs and inclusion in the CCL3. The U.S. EPA issued provisional short-term health advisories (PHA) in 2009 for two of the predominant PFAAs. The PHAs for PFOA and PFOS are 400 and 200 ng/L, respectively. In May 2009, PFOS was added to the persistent organic pollutants (POPs) list. A major producer of PFOA in the United States, Minnesota Mining and Manufacturing (3M), voluntarily ended production in 2000, but global production is ongoing. Production has shifted away from long chain PFCs toward short chain chemicals such as perfluorobutanoic acid (PFBA) and other variations like perfluoroalkyl phosphonates (PAPs).

Table 2.3. Categorization of PFASs and Precursors

Compound Group	Abbreviation	Type	Name	Abbreviation	Name	Abbreviation
Perfluoroalkyl carboxylic acid	PFCA	ionic	perfluorobutanoic acid	PFBA	perfluoropentanoic acid	PFPnA
			perfluorohexanoic acid	PFHxA	perfluoroheptanoic acid	PFHpA
			perfluorooctanoic acid	PFOA	perfluorononanoic acid	PFNA
			perfluorodecanoic acid	PFDA	perfluoroundecanoic acid	PFUnDA
			perfluorododecanoic acid	PFDoDA		
Perfluoroalkyl sulfonic acid	PFSA	ionic	perfluorobutane sulfonic acid	PFBS	perfluoropentane sulfonic acid	PFPnS
			perfluorohexane sulfonic acid	PFHxS	perfluoroheptane sulfonic acid	PFHpS
			perfluorooctane sulfonic acid	PFOS	perfluorononane sulfonic acid	PFNS
Perfluoroalkyl sulfinate	PFSiA	ionic	perfluoro-pentane sulfinate	PFPn sulfinate	perfluoro-heptane sulfinate	PFHp sulfinate
			perfluoro-octane sulfinate	PFO sulfinate	perfluoro-nonane sulfinate	PFN sulfinate
Perfluoroalkyl phosphonate	PAP	ionic	sodium perfluorodecyl phosphonate	8:2 PAP	sodium bis-perfluorodecyl phosphonate	8:2 diPAP
Fluorotelomer carboxylate	FTCA	ionic	5:2 fluorotelomer acid	5:2 FTCA	6:2 fluoro-telomer acid	6:2 FTCA
			7:3 fluorotelomer acid	7:3 FTCA	8:2 fluoro-telomer acid	8:2 FTCA
Fluorotelomer unsaturated carboxylic acid	FTUCA	ionic	6:2 fluorotelomer unsaturated acid	6:2 FTUCA	7:3 fluorotelomer unsaturated acid	7:3 FTUCA
			8:2 fluorotelomer unsaturated acid	8:2 FTUCA		

Compound Group	Abbreviation	Type	Name	Abbreviation	Name	Abbreviation
Fluorotelomer sulfonate	FTS	ionic	6:2 fluorotelomer sulfonate	6:2 FTS		
Perfluoroalkyl sulfonamide	FASA	neutral	perfluoro-octane sulfonamide	FOSA	n-methyl perfluoro-octane sulfonamide	*N*-MeFOSA
			n-ethyl perfluoro-octane sulfonamide	N-EtFOSA		
Perfluoroalkyl sulfonamide-acetic acid	FASAA	neutral	n-methyl perfluoro-octane sulfonamido acetic acid	N-MeFOSAA	n-ethyl perfluoro-octane sulfonamido acetic acid	*N*-EtFOSAA
Perfluoroalkyl sulfonamide-ethanol	FASE	neutral	n-methyl perfluoro-octane sulfonamido-ethanol	N-MeFOSE	n-ethyl perfluoro-octane sulfonamido-ethanol	*N*-EtFOSE
Fluorotelomer alcohol	FTOH	neutral	6:2 fluorotelomer alcohol	6: 2 FTOH	7:2 fluoro-telomer alcohol	7:2 FTOH
			8:2 fluorotelomer alcohol	8:2 FTOH	10:2 fluoro-telomer alcohol	10: 2 FTOH
Fluorotelomer aldehyde	FTAL	neutral	8:2 fluorotelomer aldehyde	8:2 FTAL		

2.2.1 Potential Precursors and Degradation Pathways

Although production has decreased for PFOA, PFOS, and other PFASs, these chemicals persist in water sources and can even increase in concentration. One reason is through degradation of precursors. Fluorotelomer alcohols (FTOHs) are known precursors. One research group identified PFOA, 8:2 FTAL, and fluorotelomer acids 8:2 FTCA and 8:2 FTUCA as metabolites during aerobic biodegradation of 8:2 FTOH (Dinglasan et al., 2004). The pathway involves oxidation of the alcohol to the aldehyde intermediate before proceeding to 8:2 FTCA. From there, the proposed pathway to PFOA occurs via an HF elimination reaction to form 8:2 FTUCA and oxidation by an acyl-CoA dehydrogenase type of enzyme.

In a similar biodegradation study, Wang et al. (2005) found the same four metabolites and three new ones: 7:2 FTOH, 7:3 FTUCA, and 7:3 fluorotelomer unsaturated amide (7:3 FTUA). The proposed pathway begins with oxidation of the alcohol to the aldehyde by alcohol dehydrogenase; however, the reaction is reversible and the alcohol is favored unless the aldehyde undergoes fast conversion by aldehyde dehydrogenase to the more stable metabolite 8:2 FTCA. The authors proposed three pathways for the conversion of the acid to PFOA. One pathway involves unidentified 8:1 olefin and 7:2 olefin intermediates, and another forms the amide intermediate 7:3 FTUA, which was identified with liquid chromatography–accurate radioisotope counting (LC–ARC). The third pathway includes defluorination of 8:2 FTUCA to 7:3 FTUCA, followed by conversion to 7:3 FTCA and β-oxidation to PFOA. Perfluoroheptanoic acid (PFHpA) was also identified as a metabolite in this study, but intermediates were not determined. PFOA and PFNA were confirmed as metabolic products for 8:2 FTOH in rat hepatocytes (Martin et al., 2005).

Other precursors include PAPs, fluorotelomer sulfonate (FTS), perfluoroalkyl sulfonamide-ethanol (FASEs), perfluoroalkyl sulfonamide (FASAs), and perfluoroalkyl sulfonamide-acetic acid (FASAAs). PAPs are fluorinated surfactants commonly used in food packaging. A study using microorganisms from wastewater sludge showed that monosubstituted and disubstituted PAPs will degrade to FTOHs initially and then further to PFOA (Lee et al., 2010a), as already shown in other studies (Dinglasan et al., 2004; Wang et al., 2005). Boulanger and colleagues (2005) investigated the biodegradation of a perfluorooctane surfactant, N-EtFOSE during wastewater treatment. No biodegradation was observed for anaerobic conditions, but aerobic conditions resulted in five metabolites (PFOSAA, N-EtFOSAA, FOSA, PFOS, and PFOSulfinate). In addition, the authors found PFOA, PFOS, FOSA, N-EtFOSE, and PFOSulfinate in a can of Scotchgard.

These results indicate the perfluorooctane surfactants are precursors for PFASs, and the commercial products may contain residual PFASs from production. Recently, Wang et al. (2011) examined the aerobic biotransformation of 6:2 FTS. Compared to 6:2 FTOH, it had very slow transformation, and consequently it is unlikely to be a source of PFASs in wastewater treatment or the environment. The authors hypothesized that desulfonation is the rate-limiting step for the transformation. Nonetheless, three PFCAs (FPBA, PFPnA, and PFHxA), 5:2 FTOH, one fluorotelomer ketone, and 5:3 FTCA were observed as products from 6:2 FTS degradation, which makes it a PFAS precursor.

2.2.2 Ozonation of PFASs

Several studies have shown that ozonation does not decrease PFASs concentration (Kunacheva et al., 2010; Quiñones and Snyder, 2009; Schroder and Meesters, 2005; Shivakoti et al., 2010; Takagi et al., 2008, 2011). Preliminary bench-scale research by the co-authors has shown an increase in some PFAS concentrations after ozonation of wastewater, as shown in Table 2.4. Although not discussed by the authors, results from two studies (Shivakoti et al., 2010; Schroder and Meesters, 2005) show a slight increase for some PFASs after ozonation and AOP experiments. Precursors present before ozone oxidation may generate other PFASs. For example, indirect photolysis of precursor NEtFOSE with artificial sunlight and hydroxyl radical can result in formation of PFOA (Plumlee et al., 2009). Ozonation may lead to a similar outcome.

Table 2.4. Results from Preliminary Bench-Scale Experiments Monitoring for Formation of PFASs

Wastewater Matrix	O_3:TOC Ratio	PFHxA ng/L	PFOA ng/L	PFNA ng/L
Primary Effluent	0	4.0	4.3	2.3
	0.5	37.5	6.0	3.1
	1.0	45.0	7.9	5.4

2.2.3 Accumulation in Water and Wastewater Treatment

The fate of PFASs in water treatment systems is a critical issue. Schultz et al. (2006) completed a PFAS mass flow analysis for several wastewater treatment processes, including primary clarification, conventional activated sludge (CAS), trickling filter (TF), and anaerobic digestion. PFHxS and PFDA decreased for primary clarification and TF, whereas PFHxA decreased during CAS. Both CAS and TF showed a net increase for PFOS and PFDS, which the authors hypothesized was due to precursor degradation. Coagulation and dissolved air flotation filtration (DAFF) in recycled water treatment plants in Australia showed decreases for some compounds, whereas denitrification did not have a noticeable effect (Thompson et al., 2011).

PFASs are likely to adsorb to solids during water and wastewater treatment. One group observed increases in several PFASs during CAS and no significant changes during primary clarification (Sinclair and Kannan, 2006). They also noted a preference for longer chain PFASs to partition to the sludge with PFOA as the dominant PFAS in sludge and PFOS as the dominant PFAS in the wastewater. Guo et al. (2010) and Yu et al. (2009a) found similar increases during CAS and MBR, which were attributed to precursor degradation. Decreases in PFAS concentration were attributed to sorption to sludge. Sorption studies with sludge revealed strong adsorption, with aerobic sludge having the highest capacity and a greater partitioning coefficient (K_d) for PFOS (200–4050 L/kg) as compared to PFOA (150–350 L/kg; Zhou et al., 2010). Likewise, Yu et al. (2009b) found that PFASs with the sulfonate group have higher partitioning coefficients and greater sorption to sludge. Higgins and Luthy (2006) came to the same conclusion, as well as determining that PFAS sorption to sludge increases with chain length (i.e., more CF_2 groups). Two research groups (Guo et al., 2010; Sinclair and Kannan, 2006) observed greater

concentrations of PFASs in industrial wastewater as compared to municipal wastewater. Overall, typical wastewater treatment resulted in tertiary effluent containing PFASs. Neither wetlands nor natural attenuation were shown to remove PFASs from the environment (Hoehn et al., 2007; Plumlee et al., 2008a).

2.2.4 Mitigation Strategies

2.2.4.1 Conventional Water Treatment Processes

Drinking water treatment processes exhibited some decrease in PFAS concentration but not complete removal. Sand filtration was effective for removing PFASs in the particulate phase but not the aqueous phase (Kunacheva et al., 2010). Neither rapid sand filtration nor slow filtration reduced PFAS concentration for various groundwaters and surface waters (Takagi et al., 2008). Coagulation with polyaluminum chloride (PACl) can reduce ionic PFAS concentration through electrostatic attraction to suspended solids by 90%. The dose, pH, temperature, chain length, chemical moieties, and competing ions all affect overall PFAS removal. Ionic PFASs with longer chains and a sulfonate group at a low temperature (5–15° C) and low pH (< 6) are best removed with an optimal 10 mg/L PACl dose (Deng et al., 2011).

2.2.4.2 Advanced Water Treatment Processes

Advanced treatment processes present the most likely mitigation strategies for PFASs. In one study, partial removal occurred through UF and BAC, no removal for ozonation, and almost complete removal with RO (Thompson et al., 2011). MF showed a slight decrease in PFAS concentration (Takagi et al., 2008), whereas NF showed removal greater than 90%. With the exception of small PFCs (e.g., PFPnA), RO rejection rates are greater than 95% (Steinle-Darling and Reinhard, 2008; Tang et al., 2007). In a comparison of tap water and bottled water from Thailand, the bottled waters had greater PFAS concentrations despite the use of advanced treatment (RO, ozonation, UV). The reason for this is unknown (Kunacheva et al., 2010).

Sorption techniques remove some PFASs. GAC will remove PFASs, but the results are dependent on the remaining capacity, retention time, and how often the carbon is exchanged (Shivakoti et al., 2010; Takagi et al., 2008; Yu et al., 2009b). GAC sorption is stronger than sorption to zeolite and sludge (Ochoa-Herrera and Sierra-Alvarez, 2008). Combining ultrasound with GAC increased sorption kinetics by 250 to 900% (Zhao et al., 2011). Yu et al. (2009b) found that powdered activated carbon (PAC) is suitable for PFAS removal and reached sorption equilibrium faster than GAC. The same study showed that ion exchange will remove ionic PFASs, such as PFOS and PFOA; however, the high molecular weights, small charged sites, and long nonpolar ends of PFAS molecules slow the sorption kinetics, and it may require a full day to achieve the best removal (Lampert et al., 2007).

A recent survey of several drinking water facilities revealed no significant difference between raw and effluent waters with treatment by coagulation, deep bed filtration, PAC, medium-pressure UV irradiation, or ozonation (Quiñones and Snyder, 2009). Only joint MF–RO treatment exhibited PFAS removal. Other AOPs were investigated briefly. Thompson et al. (2011) experimented with UV/H_2O_2, but the concentrations were below reporting limits after RO, and no information could be determined.

Another study investigated O_3 alone, O_3/UV, O_3/H_2O_2 and Fenton's reagent (Fe/H_2O_2) but found these AOP treatments ineffective for PFOS removal (Schroder and Meesters, 2005).

2.2.4.3 Alternative Treatments

In addition to mitigation strategies employed in water treatment today, other techniques are available to destroy PFASs. Although UV photolysis at 254 nm is not effective because most PFASs do not absorb light in this region; vacuum UV at 185 nm may exceed 90% removal through decarboxylation and loss of CF_2 units to form shorter chain PFASs (Chen et al., 2007; Giri et al., 2011). PFOA removal under UV 254 nm was improved (33 times greater) by the addition of ferric ion (Wang et al., 2008). The addition of potassium iodide or aqueous periodate during UV (243 nm) irradiation will increase removal to greater than 90 and 70%, respectively (Cao et al., 2010; Qu et al., 2010). Other photocatalysts include tungstic heteropolyacid ($H_3PW_{12}O_{40}$), persulfate, iron (III) sulfate, and gallium oxide (Fujii et al., 2007; Rayne and Forest, 2009). TiO_2 was not an effective photocatalyst (Zhao and Zhang, 2009). PFOA was successfully decomposed with zero valent iron (ZVI) and sulfate radicals, which were formed through microwave-induced oxidation of persulfate (Lee et al., 2010b). The decomposition was step-wise via the loss of CF_2 groups. As noted earlier, MF does not significantly remove PFASs, but electro-MF removes greater than 60% of ionic PFASs depending on the pH, ionic strength of the water matrix, and electrical field strength (Tsai et al., 2010). In addition, ultrasonic irradiation has been shown to degrade PFOS and PFOA. The degradation was attributed to pyrolysis at the interfacial region between the cavitation bubbles and solution rather than hydroxyl radicals or thermal destruction (Moriwaki et al., 2005a).

Chapter 3

Materials and Methods

This chapter provides detailed methods for all procedures used during this project as well as equipment descriptions for the pilot plant. The main analytical methods include nitrosamine, total nitrosamine, and PFAS analysis.

3.1 Nitrosamine Analysis

Trace analysis–grade methanol and dichloromethane (DCM) were obtained from Burdick and Jackson (Muskegon, MI). Sodium azide was purchased from Fisher Chemicals, Fisher Scientific (Fair Lawn, NJ), and sodium thiosulfate was purchased from EM Science (Merck KGaA, Darnstadt, Germany). Reagent-grade water was prepared by using a Milli-Q Gradient water purification system (Millipore, Billerica, MA). Nitrosamine standards were purchased from Ultra Scientific (Kingstown, RI), and isotopically labeled nitrosamines were purchased from Cambridge Isotope Laboratories (Andover, MA). Working stock solutions of nitrosamines and isotopically labeled nitrosamines were made in DCM. Appropriate dilutions were made in methanol for automated solid-phase extraction (ASPE) spiking solutions (nitrosamine spike mix and isotopically labeled standards). Calibration standards were made in DCM and replaced every 3 months. A minimum of seven calibration standards were made, ranging from 1.0 to 500 µg/L. All stock solutions, ASPE spiking solutions, and calibration standards were stored at -20 °C. Target nitrosamines, Chemical Abstract Services (CAS) numbers, structures, and corresponding isotopes are listed in Table 3.1.

Samples were collected in 1 L precleaned, presilanized, amber glass bottles. Aliquots of sodium azide (1%) and sodium thiosulfate (0.8%) were added to bottles prior to sampling for preservation and to quench residual oxidant. After sampling, bottles were kept on ice during transportation to laboratory and stored at 4 °C until extraction. All samples were extracted within 14 days of collection. When necessary, samples were filtered prior to extraction with 90 mm glass fiber (GF/F) filters.

ASPE was performed using a Dionex AutoTrace workstation (Thermo Scientific, Sunnyvale, CA). Samples (1 L) were processed in batches of six and spiked with 100 µL of isotope mix at 0.5 to 2.5 mg/L for a concentration of 100 to 500 µg/L in the final extract. Prepacked activated charcoal cartridges (Resprep 521, Restek, Bellefonte, PA) were sequentially conditioned with 5 mL DCM, 5 mL methanol, and 10 mL reagent-grade water with a flow rate of 15 mL/min. Samples were loaded at a rate of 15 mL/min. Cartridges were rinsed with 5 mL reagent-grade water with a flow rate of 20 mL/min and dried for 10 min with nitrogen gas. Analytes were eluted with 10 mL DCM into 15 mL conical vials (Dionex) with a flow rate of 5 mL/min. Extracts were evaporated under nitrogen gas to approximately 2 mL. Water was then removed from the DCM extracts by passing the 2 mL extract through a DryDisk separation membrane (Horizon Technology, Salem, NH). The DCM extract was collected and concentrated to a final volume of 500 µL with nitrogen gas, resulting in a 1:2000 concentration factor.

Table 3.1. Nitrosamines, CAS Numbers, Structures, and Corresponding Isotopes

Compound	CAS#	Structure	Isotope
N-nitrosodimethylamine (NDMA)	62-75-9	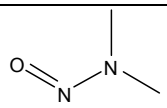	NDMA-d_6
N-nitrosomethyl-ethylamine (NMEA)	10595-95-6	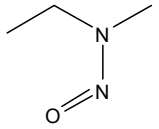	NMEA-d_3
N-nitrosodiethylamine (NDEA)	55-18-5	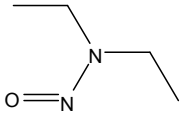	NDEA-d_{10}
N-nitrosodipropylamine (NDPA)	621-64-7	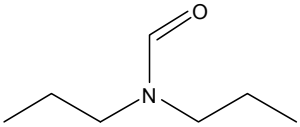	NDPA-d_{14}
N-nitrosomorpholine (NMOR)	59-89-2	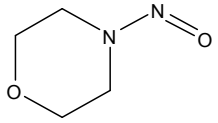	NMOR-d_8
N-nitrosodibutylamine (NDBA)	924-16-3	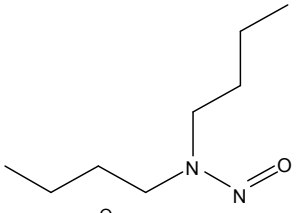	NDBA-d_{18}
N-nitrosodiphenylamine (NDPh)	86-30-6	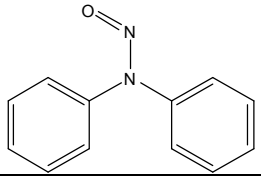	NDPh-d_6

Note: CAS=Chemical Abstract Services

A Varian (Walnut Creek, CA) CP-3800 gas chromatograph with a CP-8400 auto sampler was used for all analyses. The injector (Varian 1177) was operated in splitless mode with a Siltek™ deactivated glass liner (Restek, Bellefonte, PA) and set at 200 °C. Analytes were separated on a 30 m x 0.32 mm ID x 1.4 µm DB624 column (J & W, Agilent, Palo Alto) using a 1.4 mL/min helium flow with an initial pressure pulse of 35 psi for 0.85 min. The temperature program was as follows: 35 °C, hold for 1.0 min; 35 to 120 °C at 5 °C/min; 120 to 145° C at 3° C/min; 145 to 250 °C at 35 °C/min, hold for 4.64 min. An injection volume of 2 µL was used for all analyses. The transfer line was set at 240 °C.

Analysis was performed using a Varian 4000 ion trap mass spectrometer (Walnut Creek, CA). All analyses were performed using multiple reaction monitoring (MRM) in positive chemical ionization mode using liquid methanol. *N*-nitrosopiperidine and *N*-nitrosopyrrolidine were initially included in the analysis

but were removed because matrix interference resulted in unreliable quantification. Precursor and product ions used for quantitation and confirmation are listed in Table 3.2 for target nitrosamines as well as their molecular weights and method reporting limits (MRL). Some of the nitrosamines did not exhibit a second product ion in high enough abundance to monitor as a confirmation transition and therefore only have one quantitation transition. Because of thermal degradation upon injection, N-nitrosodiphenylamine was analyzed as diphenylamine. Quantitation was performed using isotope dilution. Method reporting limits were established at 3 to 5 times the calculated method detection limit (MDL; n=12).

Table 3.2. Molecular Weights, MRM Transition Ions, and MRLs

Compound	MW (amu)	Precursor ion (m/z)	Product ion (m/z)	MRL (ng/L)
NDMA	74	75	47 (44, 43, 58) [b]	2.5
NMEA	88	89	61 (47)	2.5
NDEA	102	103	75	5.0
NDPA	130	131	89	10
NMOR	116	117	86 (87)	5.0
NDBA	158	159	103	10
NDPhA	198 (169)[a]	170	92 (143)	10

Notes: [a]=analyzed as diphenylamine; [b]=( )-confirmation product ions; MRL=method reporting limit; MRM=multiple reaction monitoring. Refer to Table 2.3 for full list of abbreviations.

A minimum of seven calibration standards were used to construct a calibration curve for each analyte, with at least one calibration standard analyzed at or below the MRL. Correlation coefficients were required to be at least 0.990 but typically exceeded 0.995 using linear regression. A field blank was collected for each sampling event, extracted, and analyzed. A laboratory reagent blank was also included in each extract batch. Acceptance criteria for a data batch required any observable compound peaks in blanks to remain at less than 1/3 MRL; otherwise, results were flagged, and compound MRL was adjusted for all samples in batch. Laboratory fortified reagent blanks and sample matrices and a sample duplicate were incorporated into each extract batch to monitor analytical performance. Acceptance limits for recovery were set at 70 to 130% and at 30% relative difference for duplicates. Table 3.3 displays the average analytical error for replicate analysis of each compound and recovery summaries for reagent water and matrix spikes.

3.2 Total Nitrosamine Analysis

A total *N*-nitrosamine (TONO) method for wastewater was established based on previous work involving drinking water and swimming pools (Dai and Mitch, 2013; Kulshrestha et al., 2010). TONO is a nonselective method to quantify bulk *N*-nitrosamines with a wide range of polarities and molecular weights. This method consists of an extraction, a chemical redox reaction, and chemiluminescence detection.

Table 3.3. Average Recovery and Relative Standard Deviations for Target Nitrosamines in Various Water Matrices (n=6) Spiked at 25 ng/L

	Reagent Water		Finished Drinking Water		Surface Water		Tertiary Wastewater	
	Average %	RSD %	Average %	RSD %	Average %	RSD %	Average %	RSD %
NDMA	114	4.0	117	3.2	117	0.89	136	2.1
NMEA	99	3.1	98	1.5	101	2.1	99	2.8
NDEA	98	6.2	104	6.2	97	5.0	101	5.7
NDPA	109	10	82	9.9	105	7.3	78	10
NMOR	107	7.2	100	6.8	101	4.6	109	9.8
NDBA	105	6.8	98	9.1	95	7.7	47	5.7
NDPhA	84	6.1	87	5.9	89	2.8	105	4.9

Notes: RSD=relative standard definitions. Refer to Table 2.3 for definitions of abbreviations.

Unlike previously published TONO methods, which utilize a continuous liquid–liquid extraction in ethyl acetate, this method involves ASPE. Initial development began with a manual extraction using two stacked cartridges and two elution solvents. The final method was simplified to a single cartridge and two elutions, which can be automated. ASPE was performed using a Dionex AutoTrace 280 workstation (Thermo Scientific, Sunnyvale, CA). Samples (1 L) were processed in batches of six using prepacked 6 cc coconut charcoal cartridges (≤100 mesh, 2 g) from Restek. Cartridges were conditioned with 5 mL DCM, 5 mL methanol, and 5 mL reagent water at a flow rate of 15 mL/min. Samples were loaded at a rate of 15 mL/min. Cartridges were rinsed with 5 mL reagent water and dried for 15 min with nitrogen gas. Target analytes were eluted stepwise with 10 mL methanol and 10 mL DCM into separate 15 mL conical vials (Dionex) with a flow rate of 5 mL/min. Both extracts were concentrated to approximately 2 mL with nitrogen gas and then combined. The combined extract was further concentrated to a final volume of 1 mL. Extracts were stored in amber glass vials at 4 °C until analysis.

During TONO analysis, the nitrosamines are reduced to nitric oxide in a redox reaction, then oxidized by ozone in the detector, and quantified using chemiluminescence. The chemical redox reaction was performed in a jacketed glass reactor with an attached condenser. The custom-built reactor has a glass frit on the bottom of the central chamber through which nitrogen gas enters. Other features of the reactor include an inlet port sealed with a septum for introducing the sample by syringe, inlet/outlet ports for

water heated by a circulator, and an outlet port controlled with a stopcock for emptying the central chamber. The reactor was maintained at 80 °C and the condenser (50/50 mixture of water and ethylene glycol) at 0 °C. Under a nitrogen flow, 10 mL of glacial acetic acid and 1 mL of an aqueous tri-iodide solution (540 g/L potassium iodide and 114 g/L iodine) were added to the reactor. The tri-iodide is a reducing agent that reduces the nitrogen after the acid-catalyzed denitrosation reaction, which results in the formation of nitric oxide gas. After several minutes of purging, the reactor was connected to the condenser and tubing leading to a chemical trap. The chemical trap consisted of a jacketed glass cylinder with a glass frit diffuser. The inner chamber was filled with 30 mL of 1 Molar (M) sodium hydroxide, and the jacket was cooled with 50/50 ethylene glycol and water. Following the chemical trap, the gas flowed through a pressure gauge and an inline 0.2 µm syringe filter before entering the Ecomedics CLD 88 sp chemiluminescence detector.

Prior to injection, the sample extract was treated to eliminate interference from nitrite and S-nitrosothiols. First, 100 µL of 20 g/L mercuric chloride was added and allowed to react for 30 min in the dark at room temperature. Then, 100 µL of 50 g/L sulfanilamide in 1 M hydrochloric acid was added and allowed to react for 15 min in the dark at room temperature. Final concentrations were corrected for the dilution associated with eliminating interference from nitrite and S-nitrosothiols. A 50 µL aliquot was injected into the reaction chamber and monitored by viewing the peak (Microsoft Excel 2007 with CLD 1.9.98cen macro add-in). Subsequent treated extracts were injected after the signal returned to the baseline. Signal smoothing and processing were performed with ACD/Laboratories ChromProcessor (ACD/Specmanager version 12.01). The TONO sample analysis was limited to 12 samples, in addition to calibration and quality control samples, because of observed deterioration of the reaction chamber and solution.

A 7-point calibration curve (10–1000 ppb NDMA) was interspersed among the samples for every analysis. Linear regression always exceeded 0.995 for the calibration curve. During the 2-hour analysis period, peaks broadened and peak height reduced; however, peak areas remained similar (e.g., CV% within ±30% at beginning and end of entire analysis). Recovery tests for ASPE over a 5-month period are summarized in Table 3.4. Compounds included were NDMA, NMOR, NDPA, NDPhA, N-nitrosodiethanolamine (NDELA), and a nine-compound N-nitrosamine mixture (Nitro Mix). Recoveries shown are inclusive of ASPE and the reaction conversion efficiency for each nitrosamine compared to NDMA. The nitrosamines vary in how much of the compound is converted into nitric oxide and detected by chemiluminescence (Table 3.4). The NDPhA recovery was low, probably because of poor conversion. The MRL (50 ng/L) was conservatively set at approximately five times the calculated MDL (8.6 ng/L, n=12) with a signal to noise ratio greater than 3. The MDL/MRL were based on a study using only NDMA spikes as the model nitrosamine, as it correlated to the NDMA calibration too. All travel blanks and reagent water injections resulted in no observable peaks. Matrix spike recoveries for wastewater are similar to those for reagent water, which suggests that matrix effects do not adversely impact reported results. Reported results from this study were not adjusted for recovery or reaction conversion efficiency, and therefore it should be noted that these values underestimate the total nitrosamines in the samples.

Table 3.4. Average Recovery and Relative Standard Deviations for Target Nitrosamines in Reagent Water and Reaction Conversion Efficiency for Detection

	Spike Recoveries in Reagent Water				Reaction Efficiency (n=7)		
Abbreviation	Spike Conc. (ng/L)	Samples (n)	Mean Recovery (%)	RSD (%)	Spike Conc. (ng/L)	Mean Recovery (%)	RSD (%)
NDMA	400	13	39	21	500	103	8.4
NDELA	400	13	45	26	500	67	7.3
NMOR	400	3	41	13	500	56	20
NDPA	400	3	22	16	500	55	10
NDPhA	400	3	0	0	500	36	16
Nitro Mix	1800	13	34	14	450	70	8.0

Notes: RSD=relative standard definitions. Refer to Table 2.3 for definitions of abbreviations.

Table 3.5. Replicate Results, Relative Standard Deviations, and NDMA Matrix Spike Recoveries for Wastewater

Wastewater Description	Sample (ng/L)	Duplicate (ng/L)	RSD (%)	Matrix Spike Recovery (%)
Secondary WW Effluent 1	86.7	96.6	11	49
Secondary WW Effluent 2	147	142	3	38
Tertiary WW Effluent	<MRL	<MRL	0	40

Notes: WW=wastewater; MRL=method recording limit; RSD=relative standard deviations.

3.3 Perfluoroalkyl and Polyfluoroalkyl Substances Analysis

Analytical standards and isotopically labeled standards for all PFASs measured in this study (Table 3.6) were procured from Wellington Laboratories (Guelph, Ontario, Canada). This analytical suite of 23 chemicals included perfluorocarboxylic acids (PFCAs), perfluorosulfonic acids (PFSAs), and polyfluoroalkyl chemicals (PFCA and PFSA precursors). Whenever possible, matched isotope standards were used for quantitation of each PFAS. Working stock PFAS solutions and calibration standards were prepared in methanol, and appropriate dilutions were made for ASPE spiking solutions. All solutions and standards were stored at -20 °C. Trace analysis–grade methanol and methyl tert-butyl ether (MTBE) were obtained from Burdick and Jackson (Muskegon, MI). Ascorbic acid was purchased from Mallinckrod Chemicals (Phillipsburg, NJ), and concentrated sulfuric acid was obtained from EM Scientific (Merck KGaA, Darmstadt, Germany). Reagent-grade water was prepared with a Milli-Q Gradient water purification system (Millipore, Billerica, MA).

All samples shipped to the Southern Nevada Water Authority (SNWA) laboratory were collected in 1 L precleaned, wide mouth, amber high density polyethylene bottles (Rochester, NY). Samples were shipped to SNWA from several U.S. states (Kentucky, Georgia, California, Texas, Missouri, and Nevada) and Australia. An aliquot of ascorbic acid solution (0.05%) was added to all bottles prior to sampling for

chlorine quenching. After sampling, bottles were kept on ice during transportation and stored at 4° C until extraction. Samples were extracted within 14 days of collection and, when necessary, filtered prior to extraction with prewashed 90 mm glass fiber filters. Preliminary studies indicated no impact from filtration on the measured concentrations of target analytes.

ASPE was performed using Dionex AutoTrace 280 workstation (Thermo Scientific, Sunnyvale, CA). Samples (1 L) were acidified to a pH greater than 2 with concentrated sulfuric acid, then spiked with isotopically labeled standards prior to extraction. Samples were processed in batches of six. Prepacked 200 mg, 6 cc Hydrophilic-Lipophilic-Balanced (HLB) cartridges (Waters Corporation, Milford, MA) were sequentially conditioned with 5 mL MTBE, 5 mL methanol, and 5 mL reagent water at a flow rate of 15 mL/min. Samples were loaded at a rate of 15 mL/min. Cartridges were rinsed with 5 mL reagent water and dried for 30 min with nitrogen gas. Target analytes were eluted with 10 mL of methanol into 15 mL conical vials (Dionex) at a flow rate of 5 mL/min. Extracts were concentrated to a final volume of 500 µL or 1 mL with nitrogen gas.

Table 3.6. Suite of Measured PFASs in This Study

PFAS Classes	Chemical Name	Abbreviation	CAS RN	M.W. (g/ mol)	Molecular Formula	Relevant Guidance Levels
Perfluoro-carboxylic acids (PFCAs)	Perfluorobutyric acid	PFBA	375-22-4	214	$C_4HF_7O_2$	7.0 µg/L[b]
	Perfluoropentanoic acid	PFPnA	2706-90-3	264	$C_5HF_9O_2$	
	Perfluorohexanoic acid	PFHxA	307-24-4	314	$C_6HF_{11}O_2$	
	Perfluoroheptanoic acid	PFHpA	375-85-9	364	$C_7HF_{13}O_2$	
	Perfluorooctanoic acid	PFOA	335-67-1	414	$C_8HF_{15}O_2$	0.4 µg/L[a], 0.3 µg/L[b], 0.04 µg/L[c]
	Perfluorononanoic acid	PFNA	375-95-1	464	$C_9HF_{17}O_2$	
	Perfluorodecanoic acid	PFDA	335-76-2	514	$C_{10}HF_{19}O_2$	
	Perfluoroundecanoic acid	PFUnA	2058-94-8	564	$C_{11}HF_{21}O_2$	
	Perfluorododecanoic acid	PFDoA	307-55-1	614	$C_{12}HF_{23}O_2$	
Perfluoro-sulfonic acids (PFSAs)	Perfluorobutane sulfonic acid	PFBS	375-73-5	300	$C_4HF_9SO_3$	7.0 µg/L[b]
	Perfluorohexane sulfonic acid	PFHxS	355-46-4	400	$C_6HF_{13}SO_3$	
	Perfluorooctane sulfonic acid	PFOS	1763-23-1	500	$C_8HF_{17}SO_3$	0.2 µg/L[a], 0.3 µg/L[b]
	Perfluorodecane sulfonic acid	PFDS	335-77-3	600	$C_{10}HF_{21}SO_3$	
Polyfluoro-alkyl compounds	Perfluorooctane sulfonamide	FOSA	754-91-6	499	$C_8H_2F_{17}NO_2S$	
	N-methyl perfluorooctane sulfonamidoacetic acid	*N*-MeFOSAA	2355-31-9	571	$C_{11}H_6F_{17}NO_4S$	
	N-ethyl perfluorooctane sulfonamidoacetic acid	*N*-EtFOSAA	2991-50-6	585	$C_{12}H_8F_{17}NO_4S$	

PFAS Classes	Chemical Name	Abbreviation	CAS RN	M.W. (g/ mol)	Molecular Formula	Relevant Guidance Levels
	4:2-fluorotelomer unsaturated carboxylic acid	4:2 FTUCA	20825-07-4	258	$C_6H_2F_8O_2$	
	6:2-fluorotelomer unsaturated carboxylic acid	6:2 FTUCA	261503-40-6	358	$C_8H_2F_{12}O_2$	
	8:2-fluorotelomer unsaturated carboxylic acid	8:2 FTUCA	70887-84-2	458	$C_{10}H_2F_{16}O_2$	
	10:2-fluorotelomer unsaturated carboxylic acid	10:2 FTUCA	70887-94-4	558	$C_{12}H_2F_{20}O_2$	
	4:2-fluorotelomer sulfonate	4:2 FtS	36839-98-2	328	$C_6H_5F_9O_3S$	
	6:2-fluorotelomer sulfonate	6:2 FtS	27619-97-2	428	$C_8H_5F_{13}O_3S$	
	8:2-fluorotelomer sulfonate	8:2 FtS	39108-34-4	528	$C_{10}H_5F_{17}O_3S$	

Notes: [a]=U.S. Environmental Protection Agency PHA values; [b]=Minnesota Department of Health Health Risk Limits; [c]=New Jersey Department of Environmental Protection health-based drinking water guidance level; CAS RN=Chemical Abstract Services Registry Number; MW=molecular weight; PFAS=perfluoroalkyl and polyfluoroalkyl substances.

Analysis of ASPE extracts was conducted at SNWA's research and development laboratory via liquid chromatography–tandem mass spectrometry (LC–MS/MS) using a previously reported method (Quiñones and Snyder, 2009) adapted and expanded to include all analytes of interest. Briefly, an Agilent (Palo Alto, CA) G1312A binary pump and an HTC-PAL auto sampler (CTC Analytics, Zwingen, Switzerland) were used. Analytes were separated using a 150 Ö 4.6 mm Synergi Max-RP C12 column with a 4 µm pore size (Phenomenex, Torrance, CA) and a binary gradient consisting of 5.0 mM ammonium acetate (v/v) in water (A) and 100% methanol (B) at a flow rate of 800 µL/min. An injection volume of 10 µL was used for all analyses. Contaminants from the aqueous channel were removed using a 4.0 x 10 mm Hypercarb (Thermo Fisher Scientific, Waltham, MA) drop-in guard cartridge attached in-line before the instrument's purge valve. Remaining contaminants were separated from analyte peaks by installing a 75 x 4.6 mm Synergy Max-RPC12 column with a 4 µm pore size (Phenomenex, Torrance, CA) in-line upstream from the injector valve. Tandem mass spectrometry was performed using an API 4000 triple quadrupole mass spectrometer (AB SCIEX, Foster City, CA). Using electrospray ionization (ESI) operated in negative ionization mode, optimal compound-dependent parameters were determined for additional analytes, and source-dependent parameters were optimized. The concentration of each analyte was determined by isotope dilution, surrogate standard, or external calibration. MRLs were based on MDLs calculated from seven replicate measurements of deionized water samples fortified with analytes and extracted as previously described. As an added cautionary measure, MRLs for each analyte were set conservatively at least five times the MDL, higher as needed in consideration of known and unanticipated background sources. Compound-dependent analytical and quantitation parameters are detailed in Table 3.7.

Table 3.7. Compound-Dependent Analytical and Quantitation Parameters

Analyte				Calibration	
Abbreviation	**Retention Time (min)**	**MRM[a] Transition**	**Quantitation**	**Calibration Range (µg/L)**	**Method Reporting Limit (ng/L)**
PFBA	6.3	213>169	isotope dilution	0.50–125	5
PFPnA	7.1	263>219	isotope dilution	0.50–125	2
PFHxA	8.2	313>269	isotope dilution	0.10–25	0.5
PFHpA	9.4	363>319	isotope dilution	0.10–25	0.5
PFOA	10.2	413>369	isotope dilution	0.50–125	5
PFNA	10.8	463>419	isotope dilution	0.10–25	0.5
PFDA	11.4	513>469	isotope dilution	0.10–25	0.5
PFUnA	12.2	563>519	isotope dilution	0.10–25	0.5
PFDoA	13.3	613>569	isotope dilution	0.10–25	0.25
PFBS	7.1	299>99	surrogate standard	0.10–25	0.25
PFHxS	9.4	399>80	isotope dilution	0.10–25	0.25
PFOS	10.7	499>80	isotope dilution	0.10–25	0.25
PFDS	12	599>99	surrogate standard	0.10–25	0.10
FOSA	13	498>78	isotope dilution	0.10–25	0.25
N-MeFOSAA	11.8	570>419	isotope dilution	0.10–25	0.25
N-EtFOSAA	12.2	584>419	isotope dilution	0.10–25	0.25
4:2 FTUCA	7.3	257>193	surrogate standard	0.10–25	2
6:2 FTUCA	9.8	357>293	isotope dilution	0.10-25	2
8:2 FTUCA	11	457>393	isotope dilution	0.10-25	2
10:2 FTUCA	12.7	557>493	isotope dilution	0.10-25	2
4:2 FtS	8.1	327>81	external calibration	0.10–25	0.5
6:2 FtS	10.2	427>81	external calibration	0.10–25	0.5
8:2 FtS	11.4	527>81	external calibration	0.10–25	0.5

Notes: MRM=multiple reaction monitoring. Refer to Table 3.6 for definitions of abbreviations.

A minimum of seven calibration standards were used to construct a calibration curve for each analyte, with at least one calibration standard analyzed at or below the MRL. Correlation coefficients were required to be at least 0.990 but typically exceeded 0.995 using linear regression. A field blank was collected for each sampling event, extracted, and analyzed. A laboratory reagent blank was also included in each extract batch. Acceptance criteria for a data batch required that any observable compound peaks in blanks remain at less than 1/3 MRL; otherwise, results were flagged, and compound MRL was adjusted for all samples in the batch. Laboratory fortified reagent blanks and sample matrices and a sample

duplicate were incorporated into each extract batch to monitor analytical performance. Acceptance limits for recovery were set at 70 to 130% and at 30% relative difference for duplicates. Signal counts for internal and surrogate standard peaks were required to remain higher than 10% when compared to average peak counts in calibrators. Samples not meeting these criteria were reanalyzed and diluted for matrix reduction as needed. Samples where efforts did not produce acceptable quality control criteria were flagged as such. Table 3.8 displays the average analytical error for duplicate analysis of each compound and recovery summaries for reagent water and matrix spikes for the project.

3.4 City of Las Vegas Pilot-Scale Site

Primary influent or effluent from the City of Las Vegas Water Pollution Facility was pumped to an on-site pilot-scale HYDRAsub® MBR system (Hydranautics, Oceanside, CA) for further biological nutrient removal and filtration. The MBR filtrate was collected in a 300 gallon equalization tank and then fed directly to a pilot-scale HiPOx® system (APTwater, Pleasant Hill, CA) for ozone addition via direct injection. The HiPOx® systems have California Department of Public Health Title 22 certification for disinfection in wastewater and water reuse applications. Photographs of the pilot equipment are shown in Figure 3.1.

The MBR pilot skid used hollow-fiber, vacuum-type polyvinylidene fluoride (PVDF) membranes with a reinforced core, an outer diameter of 2.8 mm, and a nominal pore size of 0.40 µm. According to the manufacturer's specifications, the PVDF membranes have a high tensile strength and good chemical (particularly sodium hypochlorite) tolerance. The fibers have a dual-layer coating of PVDF on the central reinforced core. The pilot unit contained a fine screen, an anoxic tank, an aerobic tank, a membrane tank, and a filtrate tank with full automation via programmable logic controller (PLC). There were two membrane modules, which were operated as a single component (no significant difference between the modules).

For this project, the MBR was operated under various mixed liquor suspended solids (MLSS) concentrations, solids retention times (SRT), and hydraulic retention times (HRT). Specific operational parameters are provided in subsequent sections of this report. A process flow diagram of the MBR system is shown in Figure 3.2. Typical optimum operating parameters for the MBR pilot are shown in Table 3.9.

Table 3.8. Analytical Variability and Spike Recovery Data

	Variability of Replicate Samples		Spike Recoveries in Reagent Water (n=49)			Matrix Spike Recoveries (n=12)		
Abbreviation	**Average % difference (n=12)**	**Max**	**Spike Conc. (ng/L)**	**Mean Recovery (%)**	**RSD (%)**	**Spike Conc. (ng/L)**	**Mean Recovery (%)**	**RSD (%)**
PFBA	2	3	20	102	6.2	20	105	13.5
PFPnA	4	9	20	107	12.3	20	110	9.3
PFHxA	4	14	10	105	12.2	10	109	12.0
PFHpA	7	24	10	110	14.1	10	114	16.6
PFOA	9	19	20	100	14.3	20	96	13.4
PFNA	12	22	10	104	12.2	10	113	14.2
PFDA	14	34	10	103	10.9	10	106	12.3
PFUnA	15	15	10	98	14.1	10	96	18.1
PFDoA	8	8	10	106	10.9	10	109	12.3
PFBS	8	25	10	112	10.0	10	114	8.7
PFHxS	5	13	10	98	11.6	10	88	17.4
PFOS	9	20	10	104	10.4	10	114	15.9
PFDS	0	0	10	87	17.9	10	117	12.9
FOSA	16	26	10	99	12.0	10	98	16.1
N-MeFOSAA	7	9	10	112	12.4	10	102	16.4
N-EtFOSAA	6	6	10	116	13.0	10	108	15.2
4:2 FTUCA	0	0	10	101	11.5	10	83	14.7
6:2 FTUCA	0	0	10	95	9.0	10	113	11.1
8:2 FTUCA	0	0	10	108	13.3	10	110	13.6
10:2 FTUCA	0	0	10	95	12.8	10	94	8.0
4:2 FtS	0	0	10	88	21.5	10	103	28.9
6:2 FtS	9	18	10	94	23.0	10	88	28.1
8:2 FtS	2	2	10	61	27.7	10	55	46.1

Notes: RSD=relative standard deviations. Refer to Table 3.6 for abbreviation definitions.

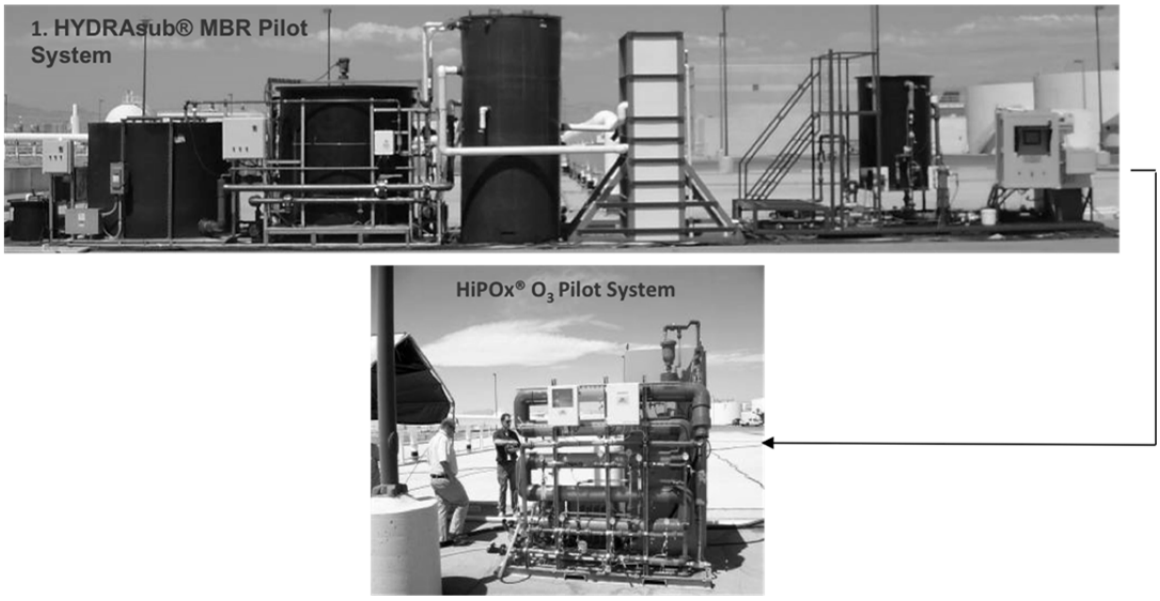

Figure 3.1. Photographs of MBR and HiPOx pilot systems.

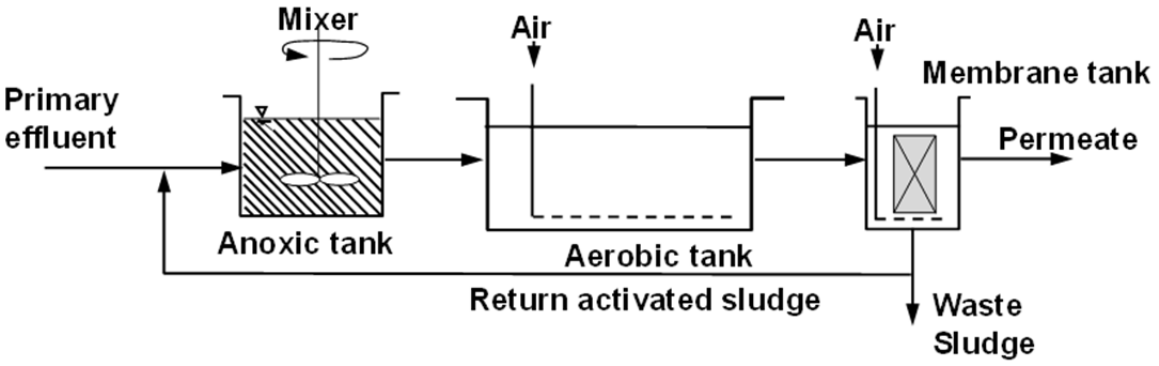

Figure 3.2. Process flow diagram of Hydranautics MBR and wastewater treatment skid.

Table 3.9. Typical Operating Parameters for Hydranautics MBR Pilot System

MBR Pilot	Parameter	Value	Unit
Fine screen	Opening	1	mm
Anoxic tank	Volume	1750	gallon
	Hydraulic retention time	1.8	hour
Aerobic zone	Total aerobic volume	3900	gallon
	Total hydraulic retention time	4.1	hour
	Solids retention time	12	days
	F:M ratio	0.1	kg BOD/day/kg MLSS
Membrane Module1	Membrane area	1345	ft^2
	Nominal pore size	0.40	µm
Membrane Module2	Design flux @ 25 °C	19.6	gfd
	Net flow	18.7	gpm
	Membrane area	807	ft^2
	Design flux @ 25 °C	19.6	gfd
	Net flow	6.2	gpm
	Tmp	2–4	psi
Filtrate tank	Volume	300	gallon

Notes: BOD=biological oxygen demand; F:M=food to microorganism ratio; MBR=membrane bioreactor; MLSS=mixed liquor suspended solids; TMP=trans-membrane pressure.

The HiPOx® pilot system was capable of operating in a variety of modes and configurations, at flow rates of 10 to 25 gpm, and at ozone doses of up to 15 mg/L. The pilot was fed using either liquid oxygen feedstock or a high purity (99.9%) oxygen gas to generate up to 10% ozone in dry gas. Ozone was added via direct injection. The HiPOx® reactor used three static mixers to maximize ozone transfer, which also contained a 60 gallon pressurized pipeline contactor with numerous sampling ports that allowed sample collection at hydraulic residence times ranging from 0 to 5.5 min at a flow rate of 10 gpm. Ozone doses were applied to match bench-scale experiments. Dosing conditions were calculated using a spreadsheet that accounted for water and oxygen flows, water temperature, and dry gas ozone concentration. Generator power was adjusted to maintain target dry gas concentration. Samples were collected at the end of the pipeline contactor and after at least one hydraulic residence time (6 min) after reaching target ozone concentration.

3.5 Bench-Scale Experimentation

A variety of bench-scale experiments were performed throughout the project. Work was completed at SNWA and the Radiation Laboratory on the University of Notre Dame campus.

3.5.1 pH and Buffering

The tested waters included laboratory grade deionized water (DI), secondary treated wastewater, and tertiary treated wastewater. DI water was buffered at neutral pH with phosphate buffer (5 mM final concentration) prepared from equal parts potassium dihydrogen phosphate (KH_2PO_4) and disodium hydrogen phosphate (Na_2HPO_4). Except for formation potential tests, the wastewater was not buffered. No additional filtration was performed, and no preservatives were added prior to bench-scale work. Collected wastewaters were stored at 4 °C prior to bench-scale experiments. Water quality characteristics for the wastewaters are described in Section 3.4.

As an initial step, wastewater pH was adjusted with 5N sodium hydroxide or 3N hydrochloric acid to pH 6, 7, or 8 depending on the test. Values were ±0.05 pH units as determined by a handheld pH meter.

3.5.2 Ozonation Batch Tests

Ozonated water was generated using an oxygen-fed generator (Model CFS-1A, Ozonia North America, Inc., Elmwood Park, NJ) to diffuse ozone into laboratory-grade water as described previously (Wert et al., 2009). DI water was stirred and cooled in a water-jacketed container as ozone bubbled in through a diffuser. Ozone venting out of the container was quenched as it bubbled through aqueous potassium iodide solutions. The ozone-saturated water was dispensed from an outlet with a stopcock near the bottom of the container.

The ozone stock was typically between 65 and 85 mg O_3/L, based on measurements by an indigo method (Rakness et al., 2010). Aliquots of the ozonated water were measured in a graduated cylinder and quickly poured into the container with the test water.

For consistency among wastewaters, the amount of ozonated water added was based on the initial TOC and the desired ratio (e.g., O_3:TOC=0.5). Dilution of the wastewater through the addition of ozonated water and DI water was taken into account when determining the final O_3:TOC ratio. After ozone addition, the container was closed and mixed. When the ozone residual was depleted, as determined through ozone decay tests, the finished water was transferred to sample containers with appropriate quenching agents for the different analyses.

Some tests required additional spikes, which were added prior to the ozonated water. These spikes included hydrogen peroxide at a 1:2 molar ratio of TOC:H_2O_2 to promote the production of hydroxyl radicals; 1000 ppm parachlorobenzoic acid (pCBA) for assessing hydroxyl radical formation; 100 mM tert-butyl alcohol (tBA) for selectively quenching hydroxyl radicals; 100 µM individual NDMA precursors; and 50 or 1200 µM bromide ion for assessing its influence on NDMA formation from precursors.

3.5.3 Formation Potential Tests

A stock chloramine solution of 14 g/L as Cl_2 was prepared from sodium hypochlorite and ammonium chloride. A procedure intended to preferentially form monochloramine rather than dichloramine was followed (Mitch and Sedlak, 2002). The initial chlorine concentration in sodium hypochlorite was determined through iodometric titration with sodium thiosulfate. Ammonium chloride and hypochlorite were combined at a Cl:N mass ratio of 3.5 to stay below breakpoint and preferentially form monochloramine. The ammonium chloride was dissolved in water with a drop of 5N sodium hydroxide.

The hypochlorite was added to the basic ammonium chloride solution while stirring rapidly. The chlorine concentration was immediately measured using iodometric titration, and the spike solution was used promptly for the formation potential tests.

The formation potential test is designed to establish the maximum amount of NDMA formed by chloramination (Mitch et al., 2003a). Phosphate buffer (10 mM final concentration) was added to ozonated and nonozonated (ambient) wastewater samples. Next, the chloramine solution was added (140 mg/L as Cl_2 final concentration). The samples were mixed and stored at room temperature in a dark location. After 10 days, the samples were quenched with sodium thiosulfate, and 0 chlorine residual was confirmed. NDMA was quantified using the standard analytical method as described in Section 3.2.

3.5.4 Radiolysis

Using a small diffuser connected to a lecture bottle, wastewater or DI water was saturated with nitrous oxide (N_2O gas) for 1 hour. Aqueous electrons, produced by gamma radiation, are scavenged by N_2O to form N_2O^-, which decomposes to N_2 and $O^{\bullet-}$. The $O^{\bullet-}$ is subsequently protonated by water to form •OH. Additional •OH was formed by direct gamma radiolysis of the water (Peller et al., 2003). Any pH adjustment was performed prior to N_2O saturation. The water was poured into amber glass containers for shipping to the radiation laboratory. Some samples were spiked with pCBA and tBA after N_2O saturation. Samples were shipped overnight and kept cool with ice packs.

Radiolysis tests were conducted to isolate the impact of hydroxyl radicals on NDMA and PFC formation. The samples were subjected to gamma irradiation (44 Gy/min) at variable time lengths to represent different hydroxyl radical concentrations. A Shepard 109-68 ^{60}Co source was used for gamma radiolysis (Peller et al., 2003). After irradiation, samples were poured into containers with appropriate quenching agents for the different analyses. Samples were shipped back overnight and kept cool with ice packs. Nitrosamines and PFASs were quantified using the standard analytical methods as described in Sections 3.1 and 3.2.

3.5.5 NDMA Precursors

Potential NDMA precursor compounds were purchased from the following suppliers: 2-furaldehyde 2,2-dimethylhydrazone (2-F-DMH) from Alfa Aesar (Heysham, Lancashire, United Kingdom); acetone dimethylhydrazone (acetone DMH), DMS, and Dacarbazine from TCI (Tokyo, Japan); 1,1,1',1'-tetramethyl-4,4'-(methylenedi-p-phenylene) TMDS from TCI America (Portland, OR); Streptozocin from Sigma (St. Louis, MO); 4-methyl-3-thiosemicabazide (4-M-3-TSC), UDMH, and DMA from Aldrich (St. Louis, MO); Atazanavir from Toronto Research Chemicals (Ontario, Canada); Daminozide from Fluka (Steinheim, Germany); *N*-{[(dimethylamino)carbonyl]oxy}-2-phenylacetamide (DMC-phenyl), *N*-1-(4-methylphenyl)-2,2-dimethylhydrazine-1-carbothioamide (DMTC-phenyl), *N'*-{[(dimethyl-amino)carbonyl]oxy}-4-(1,3-dithiolan-2-yl)benzenecarboximidamide (DMC-dithio), and *N*-1-(3-{[(2,2-dimethylhydrazino) carbonyl]amino} -4-methylphenyl)-2 ,2-dimethyl- hydrazine-1-carboxamide (DMSC) from Maybridge (Cornwall, United Kingdom).

Neat standards for new precursors (Table 6.1) and selected established precursors (Table 2.4) were individually dissolved in laboratory-grade water, acetonitrile (for solubility), or both at 10 mM, except for DMC-phenyl, DMSC, DMC-dithio, DMTC-phenyl, and Atazanavir, which were dissolved at 1000 mg/L because of a limited supply. These spike solutions were kept at 4 °C in amber vials. A phosphate buffer solution (1 M) was prepared from equal molar amounts of KH_2PO_4 and Na_2HPO_4 in laboratory-grade

water. A bromide spike solution (33.4 mg/L as Br) was prepared from sodium bromide in laboratory-grade water. A concentrated (34%) hydrogen peroxide solution was diluted to 0.1% (1000 mg/L) for use as a spike solution. All three solutions were prepared using laboratory-grade water. The phosphate salts were obtained from Fisher Scientific (Fair Lawn, NJ), the sodium bromide was from Sigma-Aldrich (St. Louis, MO), and the hydrogen peroxide solution was from EnviroTech Chemical Services (Modesto, CA).

Precursors were individually spiked into the test water at 100 µM in 125 mL amber glass bottles, except for DMC-phenyl, DMSC, DMC-dithio, DMTC-phenyl, and Atazanavir, which were spiked at 32 to 48 µM. Bromide and hydrogen peroxide (H_2O_2) spikes were added to the samples next, as appropriate. Ozonated water was added to give a final concentration of approximately 1 mM (48 mg/L), which is at a tenfold molar excess compared to the precursors. The 50 mL samples were sealed and mixed after ozone addition and left undisturbed at room temperature overnight in the dark. Based on an ozone decay curve for laboratory-grade water, the ozone residual (73 mg/L initially) was less than 0.8 mg/L after 3 hours. Therefore, leaving the bottles sit overnight was more than sufficient to eliminate the ozone residual. Ozone concentration was measured using the indigo method (Rakness et al., 2010).

3.5.6 NDMA (High Level) and pCBA Analysis

Samples for the bench-scale experiments involving NDMA precursors (Chapter 6) and the oxidant study with pCBA were not extracted and were analyzed directly via LC–MS/MS. The method did not utilize isotopic dilution or internal standards. For both pCBA and NDMA, an Agilent (Palo Alto, CA) G1312A binary pump and an HTC-PAL auto sampler (CTC Analytics, Zwingen, Switzerland) were used. A Luna C18(2) 150 x 4.60 mm, 5 micron column (Phenomenex, Torrance, CA) was used for separation.

NDMA analysis used a 20 µL injection loop and 35 µL sample injection volume. The mobile phase consisted of a binary gradient of 5 mM ammonium acetate (v/v) from J.T. Baker (Phillipsburg, NJ) in water (A) and 100% methanol (B) from Honeywell Burdick & Jackson (Muskegon, MI) at a flow rate of 800 µL/min. The gradient was as follows: 10% B held for 0.50 min, stepped to 65% B at 0.51 min and increased linearly to 100% B until 7 min. A 3 min equilibration step at 10% B at the start of each run resulted in a 10 min total run time. Tandem mass spectrometry was performed using an API 4000 triple quadrupole mass spectrometer (AB SCIEX, Foster City, CA). The mass spectrometer was operated via MRM in ESI positive ion mode with a source temperature of 375° C. Two transitions were monitored for NDMA (75/43 and 75/58). NDMA standards were purchased from Ultra Scientific (Kingstown, RI). A ten-point calibration curve for NDMA (1 to 5000 µg/L) was prepared in laboratory-grade water. Calibration standards were kept at 4 °C in amber vials.

Analysis for pCBA followed a previously published method (Vanderford et al., 2007) using the same column, mobile phases, and mass spectrometer as described previously. The gradient was as follows: 10% B held for 0.50 min, stepped to 60% B at 0.51 min, increased linearly to 100% B until 5 min, and held at 100% B for 2 min. A 5 min equilibration step at 10% B at the start of each run resulted in a 12 min total run time. Mass spectrometer parameters include ESI negative ion mode, 10 µL loop, and 30 µL injection with a flow rate of 5 µL/s, and source temperature of 550 °C. Three transitions were monitored (155/111, 155/35, and 157/37); however, the first transition did not have consistent results and was never used for quantification. A 9-point calibration curve for NDMA (0.1 to 100 µg/L) was prepared in laboratory-grade water. Calibration standards were kept at 4 °C in amber vials.

3.6 Water Quality and DOM Characterization

3.6.1 Fluorescence Excitation–Emission Matrix Spectroscopy

The quantification of subtle differences in the excitation–emission matrices (EEMs) involved the use of fluorescence regional integration (FRI) method (Chen et al., 2003), which was modified and described previously (Gerrity et al., 2011; Stanford et al., 2011). The concept of FRI is based on using specific regions of the EEM to identify (and quantify) specific components of organic matter that may be present in a given water sample. The EEM integration was based on three regions, operationally defined as described in Table 3.10 and Figure 3.3, consisting of a microbial byproducts/biopolymer region, fulvic-like substances, and humic-like substances. To avoid any bias from excitation wavelength (E(λ)), a boundary for the integration regions at [E(λ)-15 nm] was used. Similarly, to avoid any bias from the second order of the excitation wavelength, an upper boundary of [2 x E(λ) – 15 nm] was used. Hydrophobic compounds tend to have higher aromatic carbon content (Chen et al., 2003). Aromaticity is associated with a greater amount of region-specific fluorescence. Therefore, changes in FRI (and the sum of the regional volumes, Φ_T) provides a basis for quantifying changes in aromaticity (and hydrophobicity) of the organic matter in the sample. Second, FRI can be used to determine the relative contribution of types of organic matter to the overall composition of the water sample, as indicated by specific regions. As the relative distribution of organic material components changes between regions, one can assess the impact that a given treatment may be having on the quality of the organic matter.

Table 3.10. Delineation of Fluorescence Regional Integration Volumes

Region ID	Excitation–Emission Range	Description
Region I	$EX_{240\text{ to }300}$–$Em_{280\text{ to }390}$	microbial byproducts, proteins, biopolymers
Region II	$EX_{240\text{ to }300}$–$Em_{390\text{ to }580}$	fulvic-like compounds
Region III	$EX_{300\text{ to }470}$–$Em_{300\text{ to }580}$	humic-like compounds

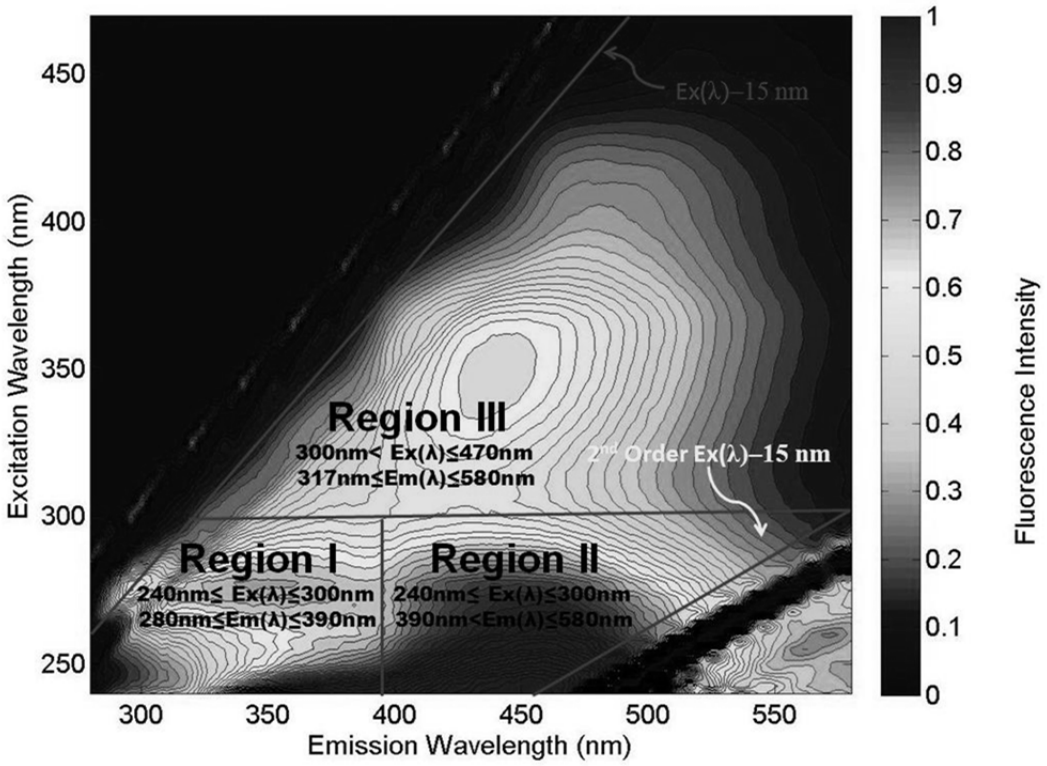

Figure 3.3. A fluorescence excitation–emission matrix image with outlined boundaries for integration regions and data collection.

3.6.2 Total Organic Carbon Analysis

For dissolved organic carbon (DOC) and total organic carbon (TOC) analysis, samples were collected into glass vials, acidified to a pH less than 3 with hydrochloric acid, and filtered through a 0.45 µm hydrophilic polypropylene filter (GHP Acrodisk, Pall Life Sciences). A Shimadzu (Shimadzu Scientific Instruments, Carlsbad, CA) TOC/total nitrogen analyzer was used for quantification.

3.6.3 UV_{254} Absorbance and Specific Ultraviolet Absorbance

Sample absorbance at 254 nm was measured using a Perkin-Elmer Lambda 45 UV-VIS spectrometer, consistent with Standard Method 5910 B. Specific UV_{254} absorbance (SUVA; $L \cdot m^{-1} \cdot mg^{-1}$) was calculated based on the following equation: $SUVA=TOC/UV_{254} \cdot 100$.

3.6.4 Dissolved Ozone

Dissolved ozone was measured using the indigo method (4500-Ozone-B; Clesceri et al., 1998; Rakness et al., 2010) and a Hach D-2000, UV/Vis spectrometer (Hach, Loveland, CO). Potassiumindigotrisulfonate was obtained from Sigma Aldrich (St. Louis, MO), potassium monobasic phosphate, American Chemical Society grade, was obtained from Fisher (Thermo Fisher Scientific, Waltham, MA). Concentrated phosphoric acid was obtained from JT Baker (Avantor Performance Materials, Phillipsburg, NJ).

3.6.5 Hydrogen Peroxide

A Hach Model HYP-1 Hydrogen Peroxide Test Kit (as H_2O_2) was used to measure hydrogen peroxide.

Chapter 4

Full- and Pilot-Scale Occurrence of Nitrosamines and Perfluoroalkyl and Polyfluoroalkyl Substances

This chapter discusses occurrence of nitrosamines and PFASs in full-scale wastewater treatment plants. Samples were collected throughout the treatment process from participating utilities, with special focus on before and after ozonation, secondary treatment, and BAC. Samples were also collected before and after chlorination, chloramination, and UV for comparison with ozonation. Analysis was completed for nitrosamines and PFASs in order to determine general occurrence in the treatment plant and changes in concentration associated with different treatment processes.

4.1 Full- and Pilot-Scale Sites

Samples were collected before and after secondary treatment, ozonation, chlorination, chloramination, UV, and BAC from the treatment trains of participating utilities. These samples were analyzed for nitrosamines and PFASs.

4.2 Nitrosamines

Out of the seven nitrosamines, four (nitrosomethylethylamine, nitrosodiproplyamine, nitrosodibutylamine, nitrosodiphenylamine) were not detected at any of the nine participating utilities. NDMA and NMOR occurred the most frequently at six sites each. Nitrosodiethylamine was detected at one site, E-GA.

For three sites (A-MO, B-KY, and D-GA), NDMA or NMOR decreased after secondary treatment (Figure 4.1). B-KY uses an oxidation ditch, whereas the other two utilities employ conventional activated sludge. No change was noticed for other sites because nitrosamines in the influent were below the reporting limit. A decrease in NDMA concentration after secondary treatment has also been reported elsewhere. Krauss et al. (2009) surveyed 21 wastewater treatment plants in Germany using activated sludge, and Sedlak et al. (2005) reported on a California wastewater treatment plant using activated sludge.

At four of six full-scale sites (A-MO, D-GA, E-GA, and F-QLD) utilizing ozone (applied O_3 doses were typically low, <2 mg/L), NDMA was higher after ozone treatment (Figure 4.2). The degree of formation is also reported in Table 4.2. For the other two sites utilizing ozone, B-KY and C-TX, NDMA was not detected in any sample. An increase of NDMA after ozone treatment was also observed at the City of Las Vegas (CLV) pilot operation (WW1 and WW2 in Table 4.1). A few other studies report an increase in NDMA concentration after ozonation during full-scale (Hollender et al., 2009; Yoon et al., 2011; Zimmermann et al., 2011) and pilot-scale (City of Reno, 2010) wastewater treatment. In addition, changes in NDMA concentration were monitored at a pilot site in California (WW4) between April and November 2011. This treatment train receives secondary effluent from full-scale treatment and uses ozone before MF membrane. Figure 4.3 shows an increase in NDMA after ozonation. NDMA formation ranged from

30 to 143 ng/L during 8 months. NDMA also increased with chloramination at H-CA, which uses MF before RO. Chloramination is performed just before MF to reduce membrane fouling. Unlike ozonation and chloramination, there was no observable change in NDMA after chlorination and UV treatment at I-NV and J-NV. This is consistent with literature on NDMA formation with various oxidants (Lee et al., 2007a; Mitch and Sedlak, 2002; Nawrocki and Andrzejewski, 2011; Pehlivanoglu-Mantas et al., 2006).

NMOR was detected at Sites A-MO and B-KY in this study (Figure 4.4, Table 4.2) and at relatively high concentrations in another study (Krasner et al., 2009). There was no formation associated with ozone for the full-scale treatment sites in this study or others (Hollender et al., 2009; Zimmermann et al., 2011).

Table 4.1 shows a summary of the sampling sites. The Appendix provides full-scale treatment process diagrams, descriptions, sampling location information, and data tables.

Table 4.1. Utilities and Treatment Trains Evaluated in This Study

Utility ID	Location	Flow (MGD)	Pretreatment[a]	3º Treatment/ Disinfection	Ozone Dose (mg/O_3/ Mg/DOC)	Effluent Total N (mg/L)	Raw Water Sampling Dates
A	MO, USA	30	1º clarifier, CAS; N/partial DN	O_3	1	12	Oct. 10, 2011, May 1, 2012
B	KY, USA	10	oxidation ditch	O_3	1	4.4	March 6, 2012
C	TX, USA	10	1º clarifier, PACT process	O_3–BAC	0.3	4	October 31, 2012
D	GA, USA	43	1º clarifier, CAS; GF/UF; N/partial DN	O_3–BAC–O_3	0.4	15	February 1, 2012
E	GA, USA	5	CAS, COAG	O_3	1	21	April 16, 2012
F	QLD, AUS	2	1º clarifier, CAS,; N/partial DN	O_3–O_3–BAC–O_3	2.0, 0.6–0.8	4.2	May 15, 2012
H	CA, USA	70	1º clarifier, CAS, DN; N	MF–RO–UV/H_2O_2	N/A	1.2	October 10, 2011
I	NV, USA	75	1º clarifier, BNR, GF; N/partial DN	chlorine	N/A	20	March 28, 2012
J	NV, USA	100	1º clarifier, BNR, COAG, GF; N/partial DN	UV, chlorine	N/A	13	March 28, 2012
Pilot	CLV NV, USA	0.032	1º clarifier, MBR; partial N	O_3	1	12–19	N/A
Pilot	CA, USA	0.032	1º clarifier, BOD removal	O_3	0.7±0.2	57	N/A

Notes: BAC=biologically activated carbon; BNR=biological nutrient removal; BOD=biological oxygen demand; CAS=conventional activated sludge; COAG=coagulation; DN=denitrification; DOC=dissolved organic carbon; GF=gravity filtration; MBR=membrane bioreactor; MF=microfiltration; N=nitrification; N/A=not applicable; PACT=powdered activated carbon treatment; RO=reverse osmosis; UF=ultrafiltration; UV=ultraviolet.

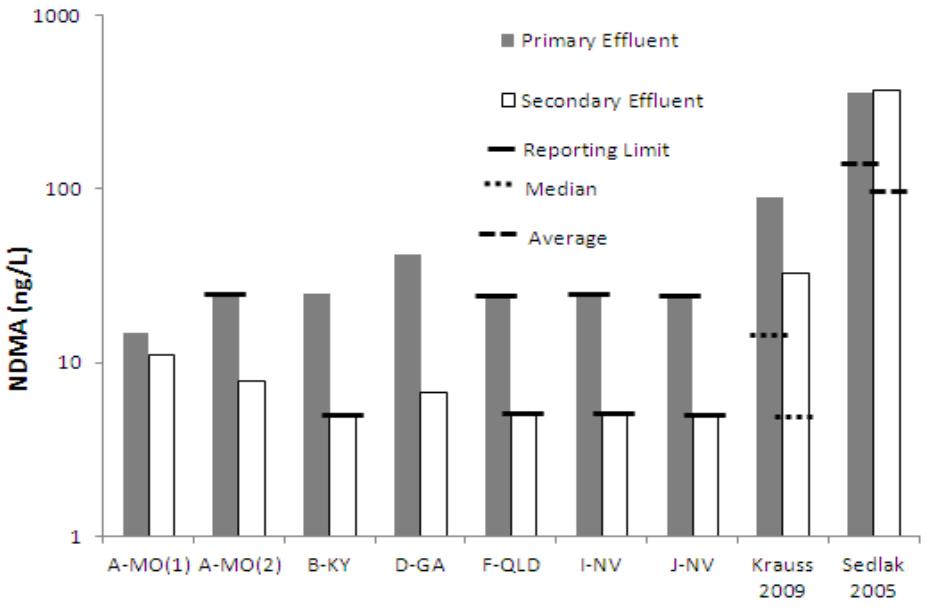

Figure 4.1. Change in NDMA concentration after full-scale secondary treatment.

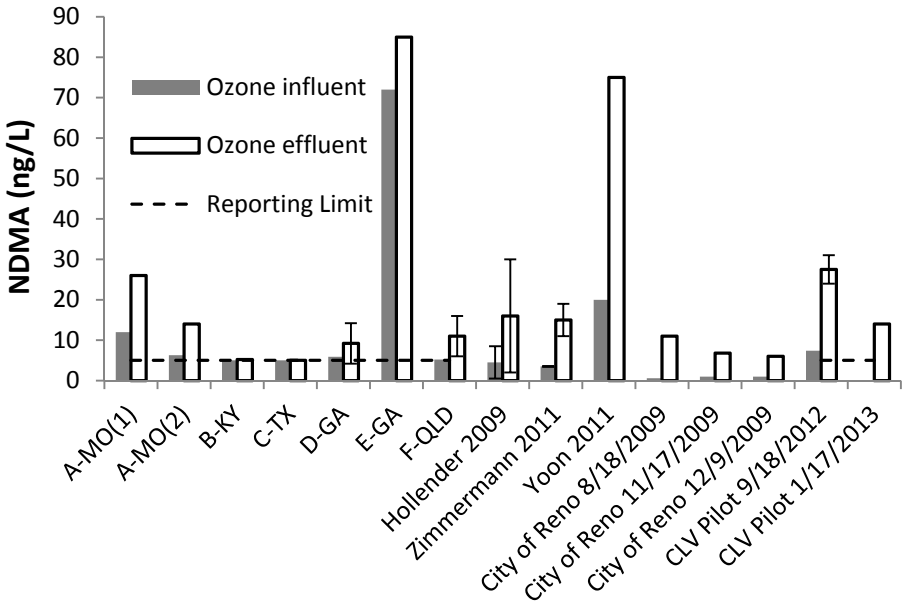

Figure 4.2. NDMA concentration before and after ozone in full- and pilot-scale (City of Reno and CLV Pilot) treatment.

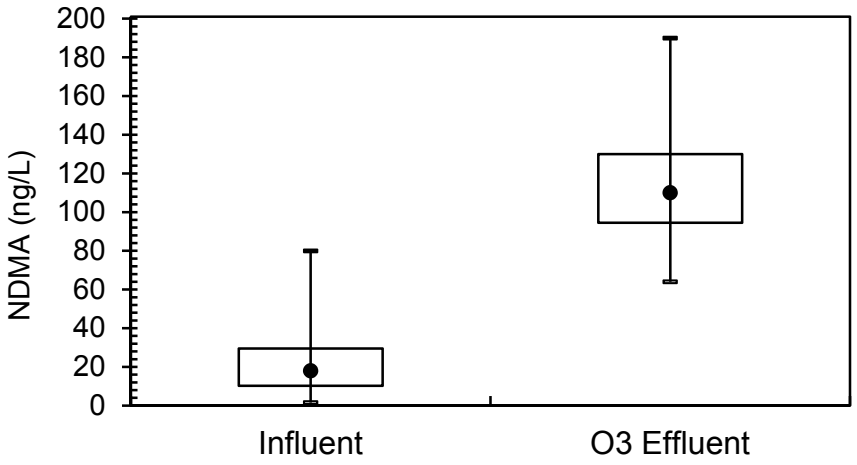

Figure 4.3. Changes in NDMA concentration from April–November 2011 at the California pilot treatment plant listed in Table 4.1.

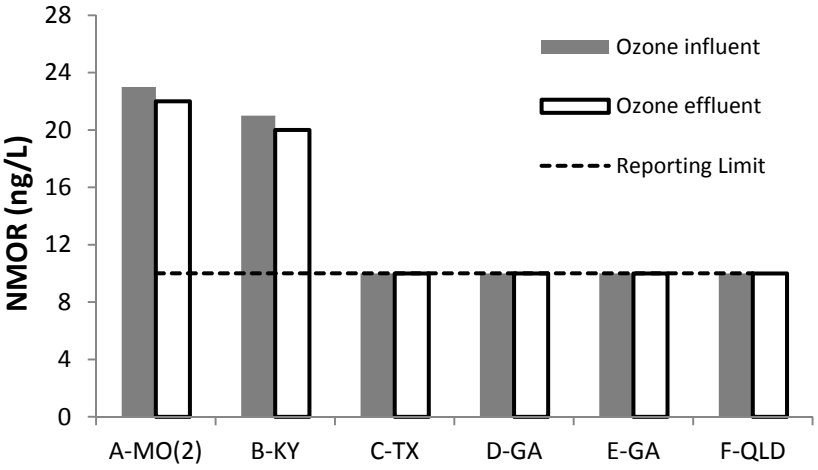

Figure 4.4. NMOR concentration before and after ozone in full-scale treatment.

Table 4.2. Selected Nitrosamine Data (ng/L)

Utility	Sampling Location	NDMA (ng/L)	NDMA Change	Nitrosomorpholine (ng/L)
A-MO(1)	Primary effluent	15	*–4*[e]	<5.0
October 2011	Secondary effluent	11		12[b]
	Combined ozone influent	12	*+14*[a]	12
	Ozone effluent	26		8.8
A-MO(2)	Primary effluent	<25		58
May 2012	Secondary effluent	7.8		22[e]
	Combined ozone influent	6.3	*+7.7*[a]	23
	Ozone effluent	14		22
B-KY	Oxidation ditch influent	25	*–>20*[e]	67
	Final clarifier effluent	<5	*+>0.2*[a]	21[e]
	Ozone effluent	5.2		20
C-TX	Primary effluent	< 25		< 25
	PACT effluent	<5.0		<5.0
	Filter effluent	<5.0		<5.0
	Ozone effluent	<5.0		6.3[a]
	BAC effluent	<5.0		7.6
D-GA	Primary effluent	42	*–35.2*[e]	<50
	Secondary effluent	6.8		<10
	Preozone influent	5.9	*+3.3*[a]	<10
	Preozone effluent	9.2	*–>4.2*[d]	<10
	BAC effluent	<5		<10
	Post-ozone effluent	<5		<10
(bench)	Primary effluent	25	*–14*[e]	<10
(bench)	Secondary effluent	11		17
E-GA	CAS influent	59	*+13*[b]	<50
	Pre-O_3/postclarifier	72	*+13*[a]	<10
	Post-ozonation	85		<10

Utility	Sampling Location	NDMA (ng/L)	NDMA Change	Nitrosomorpholine (ng/L)
F-QLD	Secondary effluent	<5.0	*+>0.4*[a]	<10
	Ozone 1 effluent	5.4	*+5.6*[a]	<10
	Ozone 2 effluent	11	*–>6.0*[d]	<10
	BAC effluent	<5.0		<10
	Ozone 3 effluent	<5.0		<10
H-CA	Microfiltration influent	16	*+26*[c]	6.9
	Microfiltration effluent	42	*–22*[d]	7.5[e]
	RO permeate	20		<5.0[d]
	RO concentrate	100		18
	UV/H_2O_2 effluent	<2.5		<5.0
I-NV	Secondary effluent	<5.0		11
	Post-chlorine	<5.0		<10
J-NV	Prechlorine	<5.0		13
	Post-chlorine	<5.0		11
	Post-UV	<5.0		<10
K-CA (pilot)	Ozone influent (median)	18	*+92*	-
	Ozone effluent (median)	110		-
CLV WW1 (pilot)	No ozone	7.4	*+20.1*[a]	<10
	O_3:toc=1.0	27.5		<10
CLV WW2 (pilot)	No ozone	<5.0	*+>9.0*[a]	<10
	O_3:toc=1.0	14		<10

Notes: -=data not available; a=increase associated with ozonation; b=increase associated with secondary treatment; c=Increase associated with chloramination; d=decrease associated with BAC and RO; e=decrease associated with secondary treatment; BAC=biologically activated carbon; CAS=conventional activated sludge; NDMA=N-Nitrosodimethylamine; PACT=powdered activated carbon treatment; RO=reverse osmosis; TOC=total organic carbon; UV=ultraviolet

4.3 Perfluoroalkyl and Polyfluoroalkyl Substances

PFASs were detected at all sites. The most commonly occurring PFASs were PFPnA, PFHxA, PFHpA, PFOA, PFNA, PFDA, PFBS, PFHxS, PFOS, and the precursor 6:2 FtS. Ten PFASs (PFUnA, PFDoA, PFDS and precursors N-EtFOSAA, 4:2 FTUCA, 6:2 FTUCA, 8:2 FTUCA, 10:2 FTUCA, 4:2 FtS, and 8:2 FtS) were detected at only one site or not at all. The highest levels were found at E-GA. Concentrations were two orders of magnitude higher at this site than at other sites. Site E-GA receives wastewater impacted by a textile industry, which could be the cause for the high PFAS levels because these chemicals may be used on clothing for waterproofing (ATSDR, 2009). Significant concentrations were also present in the digester supernatant at B-KY. Elevated PFASs concentrations in the digester supernatant indicate that PFASs adsorb to sludge and subsequently desorb during digestion.

Apparent increases and decreases of PFAA concentrations from treatment processes were observed; some were slight changes. In the following discussion of results, a 3 ng/L change in concentration was used as the criteria for observing increasing and decreasing trends.

For Sites A-MO, D-GA, E-GA, I-NV, and J-NV, PFAA concentrations increased for PFPnA, PFHxA, or PFOA following secondary treatment. The formation could be due to biological transformation of precursors or mass accumulation of these recalcitrant PFAAs during secondary treatment (Boulanger et al., 2005; Plumlee et al., 2008a; Schultz et al., 2006; Sinclair and Kannan, 2006). A mass balance evaluation around secondary treatment would need to be performed to help determine this hypothesis. Contrary to observed trends at these sites, at Site F-QLD five PFAA concentrations decreased, and PFOS decreased at B-KY and I-NV.

Several PFAAs, particularly PFHxA, PFOA, and PFBS, showed a systematic increase in concentration after ozonation at three utilities: A-MO, B-KY, and D-GA; however, no PFAA formation was apparent from ozonation at F-QLD or E-TX. In addition, there appears to be a slight increase in PFHxA after chlorination for I-NV and J-NV. UV treatment had no effect on PFAA formation or destruction.

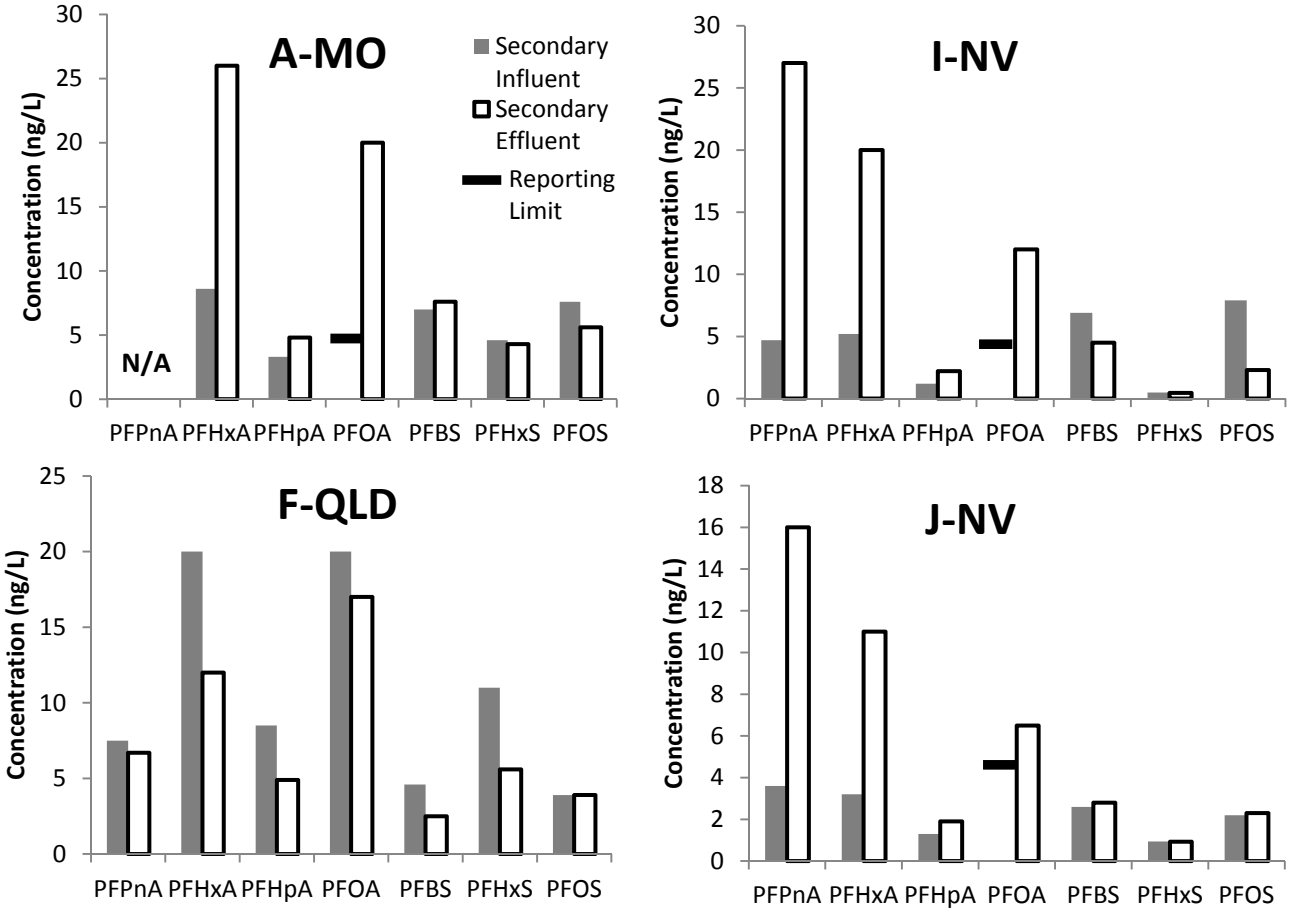

Figure 4.5. PFAAs in full-scale treatment: effects of biological treatment.

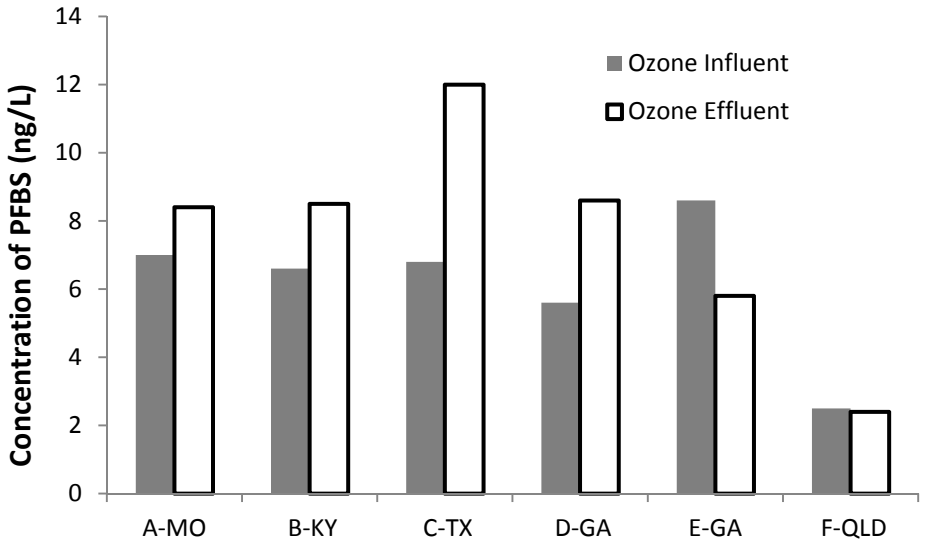

Figure 4.6. PFBS in full-scale treatment before and after ozonation.

Table 4.3. Selected PFAA Data (ng/L)

Utility	Parameter (units) Sampling Location	PFPnA (ng/L)	PFHxA (ng/L)	PFHpA (ng/L)	PFOA (ng/L)	PFBS (ng/L)	PFHxS (ng/L)	PFOS (ng/L)
A-MO(1)	Primary effluent	<20	3.2	1.8	<5.0	2.2	4.3	2.5
	Secondary effluent	15	15[a]	2.4	14[a]	2.5	3.8	4.1
	Combined O_3 infl.	16	15	3.2	15	3.5	3.7	4.8
	Ozone effluent	18	17	4.2	16	5.2	4.2	9.5[b]
A-MO(2)	Primary effluent	<40	8.6	3.3	<5.0	7	4.6	7.6
	Secondary effluent	18	26[a]	4.8	20[a]	7.6	4.3	5.6
	Combined O_3 infl.	17	24	5	19	7	4.7	6.5
	Ozone effluent	17	28[b]	5.1	20	8.4	5.1	7.4
B-KY	Oxidation ditch inf.	<40	3.5	2.3	<5.0	6.2	2.9	5.3
	Final clarifier effluent	10	5.6	1.2	<5.0	6.6	2.8	0.82[d]
	Ozone effluent	13[b]	9.3[b]	1.8	8[b]	8.5[b]	3.7	1.2
	Digester supernatant	160	60	11	100	50	<5.0	2.7
C-TX	Primary effluent	<2.0	<0.50	<0.50	<5.0	<5.0	<0.25	<5.0
	PACT effluent	40	14	2.0	15	4.1	.91	2.3
	Filter effluent	43	14	2	18	6.8	1.4	3.6
	Ozone effluent	41	14	1.8	18	12[b]	1.3	3.3
	BAC effluent	44[c]	16[c]	3.3	24[c]	17[c]	1.6	3.1

Utility	Parameter (units) Sampling Location	PFPnA (ng/L)	PFHxA (ng/L)	PFHpA (ng/L)	PFOA (ng/L)	PFBS (ng/L)	PFHxS (ng/L)	PFOS (ng/L)
D-GA	Primary effluent	7.4	<10	<10	<100	4.3	0.87	3.2
	Preozone influent	26[a]	18[a]	4.5	23	5.6	0.81	3.8
	Preozone effluent	27	22[b]	3.9	26[b]	8.6[b]	1.1	4
	BAC effluent	28	22	5	33[c]	9.6	1	3.5
	Post-ozone effluent	26	21	4.9	35[b]	13[b]	1.1	3.7
(Bench)	Primary effluent	<40	5.4	1.8	<5.0	<5.0	0.57	<5.0
(Bench)	Preozone influent	29	17[a]	3.4	20[a]	8.2[a]	1	5.4
E-GA	CAS influent	900	590	310	93	7.1	1.3	6.3
	O_3 infl. (clar. Effl.)	2900[a]	1100[a]	930[a]	220[a]	8.6	5.1[a]	22[a]
	Ozone effluent	2800	1100	760	190	5.8	4.3	24
F-QLD	Primary effluent	7.5	20	8.5	20	4.6	11	3.9
	Secondary effluent	6.7	12[d]	4.9[d]	17[d]	2.5[d]	5.6[d]	3.9
	Ozone 1 effluent	6.6	12	4.2	16	2.4	5.5	3.7
	Ozone 2 effluent	7.3	13	5	16	3.5	5.4	0.83
	BAC effluent	7.9	17[c]	7.2	32[c]	4.6	6.9	0.97
	Ozone 3 effluent	8.4	17	7.5	32	5.6	7.8	1.8
I-NV	Primary effluent	4.7	5.2	1.2	<5.0	6.9	0.49	7.9
	Secondary effluent	27[a]	20[a]	2.2	12[a]	4.5	0.45	2.3[d]
	Post-chlorine	26	23[b]	2.9	12	5.1	0.52	4.5
J-NV	Primary effluent	3.6	3.2	1.3	<5.0	2.6	0.94	2.2
	Secondary effluent	16[a]	11[a]	1.9	6.5	2.8	0.93	2.3
	Prechlorine/UV	13	10	2	7.7	5	1.3	3.7
	Post-chlorine	16[b]	13[b]	2.3	7.4	6.9	1.3	3.9
	Post-UV	13	9.6	1.9	7.3	6	1.3	4

Notes: a=increase associated with secondary treatment; b=increase associated with ozonation; c=increase associated with BAC; d=decrease associated with secondary treatment; BAC=biologically activated carbon; CAS=conventional activated sludge; PACT=powdered activated carbon treatment; UV=ultraviolet.

4.4 Summary

The occurrence of nitrosamines and PFASs in full-scale wastewater treatment plants was discussed and resulted in the following conclusions:

- Out of the seven nitrosamines monitored, NDMA and NMOR occurred the most frequently.
- Four nitrosamines (nitrosomethylethylamine, nitrosodiproplyamine, nitrosodibutylamine, and nitrosodiphenylamine) were not detected at any of the nine participating utilities. Nitrosodiethylamine was detected at one site, E-GA.
- For three sites (A-MO, B-KY, and D-GA), NDMA, NMOR, or both decreased after secondary treatment. This has also been reported for full-scale treatment plants in Germany and California.

- NDMA was higher after ozone treatment for several full- and pilot-scale treatment plants in this study and others.
- NDMA increased with chloramination at H-CA, but there was no observable change in NDMA after chlorination and UV disinfection for I-NV and J-NV.
- NMOR levels did not change during ozone treatment in this study and others, which suggests that NMOR is neither formed nor transformed during ozone treatment.
- PFASs were detected at all sites. The most commonly occurring PFASs were perfluoroalkylacids with a chain length of ten carbons or fewer.
- High PFAS levels were found at E-GA, which receives wastewater impacted by a textile industry. Concentrations were two orders of magnitude higher at E-GA than at other sites.
- Significant PFAS concentrations were present in the digester supernatant at B-KY, which indicates that PFASs adsorb to sludge and subsequently desorb during digestion.
- For several sites, PFAA concentrations increased for PFPnA, PFHxA, and PFOA following secondary treatment.
- Several PFAAs, particularly PFHxA, PFOA, and PFBS, showed systematic increasing concentrations after ozonation at some utilities, but not all.
- A slight increase in PFHxA was observed after chlorination for I-NV and J-NV. UV treatment had no effect on PFAA formation or destruction.

Chapter 5

Factors that Affect Nitrosamine Formation

This chapter discusses factors affecting the formation of the nitrosamines during ozonation. The results are broken down into three main focus areas: effects of ozone dosing, effects of the pretreatment and associated water quality parameters, and identification of principal oxidation agents. To identify critical parameters affecting NDMA formation from ozone, wastewater samples were collected from targeted participating facilities and pilot-scale systems encompassing various secondary biological treatment conditions.

5.1 Experimental Matrix

Bench-scale experiments were performed to examine factors that affect nitrosamine formation. Table 5.1 summarizes the experiments, which included ozonation of primary and secondary effluents to evaluate pretreatment, pH variation, O_3:TOC dose variation, hydrogen peroxide addition for ozone and hydroxyl radical oxidation, ozonation and tBA addition for ozone-only oxidation, and gamma radiolysis for hydroxyl radical–only oxidation.

Six wastewaters were chosen based on full-scale occurrence data and secondary treatment type, as shown in Table 5.2. Corresponding water quality parameters are shown in Table 5.3. WW1 and WW2 are from a pilot MBR plant that has been operated at distinctly different SRT and biological conditions (e.g., partial nitrification and nitrification), and WW3 is from a full-scale treatment plant (nitrification/partial denitrification/biological phosphorus removal). All three of these wastewaters use the same influent source; this was an attempt at direct comparison of NDMA formation as a result of different biological treatments.

Previous data (not shown) for WW4 (BOD removal plant) and full-scale data (Figure 4.2) for WW5 (nitrification) showed relatively high NDMA formation, making these interesting wastewaters to study. Full-scale data for WW6 (nitrification/partial denitrification) showed moderate NDMA concentrations (Figure 4.2). WW4 samples were collected over several hours starting in the morning until early afternoon to simulate a composite sample (24 hour composite sampling was not available). Primary influent (raw sewage after head works), primary effluent, and secondary effluent were collected. WW5 receives 95% of the influent flow (TOC of 120 mg/L) from a nearby industrial run-off. Ozone is used primarily for color removal. Because of such high TOC in the influent water and the large dilution factor required to achieve the targeted O_3:TOC ratios, only the secondary effluent was sampled for bench-scale ozone experiments.

Table 5.1. Experimental Matrices for Nitrosamine Bench-Scale Tests

Secondary Effluent Wastewater	Different O_3:TOC Ratios						
	pH=7						
	O_3:TOC ratio						
	0.10	0.20	0.30	0.40	0.50	0.75	1.0
WW1	x	x	x		x		x
WW2		x			x	x	x
WW3		x			x		x
WW4	x	x	x	x	x		x
WW5		x					x
WW6		x			x	x	x

pH Variation	
Secondary Effluent Wastewaters	WW1, WW3, WW4, WW5
pH:	6, 7, 8
O_3:TOC ratio (mg/mg):	0.2

H_2O_2 Addition		
pH=7, H_2O_2:O_3 ratio=1:0.5 M		
Secondary Effluent Wastewaters	O_3:TOC ratio	
	0.5	1.0
WW1	x	x
WW2		x
WW3	x	x
WW4		x
WW5		x
WW6		x

Pretreatment		
pH=7		
Primary Effluent Wastewaters	O_3:TOC Ratio	
	0.2	1.0
WW1	x	X
WW2	x	X
WW4	x	
WW6	x	X

Radiolysis		
pH=7, 1000 ppb pCBA		
Secondary effluent wastewaters	Dose	
	176 Gy	264 Gy
WW1	x	X
WW2	x	X
WW3	x	X

Notes: pCBA=parachlorobenzoic acid; Gy=gray; TOC=total organic carbon

Table 5.2. Wastewater and Treatment Process Description

Abbrev.	Location[a]	Secondary/Tertiary Treatment Type	SRT	Sampling Dates
WW1	I-NV	partial nitrification and microfiltration (MBR pilot)	4–6 days	August 1 and November 5, 2012
WW2	I-NV	nitrification, denitrification, and microfiltration (MBR pilot)	10–12 days	January 23, 2013
WW3	I-NV	nitrification, partial denitrification, biological phosphorus removal	8–12 days	August 20 and December 4, 2012
WW4		BOD removal	1–2 days	August 6, 2012
WW5	E-GA	conventional activated sludge	1–2 days	September 17, 2012
WW6	D-GA	nitrification, partial denitrification, ultrafiltration	5–10 days	October 4, 2012

Notes: [a]=these location IDs are for sites presented in Chapter 4; BOD=biological oxygen demand; MBR=membrane bioreactor; SRT=solids retention time

Table 5.3. Water Quality Parameters for Wastewaters

Parameter	Unit	WW1	WW2	WW3	WW4	WW5	WW6
COD	mg/L	54	<20	N/A	N/A	N/A	N/A
BOD	mg/L	<2	<2	6.0	N/A	7.2	N/A
Total P	mg/L	0.30	0.12	0.2	N/A	6.0	N/A
NH_4^+	mg/N/L	12.5	3.53	0.26	N/A	0.2	N/A
TKN	mg/N/L	16.0	4.2	<1.0	N/A	N/A	N/A
NO_3^-	mg/N/L	0.3	14.1	14.5	<1.0	N/A	N/A
Total nitrogen	mg/N/L	16.3	18.3	14.5	57	6.1	7.6
UV_{254}	a.u.	0.12	0.09	0.12	0.24	0.35	0.09
TOC	mg/C/L	6.1	4.5	5.1	14	17	4.1
SUVA	L/mg/m	2.09	1.92	2.27	N/A	N/A	N/A
TF	a.u	36,721	23,530	34,050	55,451	253,639	23,016
FI	a.u	1.55	1.62	1.73	1.53	1.03	1.47
TDS	mg/L	870	N/A	980	N/A	N/A	N/A

Notes: BOD=biological oxygen demand; COD=chemical oxygen demand; FI=fluorescence index; N/A=not available; P=phosphorus; SUVA=specific ultraviolet absorbance; TDS=total dissolved solids; TF=trickling filter; TOC=total organic carbon

5.2 Comparison of Water Quality for WW1–WW3

Samples were collected for bench-scale ozonation experiments for WW1 (November 5, 2012), WW2 (January 23, 2013), and WW3. Figure 5.1 shows changes in SRT and filtrate ammonia levels (NH_4^+) and indicates operational periods to produce WW1 and WW2. To produce WW1, an MBR pilot was operated such that the SRT was maintained at less than 6 days and hydraulic retention time (HRT) was approximately 4.4 hours. At these conditions, the influent ammonia decreased by approximately 50% in the filtrate. Filtrate for further bench-scale experiments with ozone was collected after at least one SRT had elapsed. For WW2, the MBR pilot was operated such that SRT was at least 15 days. Because of limited HRT, complete nitrification was not always possible.

Table 5.3 shows the water quality parameters for these three waters. WW2 was not completely nitrified, although it had significantly lower levels of NH_4^+, TKN, SUVA, and fluorescence. Therefore, it still presented a significantly different water quality than WW1. For WW3, which represents a secondary effluent after biological nutrient removal (BNR), it was completely nitrified; however, it was higher in SUVA and fluorescence than WW2. Figure 5.2 shows EEM for these wastewaters.

Ozone decay curves were completed during bench-scale experiments at various O_3:TOC ratios. Figures 5.3 and 5.4 show decay curves for WW1, WW2, and WW3 samples. These data were used to calculate ozone contact time (CT), which was plotted as a function of O_3:TOC for each wastewater and overlaid in a single plot, shown in Figure 5.5. Changes in ozone decay highlight the relative differences in water quality of these three wastewaters.

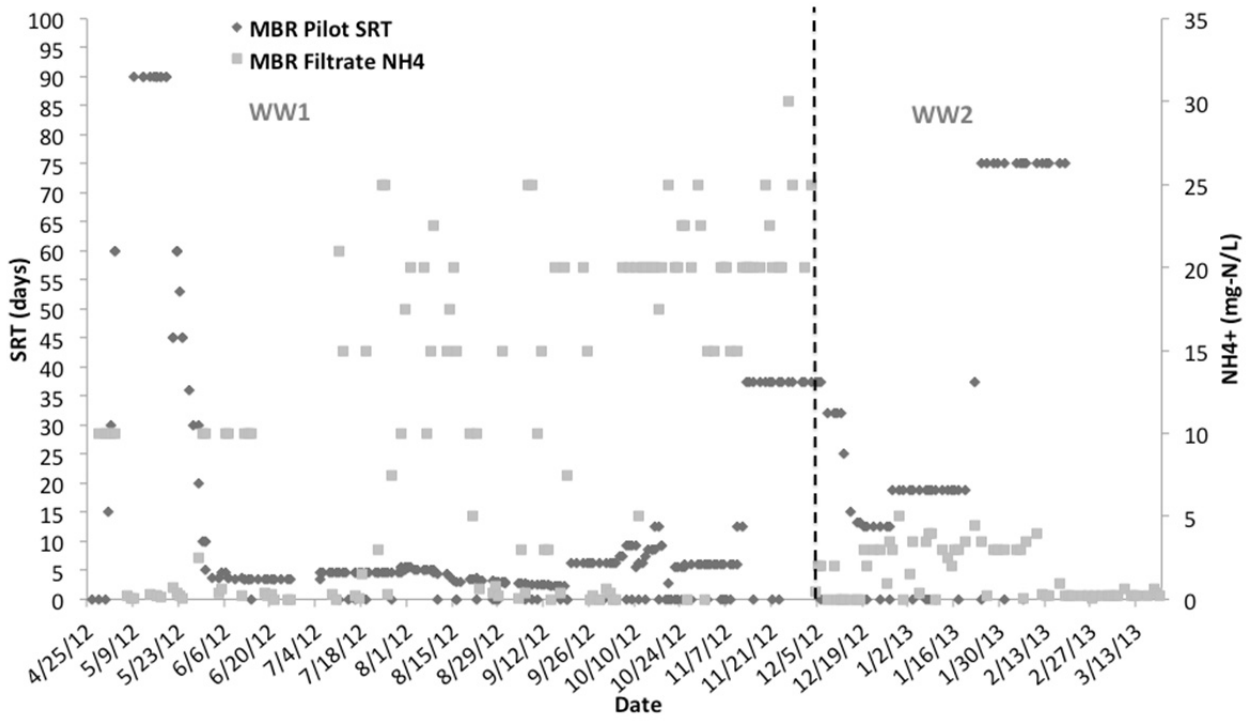

Figure 5.1. Changes in SRT and MBR filtrate NH_4^+ levels during MBR pilot operation.

Note: WW1 and WW2 were collected on 11/05/12 and 01/23/13, respectively.

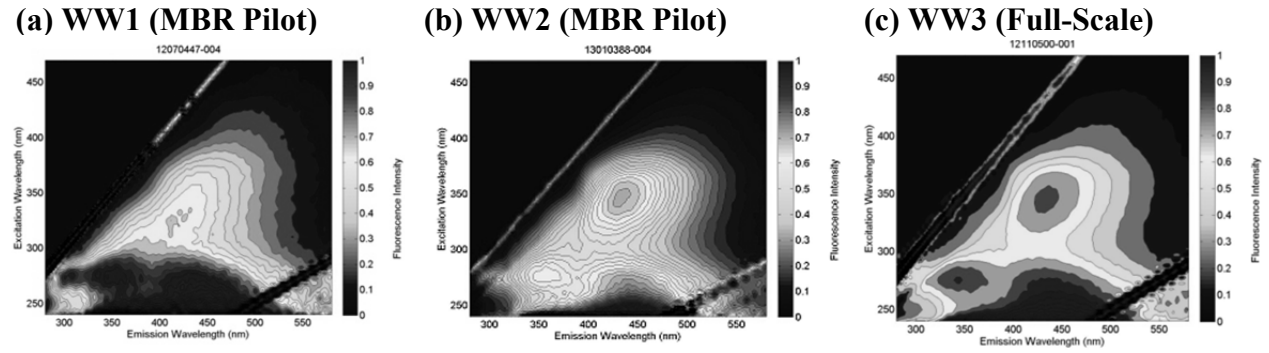

Figure 5.2. EEM of (a) WW1 and (b) WW2 produced by MBR pilot; and (c) WW3—secondary effluent from full-scale plant.

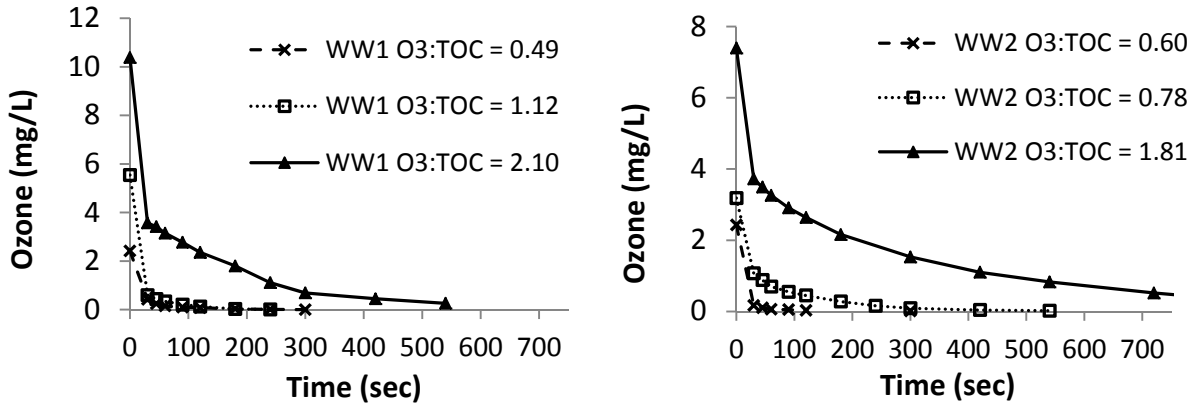

Figure 5.3. Ozone decay in WW1 and WW2 at various O_3:TOC ratios.

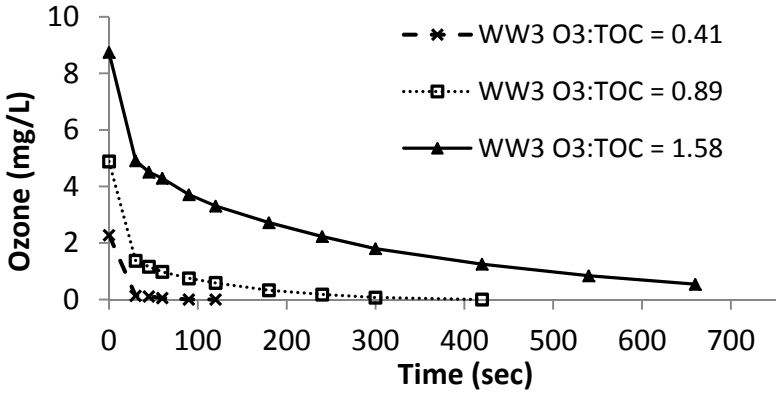

Figure 5.4. Ozone decay in WW3 at various O_3:TOC ratios.

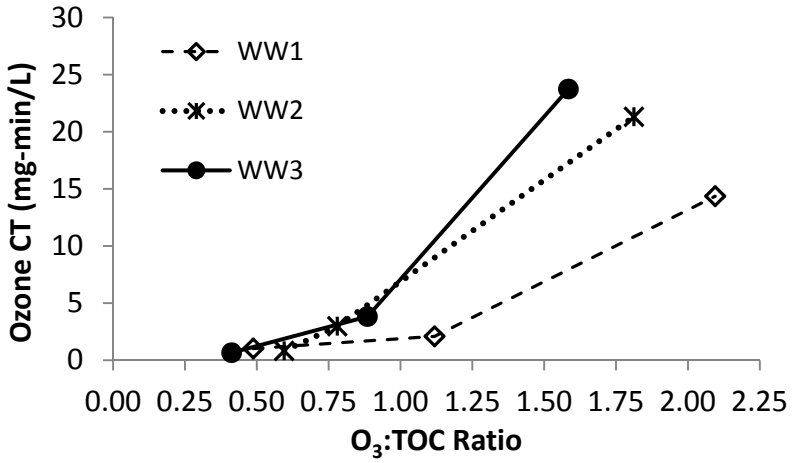

Figure 5.5. Ozone contact time CT (mg/min/L) in WW1, WW2, and WW3 at various O_3:TOC ratios.

5.3 Effect of Ozone Dose and pH on NDMA Formation

The wastewaters were ozonated at various O_3:TOC ratios to determine ozone–dose dependence of nitrosamine formation. A few wastewaters had measurable NMOR, NDEA, and NMEA, whereas NDMA was present for all wastewaters. Figure 5.6 shows formation of NDMA in six tested wastewaters. NDMA formation consistently increased with greater O_3:TOC ratios in all wastewaters. WW4 had the highest NDMA formation (55 ng/L) among the tested wastewaters, which may be due to a higher load of NDMA-forming precursors. It is interest that WW4 was the only nonnitrified wastewater. The formation of NDMA in partially and completely nitrified wastewaters (WW1, WW2, WW3, WW5, and WW6) reached near the maximum NDMA formation (8–17 ng/L) at an O_3:TOC ratio of 0.50. Formation after ozonation was minimal or did not occur for the other nitrosamines. NMEA in WW1 was below the reporting limit in the ambient sample; a slight formation (up to 8 ng/L) was observed when ozonated at O_3:TOC>0.30 (Table 5.4). This occurred on one sampling occasion; however, no NMEA was detected on a second sampling occasion. NDEA was detected in WW5 when ozonated at O_3:TOC=1.0. NMOR was present in three wastewaters (WW3, WW4, and WW6) but did not increase with greater O_3:TOC ratios. Compared to NDMA, these nitrosamines did not show a strong formation with ozonation.

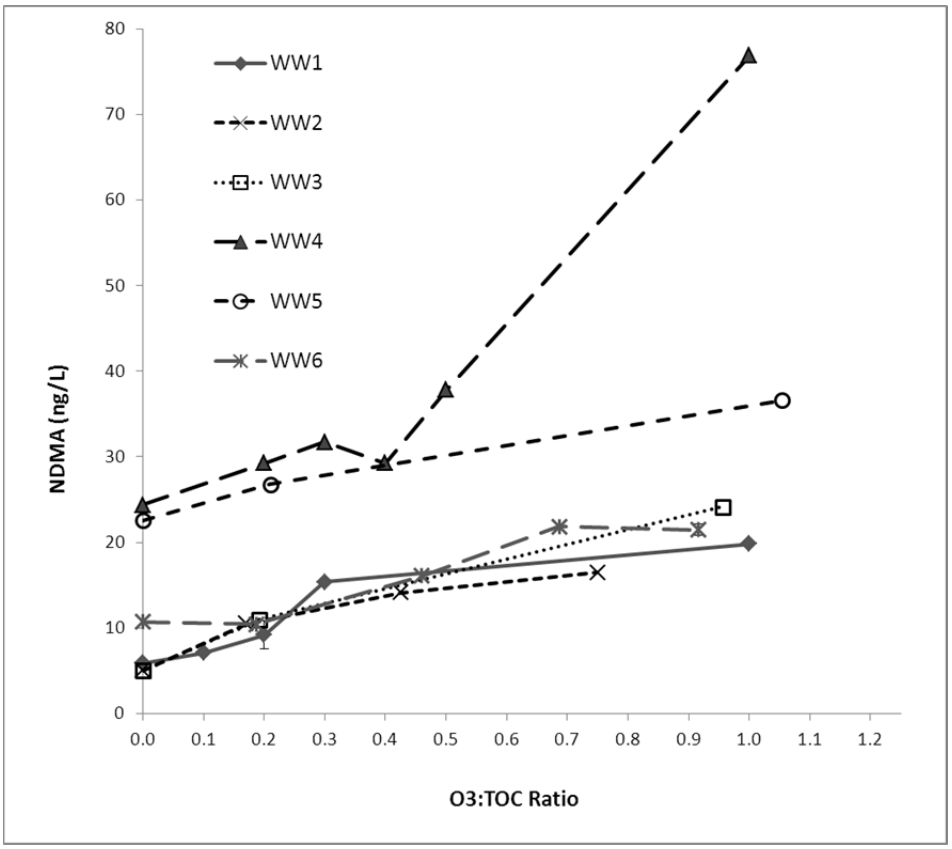

Figure 5.6. Formation of NDMA in wastewaters at various O_3:TOC ratios.

To investigate the effects of pH, separate WW1, WW3, WW4, and WW5 samples were adjusted to pH 6, 7, and 8 using HCl or NaOH and followed by the addition of ozone at a single O_3:TOC ratio of 0.20. Addition of ozone at pH 7 condition was done in triplicate. Figure 5.7 shows these results. From pH 6 to 8, there appears to be a slightly increased formation of NDMA. These data suggest that adjusting the pH will not be a useful mitigation strategy within this pH range.

Table 5.4. Changes in NMEA, NDEA, and NMOR After Ozonation

	WW1	WW5	WW3	WW4	WW6
O_3:TOC Ratio	NMEA ng/L	NDEA ng/L	NMOR ng/L	NMOR ng/L	NMOR ng/L
(no ozone)	<5.5	<14	12	<12	17
0.10	<5.5	<14		<12	
0.20	<5.5		12	<12	16
0.30	6.0			12	
0.40				<12	
0.50				<12	14
0.75					14
1.0	7.4	18	<11	13	13
1.0/H_2O_2	7.9	17	<11		16

Notes: TOC=total organic carbon; refer to Table 2.3 for definitions of abbreviations.

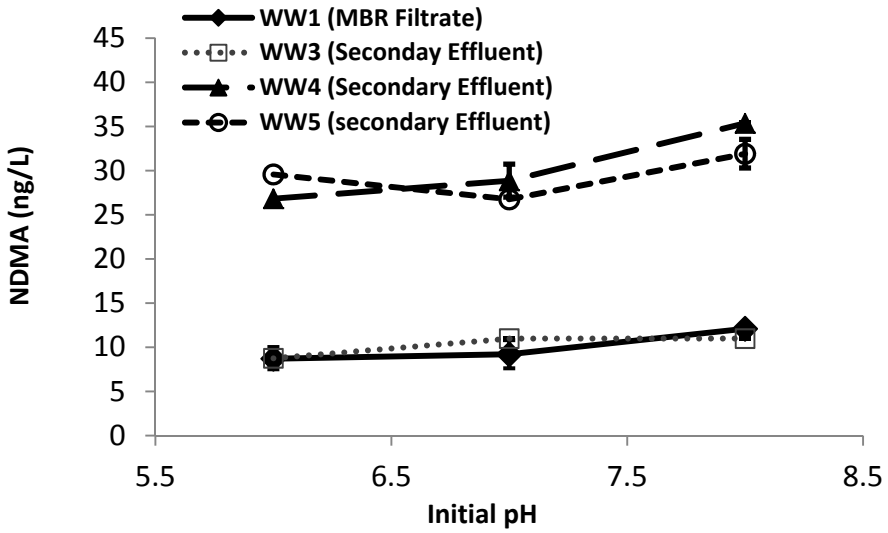

Figure 5.7. Formation of NDMA at various initial pH at the same O_3:TOC ratio of 0.20.

Note: Error bars based on n=3.

5.4 Effects of Pretreatment

The purpose of this section was to investigate changes in NDMA precursor concentrations during primary and secondary treatment processes of the selected wastewaters. Primary and secondary effluent samples were ozonated at the same O_3:TOC ratios to determine the NDMA formation potential and how it changes between treatment processes.

For all five wastewaters, ambient levels of NDMA were lower in the secondary effluent than in the primary effluent. This indicates that some of the NDMA was attenuated through secondary treatment. WW4 has the smallest change in ambient NDMA (26% reduction) and also the least extensive secondary treatment. NDMA is biodegradable (Sharp et al., 2005), so attenuation is expected, and a reduced level of secondary treatment should correspond with less biodegradation.

For most wastewaters, less NDMA formation was observed in the ozonated secondary effluent as compared to the primary effluent (Figures 5.8 through 5.10). This indicates that NDMA precursors were removed during secondary treatment, which is consistent with previous research (Krauss et al., 2010). Although WW4 and WW1 have a reduced level of secondary treatment, the lower NDMA formation in the ozonated secondary effluent suggests partial degradation of NDMA precursors. Specifically comparing WW1 and WW2, which have the same influent source and different water quality, the poorly nitrified WW1 had the lowest CT values (Figure 5.5) at similar O_3:TOC ratios, and it was slightly higher in NDMA formation than WW2 at an O_3:TOC of 1.0. The relatively small difference in results depicted by Figure 5.11 suggests that if partial nitrification is achieved, then NDMA precursors are similarly mitigated; however, it is also possible that there is temporal variation in NDMA precursor concentration. WW3 did not have the same result as the other wastewaters. At the same O_3:TOC ratios, NDMA formation was similar between primary and secondary effluents, indicating a modest removal of NDMA precursors by the BNR process.

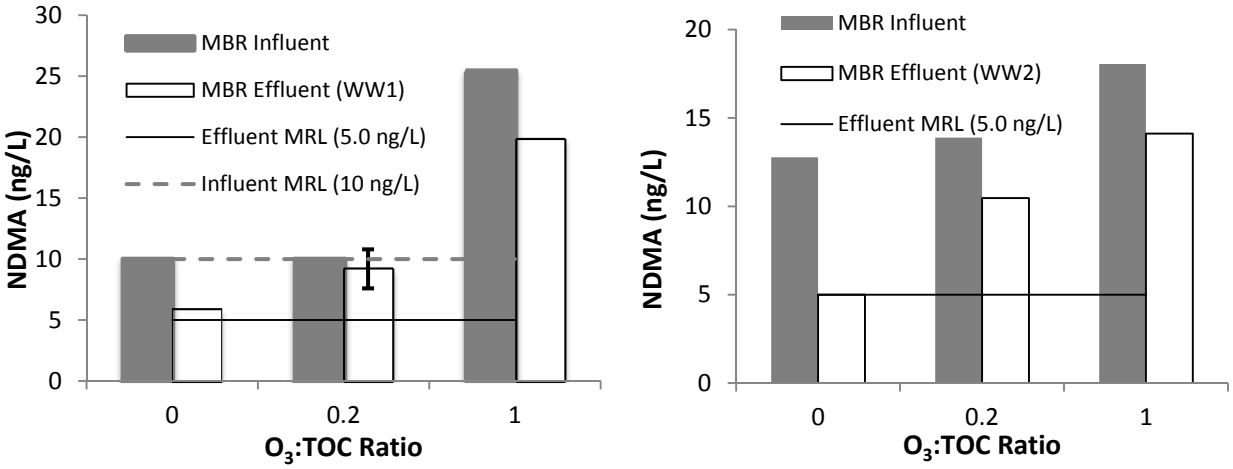

Figure 5.8. Ambient levels of NDMA in MBR influent and effluent (WW1 and WW2) and after addition of ozone at various O_3:TOC ratios.

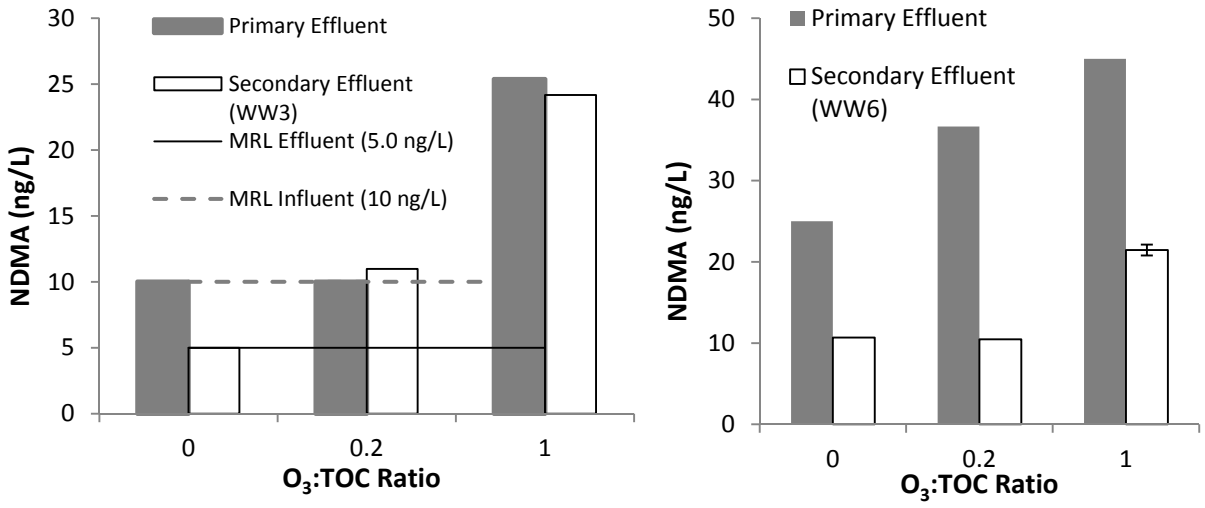

Figure 5.9. Ambient levels of NDMA in primary and secondary effluent (WW3 and WW6) and after addition of ozone at various O_3:TOC ratios.

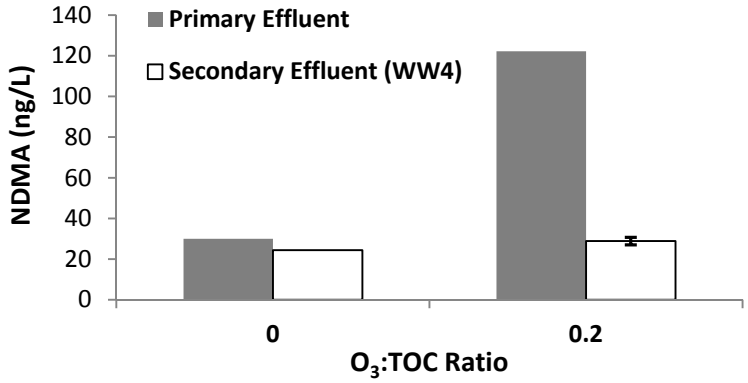

Figure 5.10. Ambient levels of NDMA in primary and secondary effluent (WW4) and after addition of ozone.

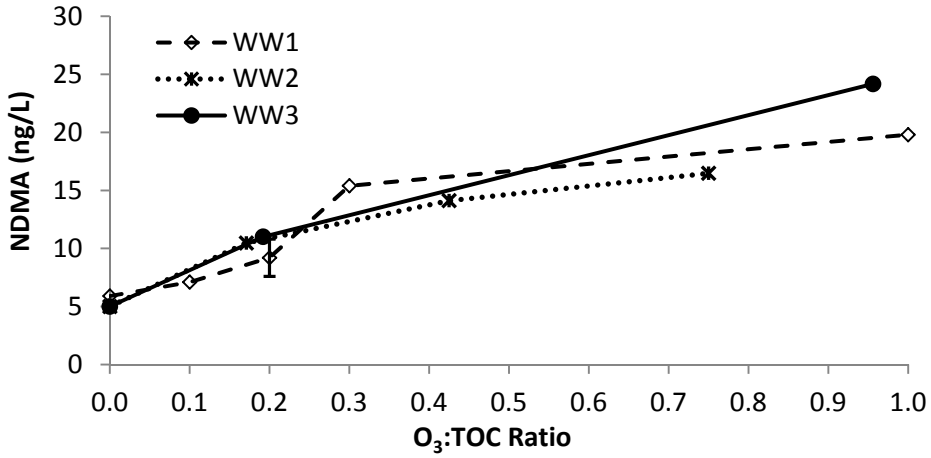

Figure 5.11. Formation of NDMA in WW1, WW2, and WW3 at various O_3:TOC ratios during bench-scale ozonation.

5.5 Impacts on Total Nitrosamine Formation

TONO analysis is a method to quantify all compounds in a sample with a nitroso group. In general, many nitrosamines are carcinogenic, but only a few are commonly measured. Many other nitrosamines may go undetected and unreported. For selected samples, TONO analysis was performed to determine if nitrosamines other than the standard seven (NDMA, NMOR, NMEA, NDEA, NDBA, NDPA, and NDPhA) were present. The reporting limit is very conservative, and TONO results underestimate the total nitrosamines in a sample because there are no corrections for recovery and reaction efficiency.

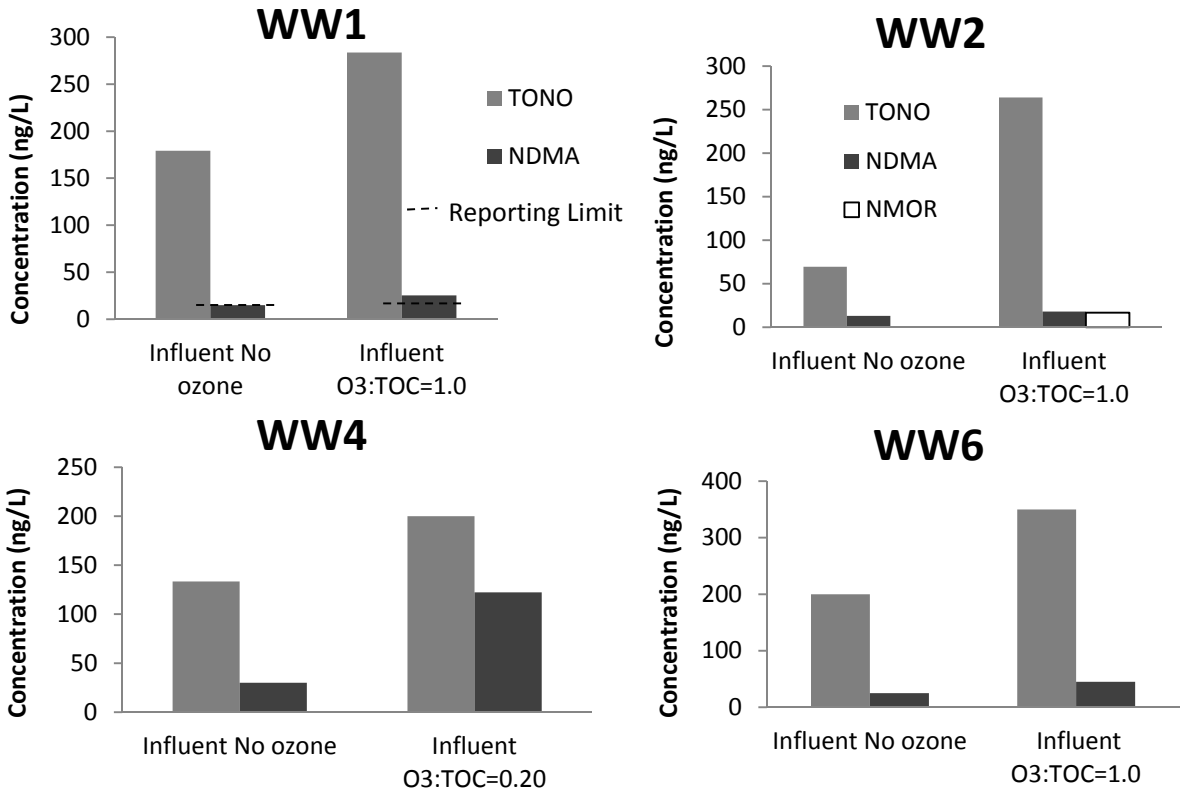

Figure 5.12. Comparison of total nitrosamines, NDMA, and NMOR for WW1, WW2, WW4, and WW6 secondary influent before and after ozonation.

NDMA and NMOR were detected using the standard analytical method, and these values were compared to the total nitrosamines measured using chemiluminescence (Section 3.3). For secondary influents, NDMA and NMOR combined made up a small fraction (9–22%) of the total nitrosamines, with the exception of the ozonated WW4 sample (61%). Based on this, a significant portion of the total nitrosamines in the influent consists of unknown nitrosamines (Figure 5.12). In secondary effluent samples, NDMA and NMOR combined were less than half of the total nitrosamines detected with TONO (Figure 5.13). For WW2, WW3, and WW4, the TONO result was below the reporting limit, and consequently, the fraction caused by NDMA and NMOR cannot be determined. With the exception of WW1, which had a reduced level of biological treatment, total nitrosamines were lower in the secondary effluent as compared to the influent. This suggests that nitrosamine precursors present in the influent are biodegraded during secondary treatment, which agrees with bench-scale results presented already in this chapter. TONO increased for WW4 and WW6 ozonated secondary effluents (O_3:TOC=0.50), which fits with ozonation bench-scale results; however, TONO decreased for WW1 and WW5 ozonated secondary effluents (O_3:TOC=0.20). Possible explanations for this are the presence of nitrosamines that are more susceptible to degradation with ozone as compared to NDMA and an ozone dose that was not sufficient for substantial nitrosamine formation.

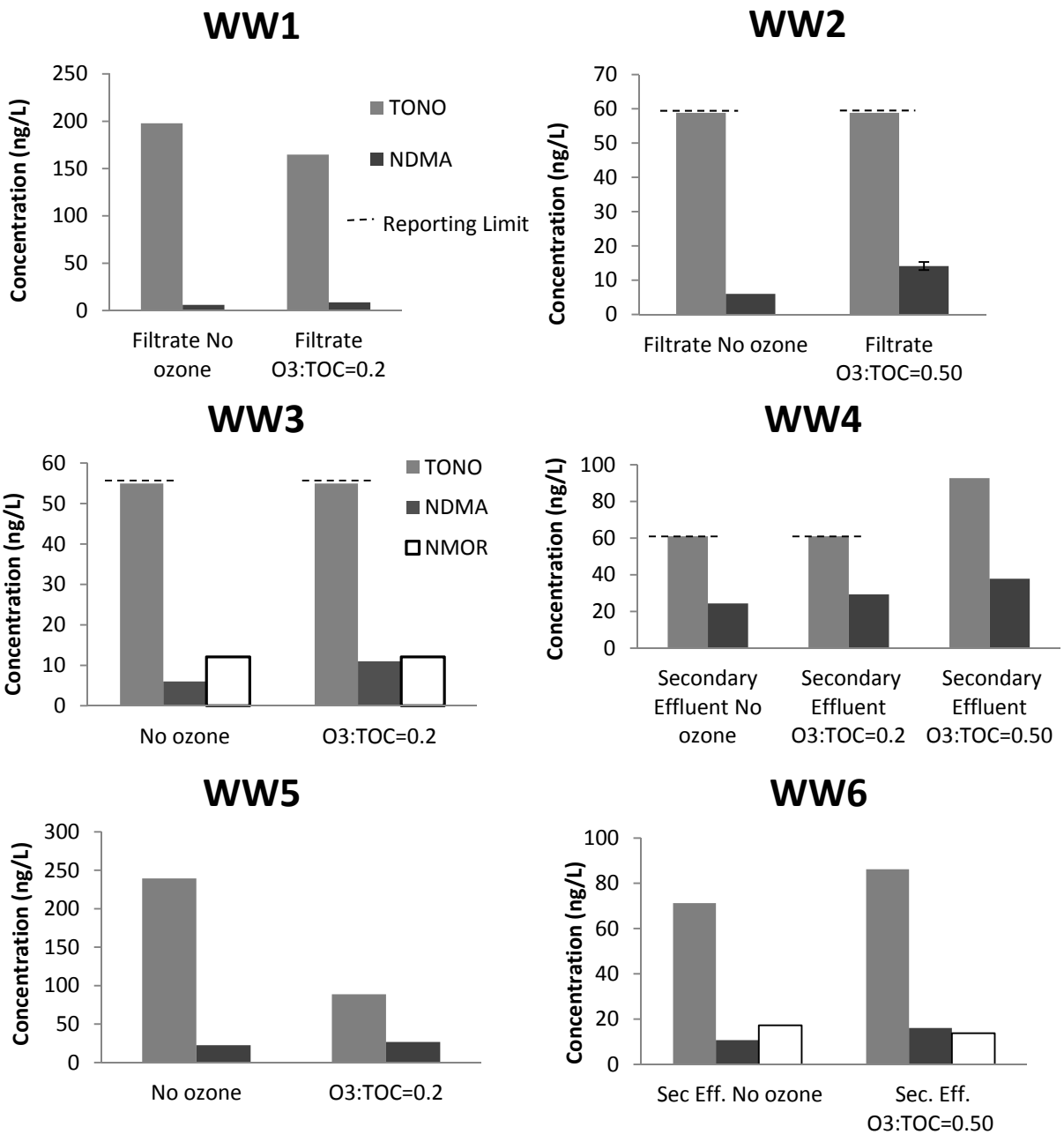

Figure 5.13. Comparison of total nitrosamines, NDMA, and NMOR for WW1–WW6 secondary effluent at various O_3:TOC ratios.

Note: Error bars based on n=3.

5.6 The Role of Ozone and Hydroxyl Radical in NDMA Formation

The objective of experiments described in the next sections was to determine whether dissolved ozone or •OH is responsible for the direct formation of nitrosamines during ozonation. Three wastewaters (WW1, WW2, and WW3) with varying secondary treatments were selected. The experimental matrix was divided into three components. In Part 1, pCBA was used to determine the overall •OH exposure with ozone and ozone/H_2O_2. In Part 2, tBA was added prior to ozone and ozone/H_2O_2 treatment. Because tBA is a strong •OH scavenger, this step isolated the effect of dissolved ozone by effectively scavenging all of •OH produced during decomposition of dissolved ozone. For Part 3, samples were spiked with pCBA for radiolysis experiments. In these experiments, only •OH was produced via exposure to gamma radiation. Change in NDMA concentration was measured for each sample before and after oxidant exposure. Specific experiments are described in greater detail below.

5.6.1 Ozone and Associated Hydroxyl Radical Exposure

A large number of published works describe decomposition of ozone in wastewater to be complex and typically involving many reactions. Hydroxyl radicals are produced during reactions of ozone, EfOM, and other water constituents. To assess the hydroxyl radical exposure, pCBA was spiked into samples and monitored for changes before and after ozonation at various O_3:TOC ratios. Prior to exposure to ozone, sample solutions were adjusted to pH 7.0 using solutions of HCl, NaOH, or both. Figure 5.14 shows decomposition of pCBA in WW1, WW2, and WW3 after ozone exposure at various O_3:TOC ratios.

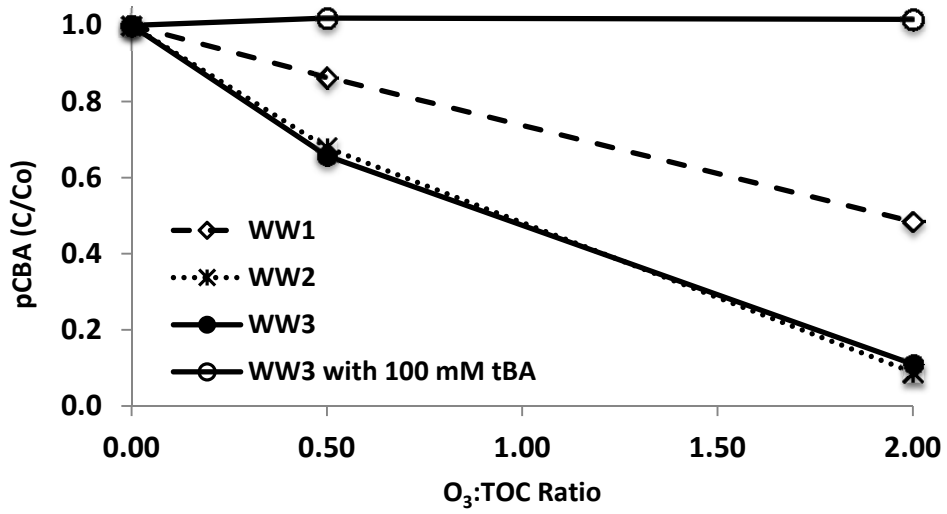

Figure 5.14. Decomposition of pCBA in WW1, WW2, and WW3 at various O_3:TOC ratios during bench-scale ozonation experiments.

Similar to results in the previous section describing how WW1 had the lowest ozone CT as compared to WW2 and WW3, the pCBA data show that effectively there is more •OH scavenging in WW1. With a more effective scavenging of •OH, degradation of various compounds (e.g., potential precursors) may be hindered. Note that with the addition of tBA at 100 mM, no pCBA degradation is observed, and effectively all of •OH is scavenged.

5.6.2 Effects of Addition of H_2O_2 on NDMA Formation

No significant differences in NDMA formation were observed between samples exposed to ozone only and samples exposed to ozone and hydrogen peroxide. Figure 5.15 shows formation of NDMA during ozonation with and without addition of hydrogen peroxide.

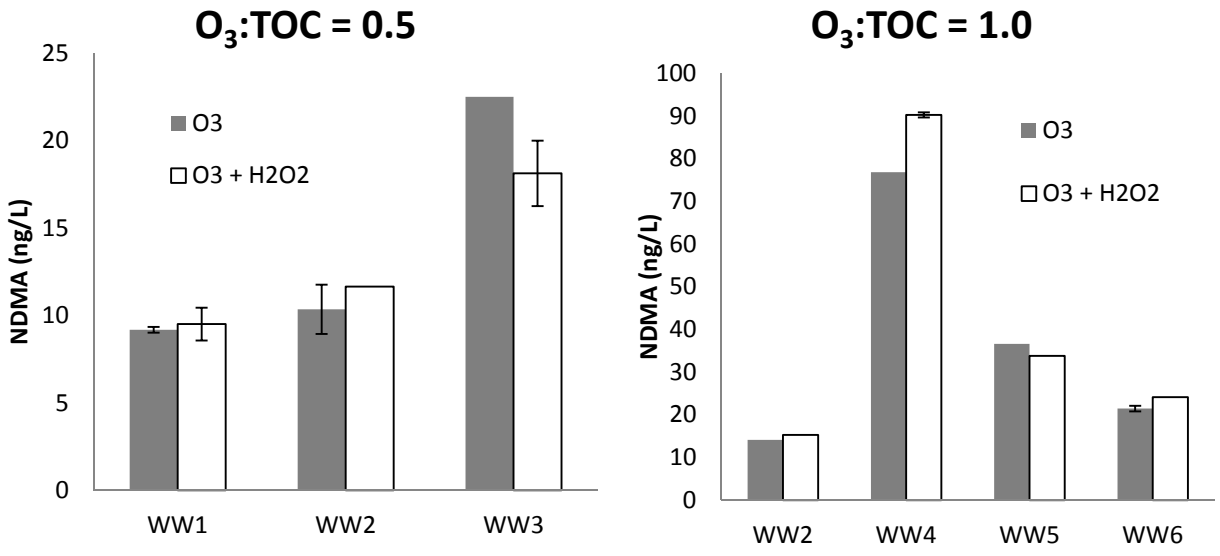

Figure 5.15. Formation of NDMA at the same O_3:TOC ratios (0.5 and 1.0), with and without addition of H_2O_2 at initial pH 7.

Note: Error bars based on n=2.

Because of significant •OH exposure already produced during ozone decomposition, the addition of hydrogen peroxide did not significantly increase the yield of •OH exposure, as shown by Table 5.5. Therefore, these results did not provide a definitive conclusion on relative contribution of ozone and hydroxyl radical to NDMA formation.

5.6.3 Effects of Molecular Ozone and Hydroxyl Radical

Results described in this section attempt to show evidence of primary oxidant species responsible for NDMA formation in wastewater. WW1, WW2, and WW3 were ozonated at approximately the same O_3:TOC ratio. A hydroxyl radical probe, pCBA, was spiked to achieve 1000 µg/L in wastewater samples; tBA was used to effectively scavenge hydroxyl radical exposure as a result of ozone decomposition. Initial experiments indicated there were no significant differences in NDMA formation in the ozonation (O_3:TOC ratio of 0.2) of WW1 samples with or without addition of tBA. At O_3:TOC=0.2 (without tBA), pCBA decreased only 10% in this matrix. The experiments were repeated at a higher O_3:TOC ratio of 0.5 in order to quantify expected differences in NDMA formation. This series of experiments was performed in duplicate.

Table 5.5. Hydroxyl Radical Exposure [•OH]ss (M•s) in WW1, WW2, and WW3 at Various O_3:TOC Ratios and with Addition of Hydrogen Peroxide

Sample Description	WW1	WW2	WW3
O_3:TOC=0.50	2.92E-11	7.76E-11	8.40E-11
O_3:TOC=0.50 (H_2O_2)	2.06E-11	6.68E-11	1.31E-10
O_3:TOC=2.0	1.45E-10	4.86E-10	4.41E-10
O_3:TOC=2.0 (H_2O_2)	1.76E-10	5.72E-10	5.32E-10

NDMA formation was monitored in samples with and without addition of tBA and H_2O_2 during the same ozone dosing at O_3:TOC ratio of 0.5 and adjustment of initial pH to 7 using a solution of HCl, NaOH, or both. As shown in Section 6.5.1, the tBA spike at 100 mM effectively scavenges all of •OH at an O_3:TOC of 2.0. Figures 5.16 and 5.17 show NDMA formation in WW1, WW2, and WW3 at various conditions. As discussed earlier, similar formation of NDMA was observed with and without addition of H_2O_2; however, significantly more NDMA was observed with the addition of tBA prior to ozonation. This result suggests that in fact NDMA formation is a product of ozone decomposition reactions. With addition of O_3/H_2O_2 and tBA spike, more NDMA was formed.

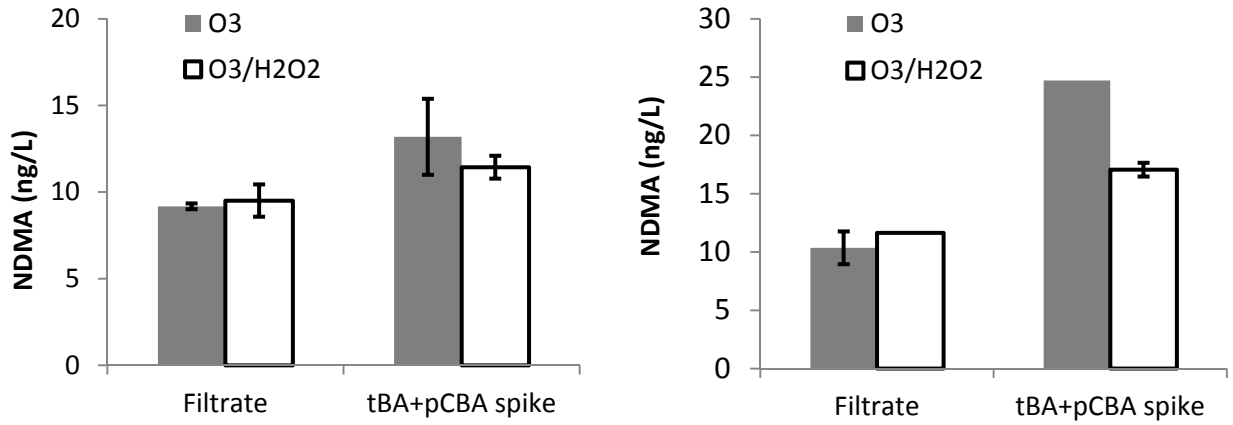

Figure 5.16. Formation of NDMA in WW1 and WW2 at the same O_3:TOC ratio of 0.5, with and without addition of H_2O_2, tBA, or both, and pCBA at initial pH 7.

Note: Error bars based on n=2.

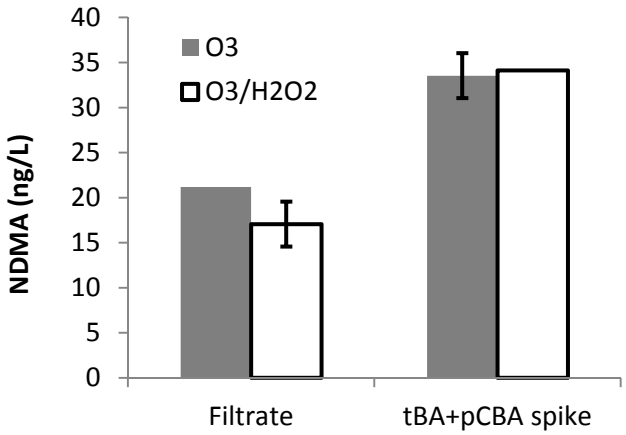

Figure 5.17. Formation of NDMA in WW3 at the same O_3:TOC ratio of 0.5, with and without addition of H_2O_2, tBA, or both, and pCBA at initial pH 7.

Note: Error bars based on n=2.

Effective scavenging of •OH radicals by tBA must have increased the available molecular ozone for reactions with unknown precursors, thereby resulting in more NDMA formation. In practice, these results suggest that wastewater with higher •OH scavenging may also lead to higher NDMA formation. Higher •OH scavenging is typically associated with a poorer wastewater quality.

Gamma radiation experiments targeted similar exposures that were generated during ozonation experiments. Changes in pCBA concentration were used to assess the •OH exposure ($[•OH]_{ss}$). Table 5.6 shows actual hydroxyl radical during radiolysis experiments. In general, the •OH exposures were quite comparable to those shown in Table 5.5.

For radiolysis experiments, there was no NDMA formation observed in any of the wastewater samples. This confirms that formation is due to reactions associated with molecular ozone. In addition, a control experiment was performed with NDMA spiked at 500 µg/L to assess NDMA degradation during these experiments, in order to verify that the radiolysis did not destroy NDMA at a rate possibly greater than it was formed. Figure 5.18 shows changes in NDMA concentration at various radiation doses. Even at the highest tested dose of 223 Gy, there was less than 4% degradation. Based on these results and those discussed in previous sections, it is evident that •OH is not responsible for NDMA formation and, though considerable •OH exposure may be generated during ozonation experiments, no significant degradation of NDMA is expected from •OH reactions.

Table 5.6. Hydroxyl Radical Exposure [•OH]ss (M•s) in WW1, WW2, and WW3 at Various Gamma Radiation Exposures

Radiation Dose (Gy)	WW1	WW2	WW3
88	6.01E-11	N/A	N/A
176	1.27E-10	7.61672E-10	6.83E-10
264	2.01E-10	1.37409E-09	1.07E-09

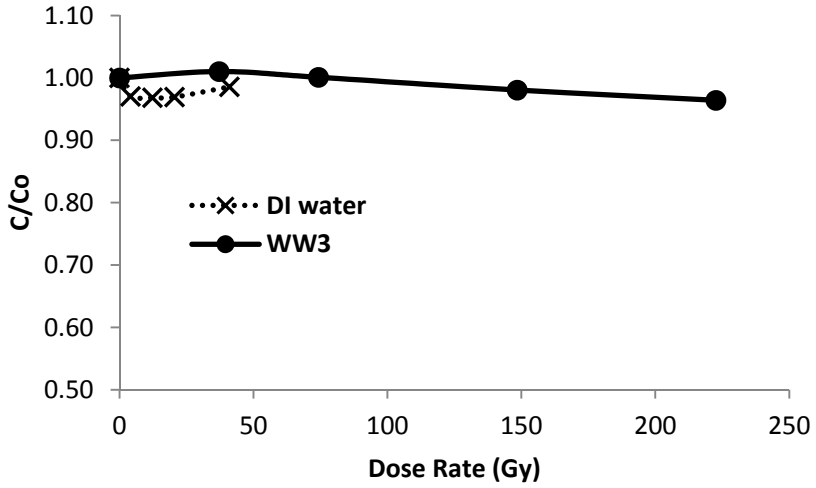

Figure 5.18. Changes in NDMA in DI water and WW3 during gamma radiation exposures.

5.7 Summary

Several factors affecting nitrosamine formation were studied and resulted in the following conclusions:

- The ambient level of NDMA and the level of NDMA formation at the same O_3:TOC ratio were lower in the secondary effluent than in the primary effluent. This indicates that the secondary treatment was effective in lowering NDMA as well as NDMA precursors.
- NDMA was the dominant nitrosamine formed during ozonation; however, TONO results suggest that NDMA may only be a fraction of total nitrosamines in the wastewater.
- Formation after ozonation was minimal or did not occur for the other nitrosamines, except slight formation of NMEA and NDEA was observed for WW1 and WW5, respectively.
- NMOR was detected in WW3, WW4, and WW6, but its level did not change during ozonation.
- NDMA formation during ozonation in non-nitrified wastewaters, such as WW4, was higher relative to wastewaters that had undergone a partial or complete nitrification process.

- NDMA formation during ozonation of wastewater is strongly dependent on the ozone concentration and continues to increase until ozone has been added in excess. At higher O_3:TOC ratios (e.g., O_3:TOC>0.5), NDMA formation typically was near its maximum.

- The hydroxyl radical is not responsible for NDMA formation, and this suggests that NDMA formation is due to reactions with molecular ozone.

- Degradation of NDMA caused by the hydroxyl radical is inefficient in wastewater.

- On the basis of controlled experiments with tBA, wastewaters with higher effective •OH scavenging may lead to higher NDMA formation during ozonation.

Chapter 6

Examination of NDMA Precursor Model Compound Structures

The objective of this task was to identify specific organic precursors that may contribute to the direct formation of NDMA by ozonation. Only a few precursors have been identified in the literature, and there is much to gain in understanding which compounds lead to NDMA formation. Information about precursors could be a tool for mitigation. If precursors can be identified, then specific strategies could be utilized to remove the precursors prior to oxidation.

6.1 Selection of Precursor Structures for NDMA

To narrow the scope of relevant nitrosamine precursors, NDMA was chosen as the single nitrosamine to study. Previous experimental research by the Project Team and the literature suggest that certain structures are more likely to form NDMA by ozonation. Preliminary tests were conducted with nitrogen-containing pharmaceuticals (atenolol, atrazine, carbamazepine, N,N-Diethyl-meta-toluamide, diclofenac, meprobamate, phenytoin, primidone, sulfamethoxazole, and trimethoprim) spiked at two to three orders of magnitude higher than the ambient occurrence levels in a fully nitrified secondary effluent. Compared to the background level, there was no additional NDMA formed after ozonation. Subsequently, the Project Team compiled a list of known and potential NDMA precursors. The focus was on compounds sharing similar structural moieties, such as a dimethyl amine group, hydrazine, sulfamide, hydrazone, and carbamate. The selected compounds contain the dimethylamine group and at least one other nitrogen, which forms the building block for NDMA. In some compounds, the building block is located on the end of the structure (e.g., DMSC), and for other compounds it is more centrally located (e.g., Atazanavir). In most compounds, DMA is bonded to the additional nitrogen; however, the carbamates have a CO_2 group separating the nitrogens. The precursors were identified using structure search tools for compounds available for purchase, which is not necessarily an indication of commercial or industrial use. Table 6.1 shows the new precursors selected by the Project Team.

6.2 Experimental Design for NDMA Precursors

Precursors were individually spiked into the test water at 32 to 100 μM. Bromide and hydrogen peroxide spikes were added to the samples next, as appropriate. Ozonated water was added to give a final concentration of approximately 1 mM (48 mg/L), which is at least a tenfold molar excess compared to the precursors. NDMA concentration was measured before and after ozone spike addition. The 50 mL samples were sealed and mixed after ozone addition and left undisturbed at room temperature overnight in the dark.

Chloramination formation potential (FP) tests were carried out as described in Section 3.6. 3. An LC–MS/MS method was used to quantitate NDMA. The MRL of the method used was 25 μg/L, thus allowing evaluation of molar yields in the range of 0.34 to 100%. Individual precursor concentrations were assumed based on prepared solutions and were not directly quantified. Molar yields were calculated as shown:

$$\text{Molar Yield (\%)} = 100 * [NDMA_{final}\ (\mu M)] / [Precursor_{initial}\ (\mu M)]$$

Table 6.2 summarizes the various experiments that were completed with the precursors.

6.3 NDMA Molar Yields

6.3.1 Molar Yields in Buffered Deionized Water

Figure 6.1 shows the molar yields of NDMA formed by ozonation of the various precursors in buffered DI water. Molar yields varied widely, from 0 to 78%. Error bars represent one standard deviation (n=2). There was no NDMA formation observed for Atazanavir and Streptozocin. Ozone may react with these compounds, but not in a manner that results in NDMA. As expected, DMS and DMA did not result in NDMA formation. DMS requires bromide (Schmidt and Brauch, 2008), which was not present in this test. DMA reacts with dichloramine to form NDMA, but ozonation of amines mainly results in the formation of aldehydes (Munoz and von Sonntag, 2000). A very low molar yield (<0.4%) for ozonation of DMA was shown by one group (Andrzejewski et al., 2008), but the reaction may have been due to nitrosation rather than ozonation.

Several of the proposed compounds do form NDMA by ozonation. The hydrazones, acetone DMH and 2-F-DMH, are similar to the known precursor UDMH. DMSC and DMTC-phenyl are similar to the known precursor TMDS. DMC-phenyl and DMC-dithio are related to DMS in that the nitrogen atoms are separated by a good leaving group (e.g., SO_2, CO_2). This is a new structure that has not been examined previously for NDMA formation; it appears that during ozonation the nitrogen atoms are joined as CO_2 leaves. Other carbamate pesticides may potentially be precursors.

Structure appears to make a difference in the overall molar yield. 2-F DMH had a higher conversion to NDMA than acetone dimethylhydrazone. This was expected because 2-F DMH has an electron donating group (furfural), whereas acetone dimethylhydrazone does not (Shen and Andrews, 2011). Electron donating groups and branched alkyl groups may lead to the formation of stable carbocations, which can increase NDMA formation (Selbes et al., 2013). Another hydrazone, dacarbazine, showed no NDMA formation, which could be due to ozone reacting preferentially at other sites to form compounds other than NDMA. DMSC and DMTC-phenyl have similarities but differ in the carbonyl (C=O) and thiol (C=S). Even when dividing the molar yield of DMSC by two in order to account for the two potential NDMA building blocks, DMTC-phenyl has a much lower yield. This could be due to a greater electron withdrawing effect by the thiol.

Table 6.1. Compounds Selected as Precursors for NDMA

Compound	Structure	Moiety	Notes
Acetone dimethylhydrazone (acetone DMH)		hydrazone+ DMA	synthesis building block
2-furaldehyde 2,2-dimethylhydrazone (2-F-DMH)	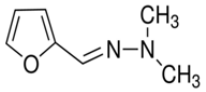	hydrazone+ DMA	synthesis building block
N-1-(3-{[(2,2-dimethyl hydrazino)carbonyl]amino}-4-methylphenyl)-2,2-dimethylhydrazine-1-carboxamide (DMSC)	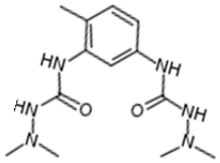	urea+DMA	no known uses
N-1-(4-methylphenyl)-2,2-dimethylhydrazine-1-carbothioamide (DMTC-phenyl)	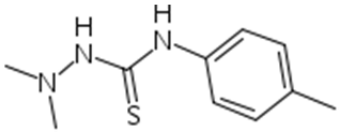	thiourea+ DMA	no known uses
N'-{[(dimethylamino) carbonyl]oxy}-4-(1,3-dithiolan-2-yl)benzenecarboximidamide (DMC-dithio)	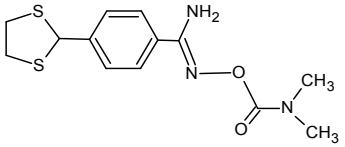	carbamate+ DMA	no known uses
N-{[(dimethylamino) carbonyl]oxy}-2-phenylacetamide (DMC-phenyl)	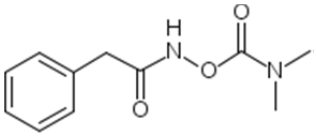	carbamate+ DMA	no known uses
Atazanavir	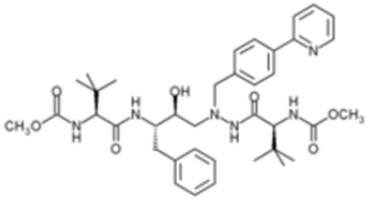	hydrazine (centrally located)	antiretroviral drug for HIV
Dacarbazine	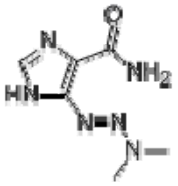	hydrazone+ DMA	antineoplastic agent for melanoma
Streptozocin	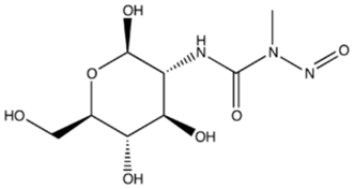	NDMA	antibiotic produced by Streptomyces achromogenes

Notes: DMA=dimethylamine; HIV=human immunodeficiency virus; NDMA=N-nitrosodimethylamine.

Table 6.2. Experiments Completed for NDMA Precursors

Precursors	Test Waters		Ozone Conc. (mM)	Bromide Spike			H_2O_2 Spike	Chloram. FP Test
	5 mM Phosphate Buffered DI Water	Secondary Effluent WW		0 (µg/L)	50 (µg/L)	1200 (µg/L)		
All 14	X		1	X	X	X		
		X	1	X	DMS only			
	X							X
TMDS and 2-F-DMH	X		1	X			X	
	X		0.1–1.5	X				

Notes: DI=deionized; DMS=dimethylsulfamide; FP=formation potential; TMDS=disemicarbazide; WW=wastewater.

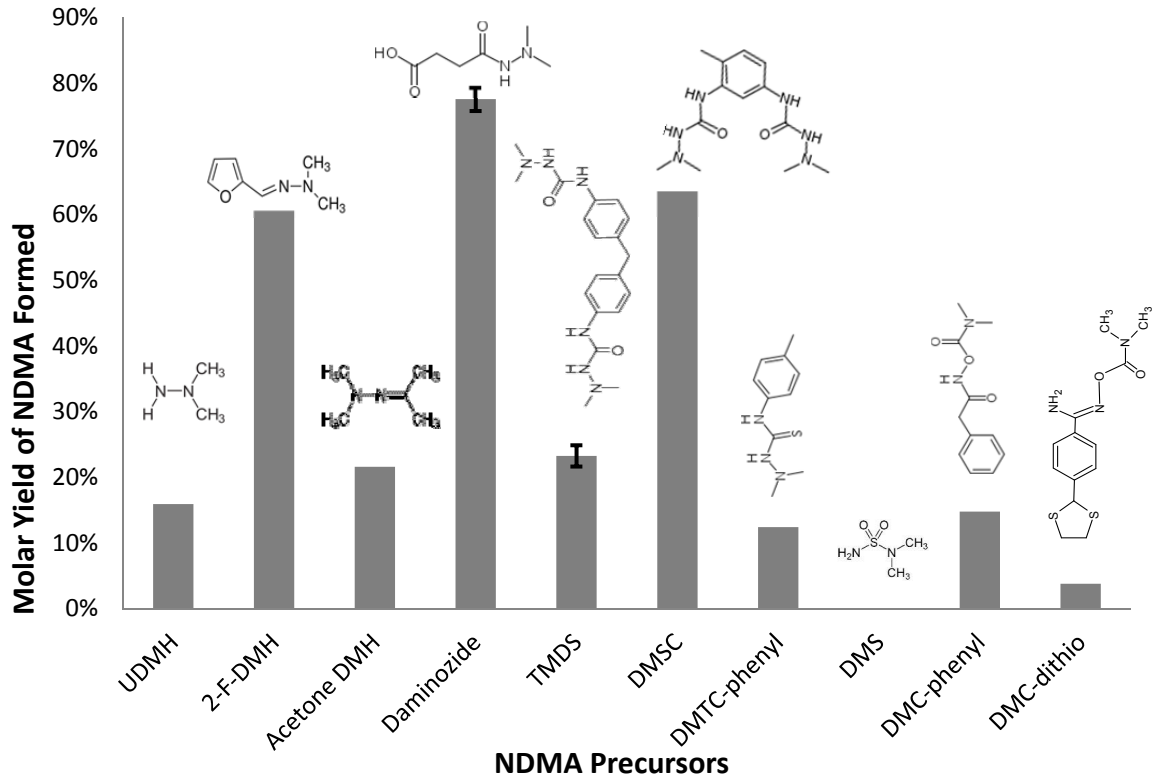

Figure 6.1. NDMA formation by ozonation (O_3=1 mM) of precursors in buffered DI water at pH 7.

Molar yields may also be affected by hydrolysis prior to ozonation (Padhye et al., 2013). Compared to previous studies, the molar yields for UDMH and DMS were much lower. Precursor stock solutions were

not prepared daily. Hydrolysis may have altered the precursors, which can explain the lower molar yields in this study.

6.3.2 Effect of Bromide on NDMA Formation

The ozonation bench-scale experiments in buffered DI water were repeated with two different bromide spikes. Figure 6.2 shows a plot of NDMA formation in buffered DI solutions at different starting bromide concentrations. Error bars represent one standard deviation (n=2). As seen in Figure 6.2, molar yields for some compounds are enhanced by bromide, whereas others remain constant. Although there is a slight decrease in molar yield for 2-F-DMH, Daminozide, and TMDS, this is probably the effect of increased ozone demand caused by the bromide spike. A greater ozone demand could result in lower NDMA formation.

As expected, there was considerably more NDMA formed in solutions of DMS containing higher initial bromide concentration. Bromide concentration was also significant for NDMA formation in solutions of UDMH and acetone DMH. DMC-phenyl and DMC-dithio did not show increased formation with bromide. This suggests that the reaction pathway for these compounds is different than the bromide-catalyzed, SO_2-leaving reaction for DMS. In general, it appears that there is not just one common reaction pathway for NDMA precursors that react with ozone.

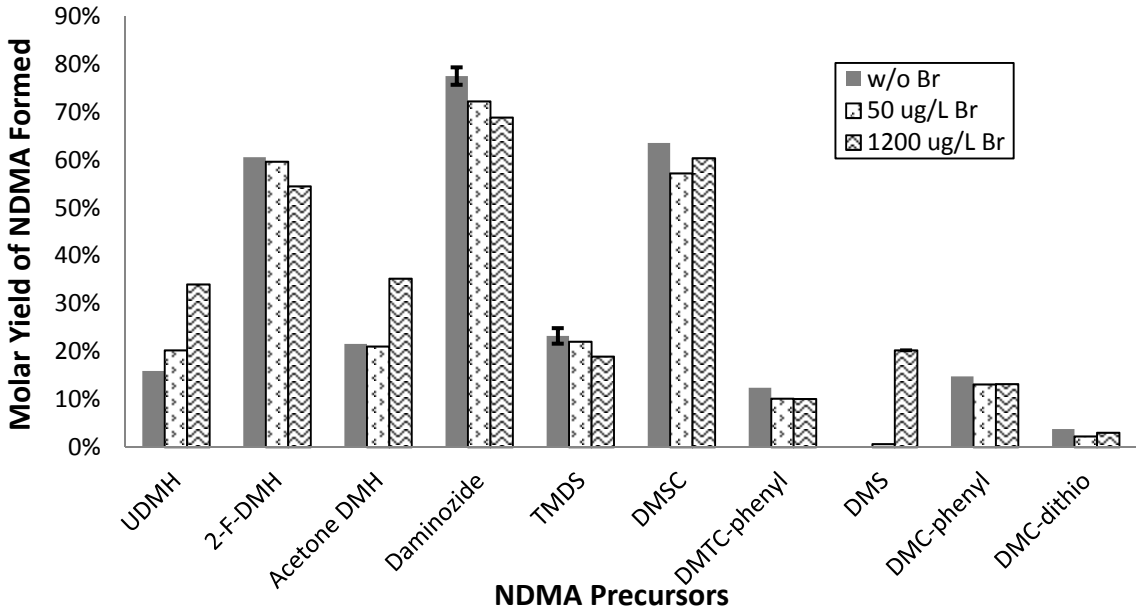

Figure 6.2. NDMA formation by ozonation (O_3=1 mM) in buffered DI water at pH 7 with bromide addition.

6.3.3 Molar Yields in Wastewater

NDMA formation was examined in a wastewater matrix using the same procedure (i.e., 32–100 µM precursors and 1 mM ozone). Tertiary treated wastewater was obtained from the MBR pilot-scale plant at I-NV. The final pH of the solution was near neutral (pH 6.7–7.1). Recovery for the matrix spike was 102%, and NDMA in the ozonated ambient wastewater was below the reporting limit. Results comparing NDMA formation in buffered DI water and wastewater are shown in Figure 6.3. Error bars represent one standard deviation (n=2).

NDMA formation was affected by the water matrix for a few compounds. It was anticipated that the ozone demand presented by the wastewater might decrease the NDMA molar conversion yields, but this was not seen. For four compounds (UDMH, acetone DMH, TMDS, and DMSC), the NDMA molar conversion yield was significantly greater in the wastewater matrix compared to phosphate-buffered DI water. This trend was also seen by a group of researchers comparing NDMA formation by ozonation of two dyes in river water and DI water matrices at pH 7 (Oya et al., 2008). Higher NDMA formation occurred in the river water matrix, and the low levels of bromide and nitrite could not account for this increase. At this time, no conclusions can be made regarding the constituents in wastewater that are responsible for increased formation; however, further research should assess the effects of ionic strength, effluent organic matter, and other ions (e.g., metals, bicarbonate, phosphate, nitrate, chloride, and sulfate ions). Table 6.3 shows a comparison of the molar conversions from this study and the literature.

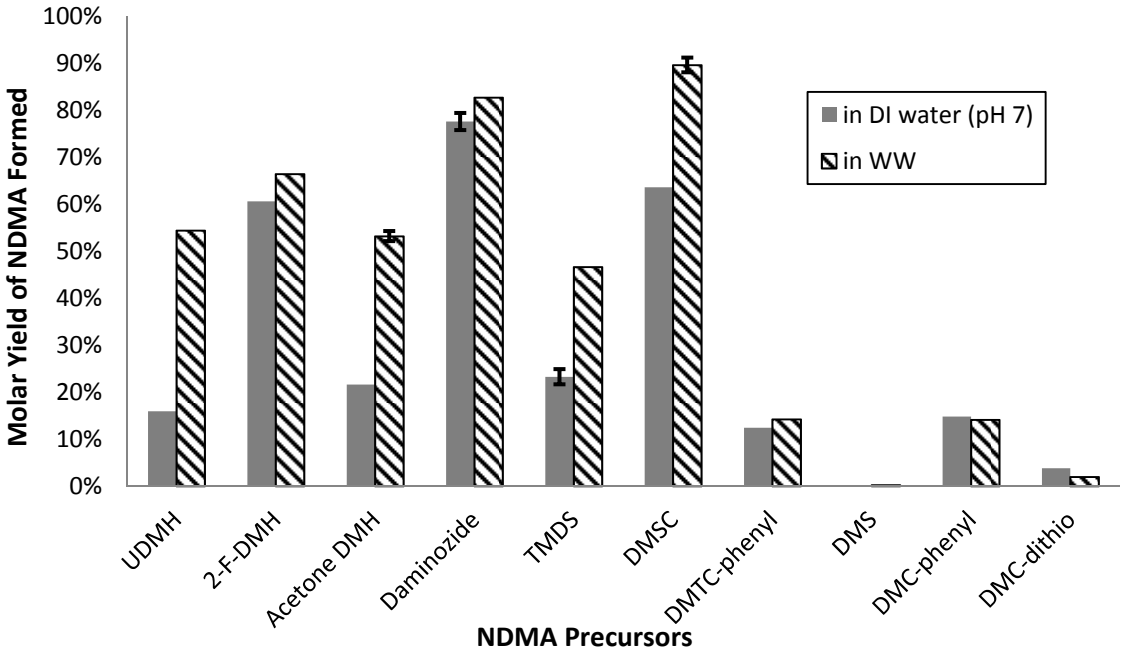

Figure 6.3. NDMA formation by ozonation (ozone=1 mM) in wastewater.

Table 6.3. Comparison of NDMA Molar Conversion Yields with Ozone for Various Precursors

Compound	This Study DI (1 mM O_3)	This Study WW (1 mM O_3)	Schmidt et al., 2008	Kosaka et al., 2009	Andrzejewski et al., 2008
UDMH	16	54	80		
DMS	20[a]	2.5[b]	52[c]		
TMDS	23	47		27	
DMA	0	0	0	0.01	0.4
Daminozide	78	83	55		
2-F-DMH	61	66			
DMSC	64	90			
DMTC-phenyl	12	14			
DMC-phenyl	15	14			
DMC-dithio	3.8	2			
Acetone DMH	22	53			

Notes: [a]=bromide spiked at 1350 µg/L; [b]=bromide spiked at 250 µg/L; [c]=bromide concentration not specified; DI=deionized water; WW=wastewater. Refer to Table 6.1 for definitions of abbreviations.

6.4 Chloramination Formation Potential

NDMA formation potential (NDMA-FP) for the targeted precursors was investigated. It was hypothesized that because all of the precursors contain dimethylamine groups, they would also react strongly with chloramines to form NDMA. Therefore, 10 day NDMA-FP tests in buffered DI water at 2 mM (140 mg/L) as Cl_2 before and after ozonation were conducted. Experimental parameters (32–100 µM precursors, 1 mM ozone, and pH 7) were kept the same for comparison to previous tests. One set of samples was spiked with chloramines. The other set of samples was spiked with ozone and allowed to react for 24 hours before spiking with chloramines.

Figure 6.4 shows a comparison of NDMA formation in buffered DI water after ozonation only and after chloramination only. Error bars represent one standard deviation (n=2). The NDMA molar conversion yields are summarized in Table 6.4. With the exception of DMA, all yields for chloramination were less than 3%, and most were less than 1.5%. These precursors have a much higher NDMA formation with ozone as compared to chloramines. As expected, DMA had the highest molar conversion yield with chloramines. NDMA-FP decreased after ozonation for DMA (data not shown), which agrees with previous research that ozonation can reduce NDMA-FP associated with chloramination (Pisarenko et al., 2012).

Molar yields for UDMH and acetone DMH increased slightly for chloramination following ozonation (Figure 6.5). This suggests that transformation products from the ozonation reaction may be NDMA chloramination precursors. Ozonation of tertiary amines can result in DMA formation (Lee et al., 2007a), which would result in NDMA with subsequent chloramination.

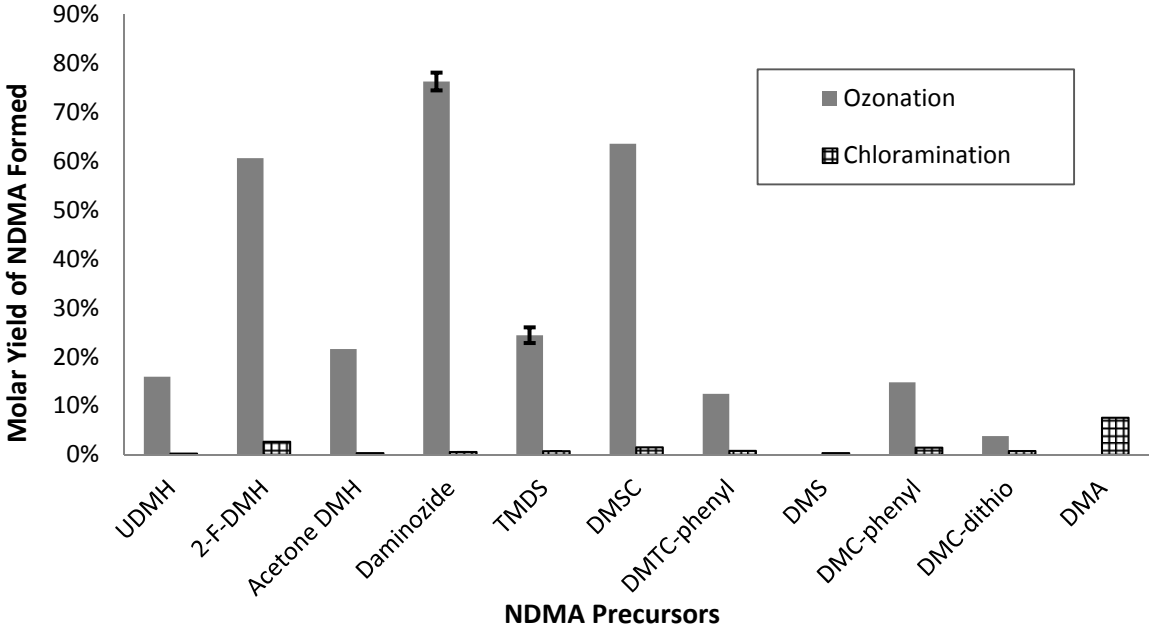

Figure 6.4. Comparison of NDMA formation for ozonation (O_3=1 mM) and chloramination (2 mM as Cl_2) in buffered DI water at pH 7.

Table 6.4. Comparison of NDMA Molar Conversion Yields for Ozonation and Chloramination in Buffered DI Water at pH 7

Compound	Ozone (1 mM O_3)	Chloramines (2 mM as Cl_2)
UDMH	16	0.2
DMS	20[a]	0.3[b]
TMDS	23	0.7
DMA	0	7.5
Daminozide	78	0.5
2-F-DMH	61	2.6
DMSC	64	1.5
DMTC-phenyl	12	1.4
DMC-phenyl	15	0.8
DMC-dithio	3.8	0.8
Acetone DMH	22	0.3

Notes: [a]=bromide spiked at 1350 µg/L; [b]=bromide spiked at 250 µg/L. Refer to Table 6.1 for definitions.

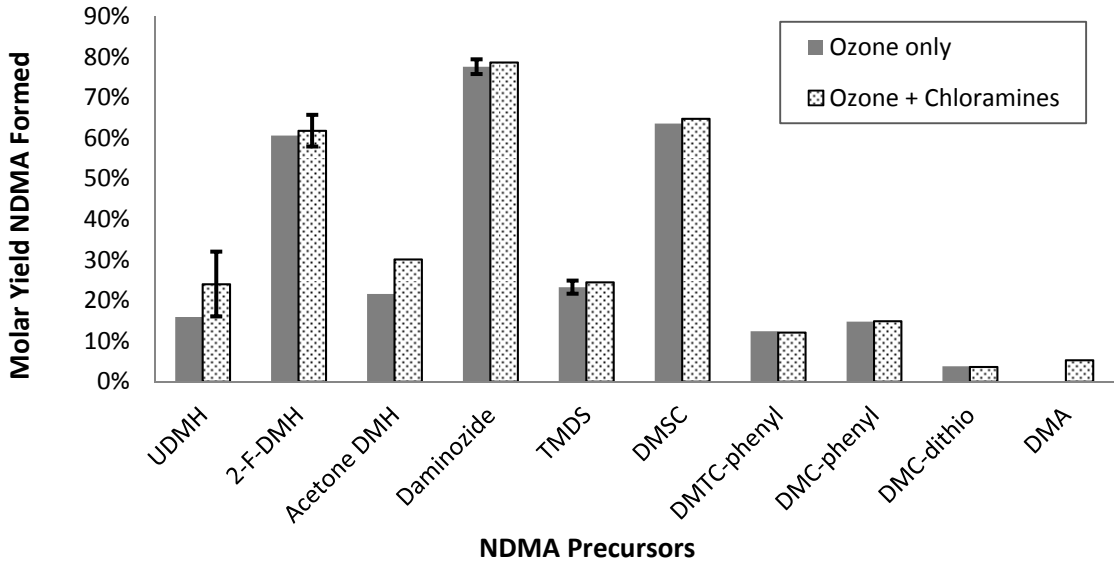

Figure 6.5. Comparison of NDMA formation with ozonation only and ozonation–chloramination in buffered DI water at pH 7.

6.5 Effect of Ozone Dose and Hydrogen Peroxide Addition on NDMA Formation

The effects of ozone dose and hydrogen peroxide on NDMA formation were investigated for two compounds (TMDS and 2-F-DMH) in phosphate-buffered DI water at pH 7. As seen in Figure 6.6, the addition of hydrogen peroxide had no impact on NDMA formation or destruction. This was also seen by Oya et al. (2008). Based on this, ozone/H_2O_2 is not expected to be a useful mitigation strategy for NDMA in wastewater matrices.

Initial ozone dose affected the extent of NDMA formation. For 2-F-DMH, NDMA formation increased from 0.1 to 0.5 mM O_3 and then leveled off (Figure 6.7). The maximum molar conversion yield was 70%. It is unlikely that increasing the ozone dose to greater than 0.5 mM would cause more NDMA formation because the precursor had reacted completely to form NDMA and other transformation products. In the case of TMDS, there was a linear correlation (R_2=0.982) between NDMA formation and ozone dose in the tested range. No maximum molar conversion yield was achieved.

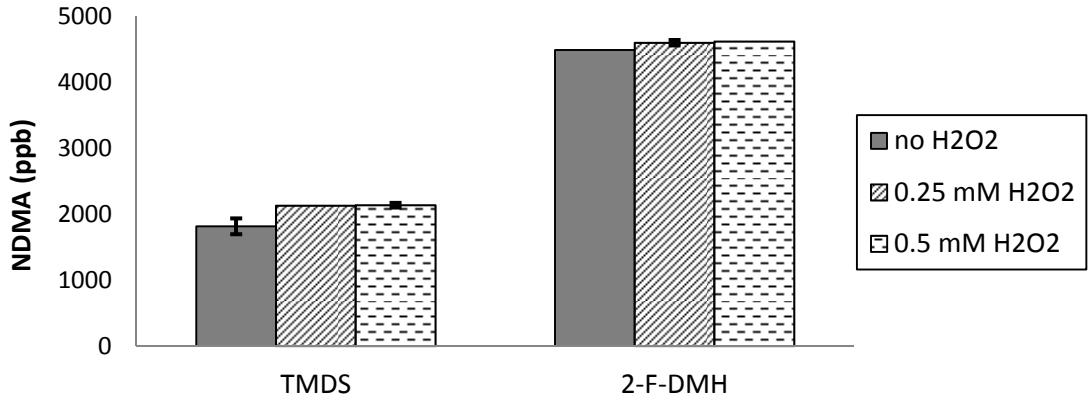

Figure 6.6. Effect of hydrogen peroxide addition on NDMA formation by ozonation (O_3=1 mM) in buffered DI water at pH 7.

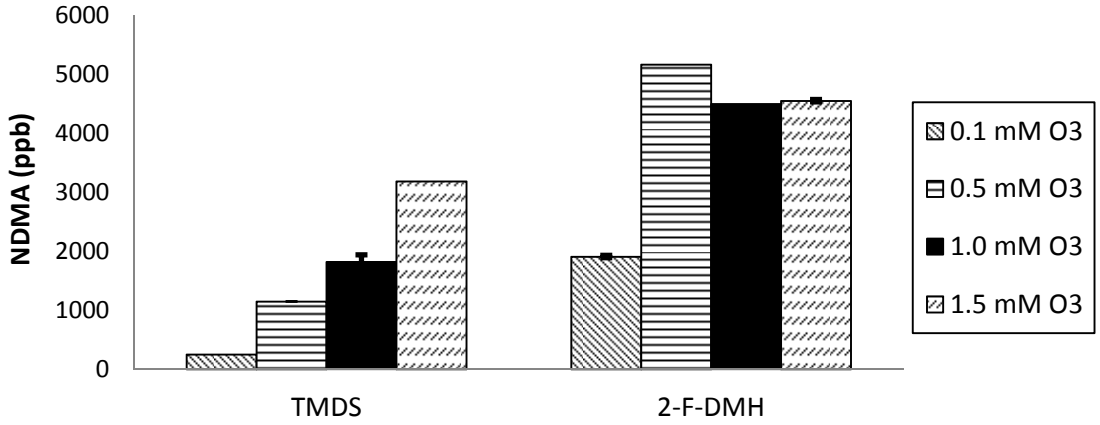

Figure 6.7. Effect of ozone dose on NDMA formation by ozonation (O_3=1 mM) in buffered DI water at pH 7.

6.6 Summary

Experiments with known and potential NDMA precursors resulted in the following findings on NDMA formation by ozonation:

- Out of nine compounds selected based on structural characteristics, six new compounds were identified as NDMA precursors. Two are hydrazones, two are semicarbazides, and two are carbamates.

- Bromide concentration was significant for NDMA formation in solutions of DMS, UDMH, and acetone dimethylhydrazone. Bromide showed no enhancing effect on NDMA formation on other compounds.

- For compounds with similar structures, NDMA molar conversion was higher for compounds with an electron donating group (e.g., 2-F-DMH) and lower for compounds with a greater electron withdrawing effect (e.g., DMTC-phenyl).

- Higher NDMA formation was observed in wastewater than ultrapure water for several precursors. Wastewater may contain constituents that promote NDMA formation.

- Although all the precursors tested contain a dimethylamine that reacts with chloramine to form NDMA, the reaction with ozone results in significantly higher NDMA formation. This group of precursors could be distinctly different than other dimethylamine-containing compounds.

- Transformation products from the ozonation reaction of UDMH and acetone DMH may be NDMA chloramination precursors.

- The addition of hydrogen peroxide had no impact on NDMA formation or destruction.

Chapter 7

Factors that Affect Perfluoroalkyl Acid Formation

This chapter discusses factors affecting the formation of PFAA during ozonation. These efforts are broken down into three main focus areas: effects of ozone dosing, effects of the pretreatment and associated water quality parameters, and identification of principal oxidation agents. To identify critical parameters affecting PFAA formation from ozone, facilities and pilot-scale systems encompassing various secondary biological treatment conditions were targeted.

7.1 Experimental Matrix

Six wastewaters were chosen based on full-scale occurrence data and secondary treatment type, as shown in Table 7.1. Corresponding water quality parameters are shown in Table 7.2. WW1 and WW2 are from the pilot MBR plant that has been operated at distinctly different SRT and biological conditions (e.g., partial nitrification or nitrification), and WW3 is from a full-scale treatment plant (nitrification/partial denitrification/biological phosphorus removal). All three of these wastewaters, WW1 through WW3, used the same influent source for a direct comparison of PFAA formation as a result of different biological treatments.

WW4 was selected based on this site using a reduced level of wastewater treatment. WW5 was selected based on PFAA formation observed in full-scale data (Table 5.1) and represents a highly treated wastewater. WW4 samples were collected over several hours starting in the morning until early afternoon, to simulate a composite sample (24 hour composite sampling was not available). Primary influent (raw sewage after head works), primary effluent, and secondary effluent were collected. WW5 receives 95% of the influent flow (TOC of 120 mg/L) from a nearby industrial run-off. Ozone is used primarily for color removal. Because of such high TOC in the influent water and the large dilution factor required to achieve the targeted O_3:TOC ratios, only the secondary effluent was sampled for bench-scale ozone experiments.

Table 7.1. Wastewater and Treatment Process Description

Abbrev.	Location[a]	Secondary/Tertiary Treatment Type	SRT	Sampling Dates
WW1	I-NV	Partial nitrification and microfiltration (MBR pilot)	4–6 days	August 1 and November 5, 2012
WW2	I-NV	Nitrification, denitrification, and microfiltration (MBR pilot)	10–12 days	January 23, 2013
WW3	I-NV	Nitrification, partial denitrification, biological phosphorus removal	8–12 days	August 20 and December 4, 2012
WW4		BOD removal	1–2 days	August 6, 2012
WW5	E-GA	Conventional activated sludge	1–2 days	September 17, 2012
WW6	D-GA	Nitrification, partial denitrification, ultrafiltration	5–10 days	October 4, 2012

Notes: [a]=These location IDs are for sites presented in Chapter 4; BOD=biological oxygen demand; MBR=membrane bioreactor.

Table 7.2. Water Quality Parameters for Wastewaters

Parameter	Unit	WW1	WW2	WW3	WW4	WW5	WW6
COD	mg/L	54	<20	N/A	N/A	N/A	N/A
BOD	mg/L	<2	<2	6.0	N/A	7.2	N/A
Total P	mg/L	0.30	0.12	0.2	N/A	6.0	N/A
NH_4^+	mg-N/L	12.5	3.53	0.26	N/A	0.2	N/A
TKN	mg-N/L	16.0	4.2	<1.0	N/A	N/A	N/A
NO_3^-	mg-N/L	0.3	14.1	14.5	<1.0	N/A	N/A
Total Nitrogen	mg-N/L	16.3	18.3	14.5	57	6.1	7.6
UV_{254}	a.u.	0.1245	0.0866	0.1160	0.2380	0.3460	0.0870
TOC	mg-C/L	6.1	4.5	5.1	14	17	4.1
TF	a.u	36,721	23,530	34,050	55,451	253,639	23,016
FI	a.u	1.55	1.62	1.73	1.53	1.03	1.47

Notes: BOD=biological oxygen demand; COD=chemical oxygen demand; FI=fluorescence index; N/A=not available; P=phosphorus; TF=trickling filter; TOC=total organic carbon; UV=ultraviolet

Table 7.3. Experimental Matrices for PFAS Bench-Scale Tests

Different O_3:TOC Ratios								
Secondary Effluent Wastewater	pH=7							
	O_3:TOC Ratio							
	0.1	0.2	0.3	0.4	0.5	1.0	1.5	2.0
WW1	x	x	x			x		
WW2					x	x	x	x
WW3		x				x		x
WW4	x	x	x	x	x	x		
WW5		x				x		
WW6					x	x	x	x

pH Variation	
Secondary Effluent Wastewaters	WW1, WW3, WW4, WW5
pH:	6, 7, 8
O_3:TOC ratio (mg/L)	0.2
H_2O_2 Addition	
pH=7, H_2O_2:O_3 ratio=1:0.5 M	

Secondary Effluent Wastewaters	O_3:TOC Ratio		
	1.0	1.5	2.0
WW1	x		
WW2		x	
WW3	x		x
WW4	x		
WW5	x		
WW6	x		

Pretreatment		
pH=7		
Primary Effluent Wastewaters	O_3:TOC Ratio	
	0.2	1.0
WW1	x	x
WW2	x	x
WW4	x	
WW6	x	x

Radiolysis		
pH=7, 1000 ppb pCBA		
Secondary Effluent Wastewaters	Dose	
	176 Gy	264 Gy
WW1	x	x
WW2	x	x
WW3	x	x

Note: pCBA=parachlorobenzoic acid.

Bench-scale experiments were performed to examine factors that affect PFAA formation. Table 7.3 summarizes the experiments, which included ozonation of primary and secondary effluents to evaluate pretreatment, pH variation, ozone:TOC dose variation, hydrogen peroxide addition for ozone and hydroxyl radical oxidation, ozonation and tBA addition for ozone-only oxidation, and gamma radiolysis for hydroxyl radical–only oxidation.

7.2 Effect of Ozone Dose and pH on PFAA Formation

A series of ozone doses were applied to the wastewaters to determine the effect on PFAA formation (Figures 7.1–7.5). In general, some PFAAs are formed after ozonation of secondary treated samples. Among the wastewaters, the extent of formation and the PFAA that increased varied. The most notable formation was for PFHxA. For each wastewater, the PFHxA levels increased as a function of O_3:TOC ratio (except for WW3). For WW1 and WW4, PFHxA continued to increase to the highest concentration level up to an O_3:TOC ratio of 1.0. A similar trend occurs for PFPnA for WW1. Both WW1 (partial nitrification; SRT 4–6 days) and WW4 (BOD removal; SRT 1–2 days) have reduced treatment compared to WW2, WW3, and WW6; however, for WW2 and WW6, the PFHxA formation plateaus between 0 and 0.50 O_3:TOC ratio. This suggests that highly treated secondary wastewaters have a lower percentage of PFHxA precursors present that can react during subsequent ozone treatment compared to WW4 and WW1. For WW5 (data not shown), PFHxA levels continued to increase with higher O_3:TOC ratios. A similar trend was observed for PFBA in WW5. This was the only wastewater in which this trend was observed. PFBA levels were below the reporting levels for the other wastewaters.

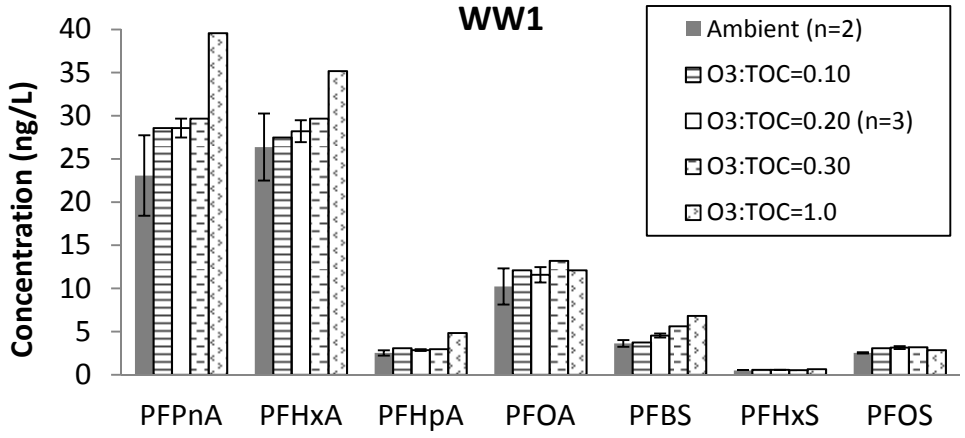

Figure 7.1. Change in PFAA in WW1—MBR filtrate (partial nitrifcation) at various O_3:TOC ratios.

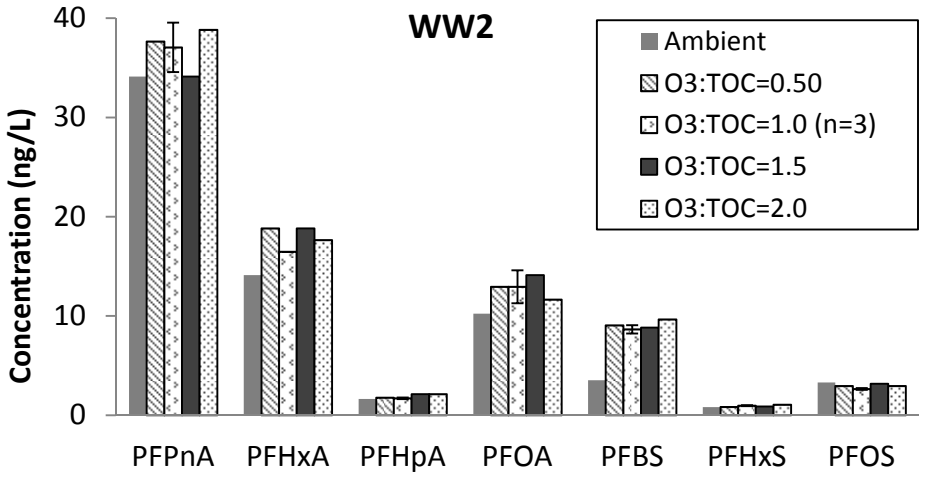

Figure 7.2. Change in PFAA in WW2—secondary effluent (nitrification) at various O_3:TOC ratios.

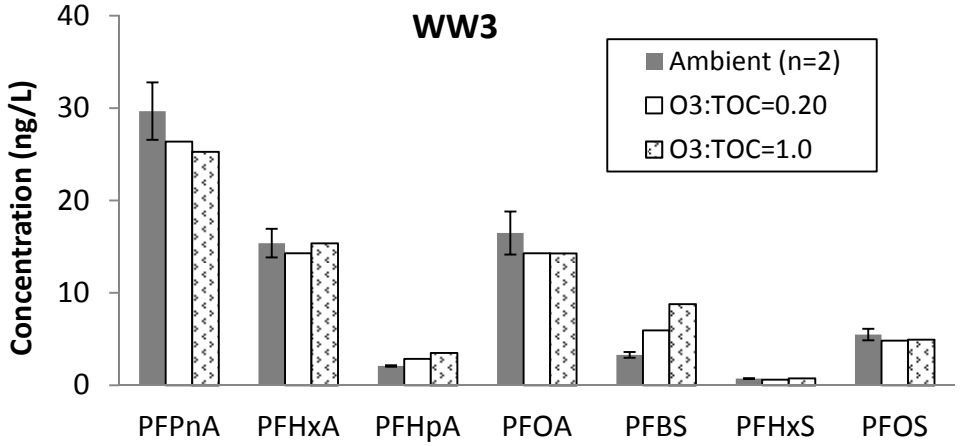

Figure 7.3. Change in PFAA in WW3—secondary effluent (nitrification/denitrification) at various O_3:TOC ratios.

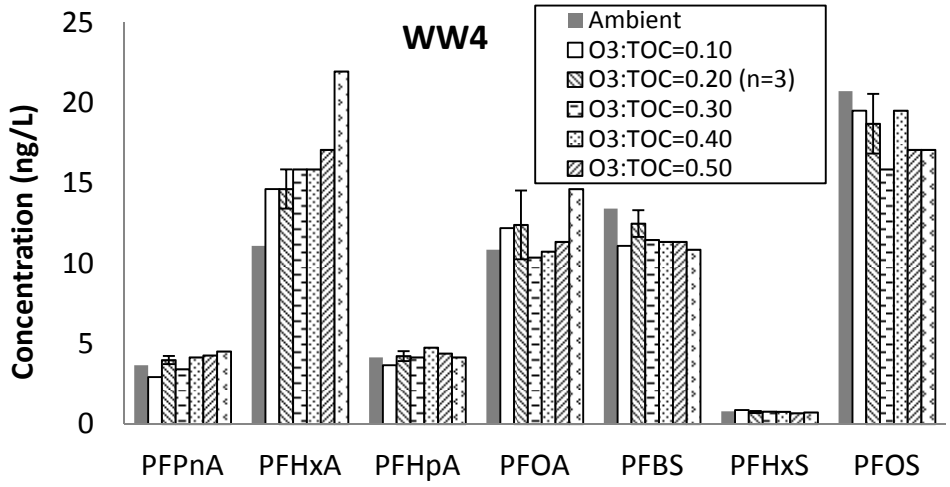

Figure 7.4. Change in PFAA in WW4—secondary effluent (BOD removal) at various O_3:TOC ratios.

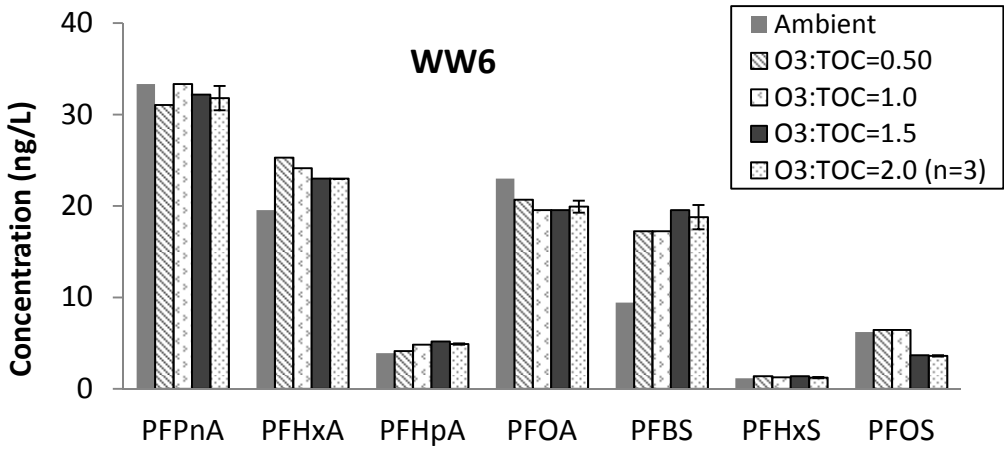

Figure 7.5. Change in PFAA in WW6—secondary effluent (nitrifying/denitrifying) at various O_3:TOC ratios.

Varying pH had little impact on PFAS formation with ozonation. For brevity, only two figures showing PFAS formation at different pH are presented (Figures 7.6 and 7.7). WW1 has lower levels of PFAS, whereas WW5 has high levels. In both cases, there is no significant change with pH adjustment. These data suggest that adjusting the pH will not be a useful mitigation strategy within this pH range.

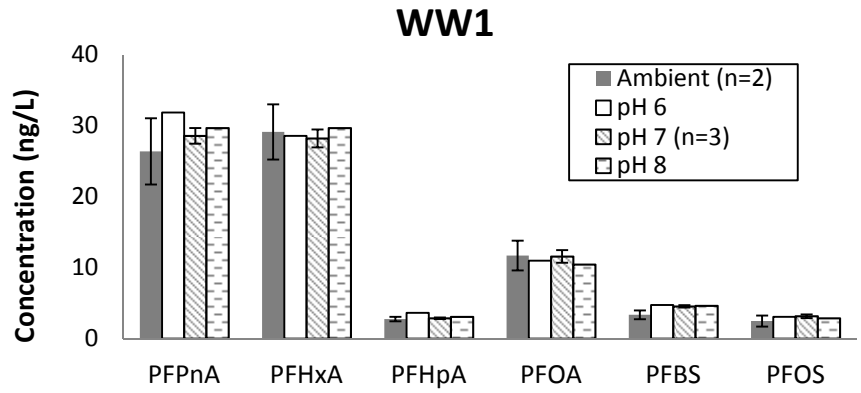

Figure 7.6. Change in PFAA formation in WW1 at various pH and O_3:TOC=0.20.

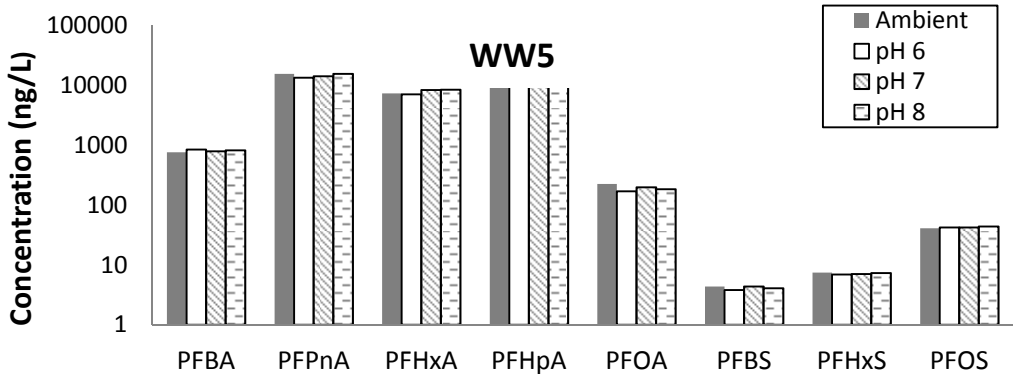

Figure 7.7. Change in PFAA formation in WW5 at various pH and O_3:TOC=0.20.

Note: Notice the logscale y-axis.

7.3 Effects of Pretreatment

PFAA formation was monitored at ambient and several O_3:TOC ratios for primary and secondary effluent to determine the effect of pretreatment. As seen with the full-scale data (Figure 4.5), several PFAAs (e.g., PFHxA, PFOA) increased after secondary treatment in Figure 7.8. Although grab samples are not hydraulically connected and tend to have high variability, there is a consistent increase after secondary treatment. The increase could be due to biological transformation of precursors.

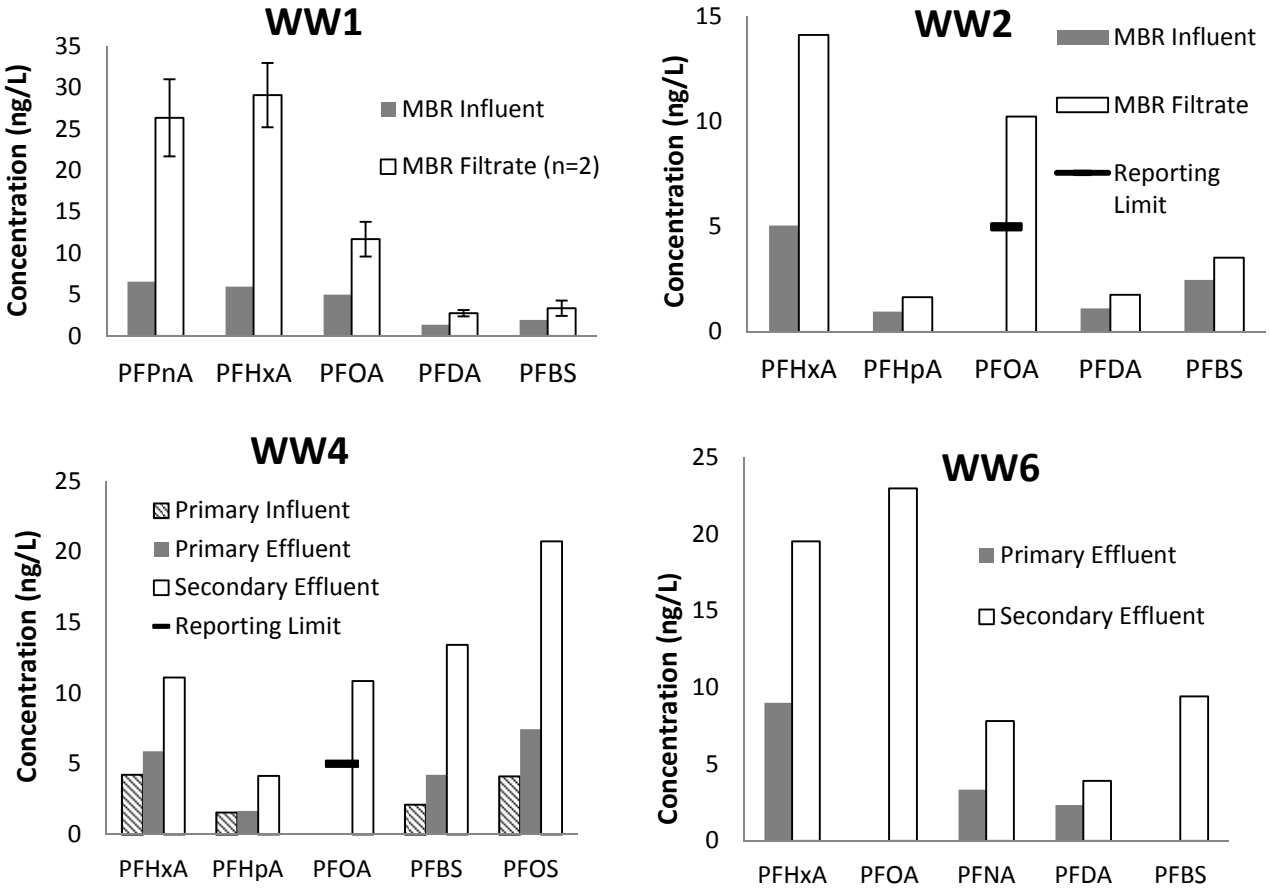

Figure 7.8. Ambient levels of PFAA in primary and secondary treated wastewaters.

Table 7.4 reports the PFHxA levels before and after ozone treatment at an O_3:TOC ratio of 1.0. For WW1, WW2, WW6, and WW3, the PFHxA formation from ozone treatment ranged from 1 to 6 ng/L (average 3.8±1.4 ng/L). WW5 was an outlier with an exceptionally high concentration. Excluding WW5, PFHxA formation was highest in WW4, which corresponds with WW4 having the least treated wastewater. If similar PFHxA precursors are present before secondary treatment for these wastewaters, then BOD removal plants with an SRT of 1 to 2 days could have a higher level of PFHxA precursors present after secondary treatment.

As discussed previously, PFAAs, such as PFHxA, can form during both secondary treatment and subsequent ozone treatment. This was evaluated at I-NV, where different treated wastewaters were produced (WW1–3). WW1 (partial nitrification; 4–6 days) and WW2 (nitrification; 10–12 days) are from a pilot-scale MBR system located at the I-NV site, which was operated at different SRTs. The MBR influent came from the primary effluent of the onsite full-scale plant. WW3 is from a full-scale plant (nitrification, partial denitrification; SRT 8–12 days). The PFHxA levels for secondary influent and nonozonated and ozonated secondary effluent are presented in Figure 7.9. WW1, sampled in August 2012, has a greater PFHxA concentration after biological treatment, but this could be caused by varying influent concentrations. In general, these results show the final PFHxA level after ozone treatment (O_3:TOC=1.0) does not vary as a function of the pretreatment.

Table 7.4. PFHxA Concentrations (ng/L) in Secondary Effluent Before and After Ozonation

WW	Date	Secondary Effluent Ambient (no ozone)	Secondary Effluent (O_3:TOC=1.0)	Formation Increase
WW1	08/01/2012	31.9	35.2	3.3
WW1	11/05/2012	10.9	14.8	4.0
WW1	09/18/2012	9.9	13.5	3.6
WW2	01/23/2013	14.1	16.5	2.4
WW2	01/17/2013	11.0	16.0	5.0
WW3	08/21/2012	14.3	15.4	1.1
WW3	12/04/2012	18.8	23.1[a]	4.4
WW4	08/02/2012	11.1	22.0	10.9
WW5	09/17/2012	5200	6500	1300
WW6	10/04/2012	19.5	24.1	4.6

Note: [a]=different ozone dose applied (O_3:TOC = 2.0).

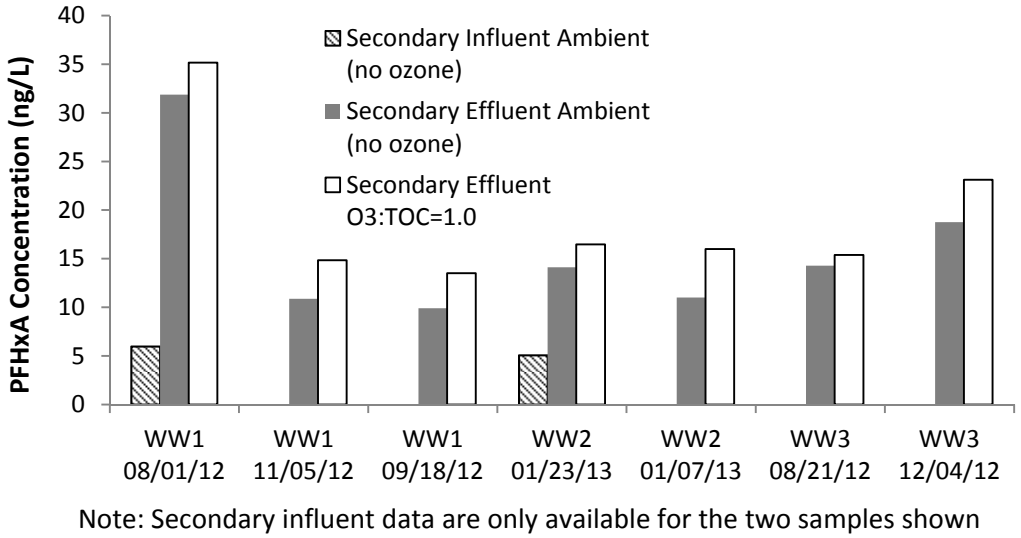

Figure 7.9. PFHxA concentrations (ng/L) for secondary influent, secondary effluent, and ozonated secondary effluent for WW1–WW3.

7.4 The Role of Ozone and Hydroxyl Radical in PFAA Formation

Experiments were designed to determine whether dissolved ozone or •OH is responsible for the direct formation of PFAA during ozonation. Three wastewaters (WW1, WW2, and WW3) with varying secondary treatments were selected. The experimental matrix was divided into three components that isolated the effect of the oxidants. In Part 1, pCBA was used to determine the overall •OH exposure with ozone and ozone/H_2O_2. In Part 2, tBA was added prior to ozone and ozone/H_2O_2 treatment. Because tBA is a strong •OH scavenger, this step isolated the effect of dissolved ozone by effectively scavenging all of •OH produced during decomposition of dissolved ozone. For Part 3, samples spiked with pCBA were subjected to gamma radiolysis. In these experiments, only •OH was produced in the wastewater samples. Changes in PFAA concentration were measured for each sample before and after oxidant exposure.

7.4.1 Ozone and Associated Hydroxyl Radical Exposure

In order to have a comparable hydroxyl radical exposure between ozonation and radiolysis, it was necessary to determine the overall •OH exposure using pCBA. In addition, it was verified that the tBA dose was effective in scavenging the •OH produced during dissolved ozone decomposition and radiolysis. As shown in Figure 7.10, the wastewaters received similar •OH exposure during ozonation with and without H_2O_2. Radiolysis samples received •OH exposure similar to that of the ozonation samples (Figure 7.11).

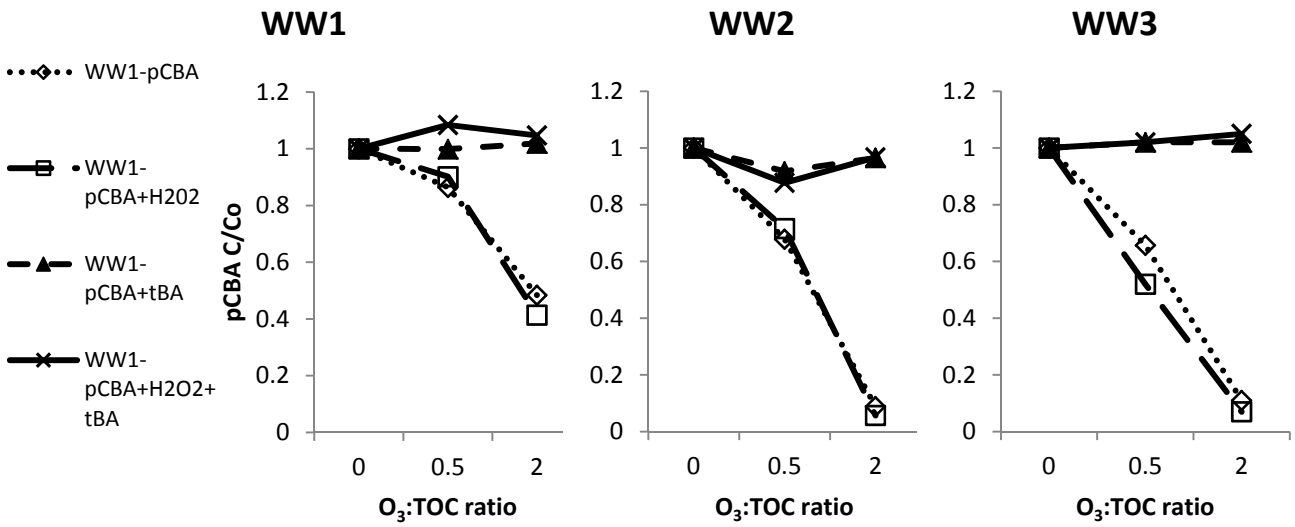

Figure 7.10. Hydroxyl radical exposure for WW1–WW3 after ozonation with and without H_2O_2 addition at various O_3:TOC ratios.

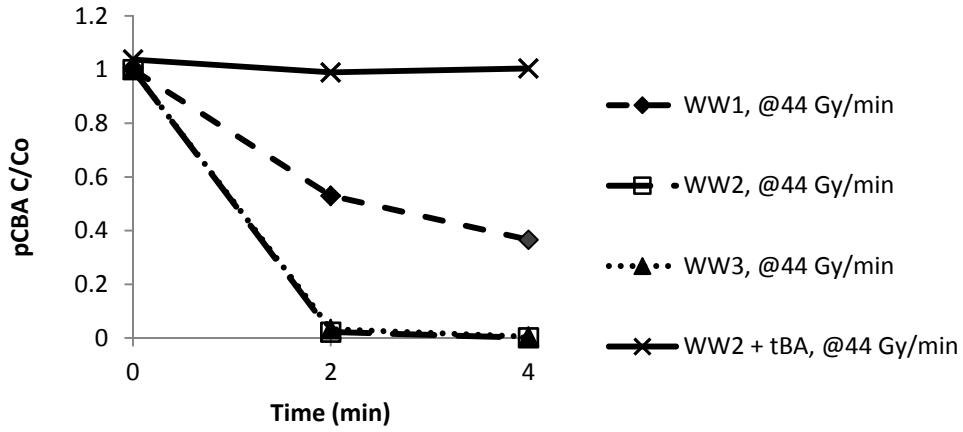

Figure 7.11. Hydroxyl radical exposure for WW1–WW3 after radiolysis.

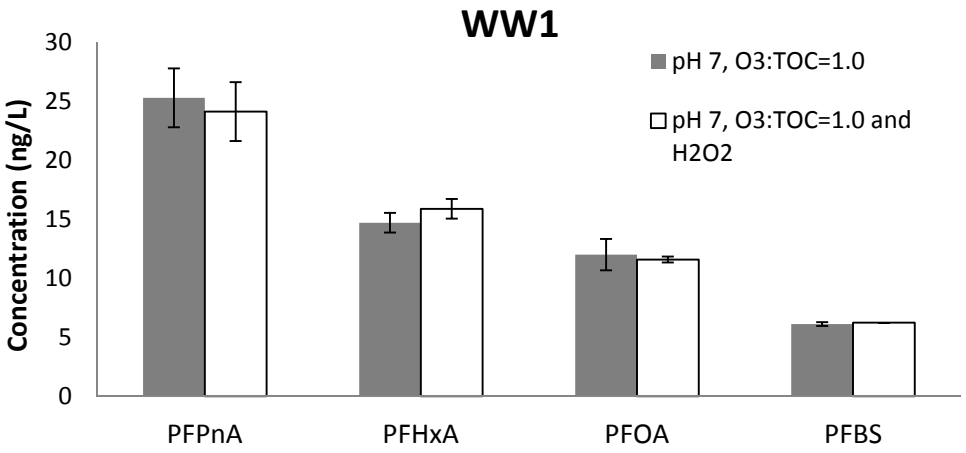

Figure 7.12. PFAA formation for WW1 after ozonation with and without H_2O_2 addition at O_3:TOC=1.0.

7.4.2 Effects of Addition of H_2O_2 on PFAA Formation

No significant differences in PFAA formation were observed between samples exposed to ozone only and those exposed to ozone and hydrogen peroxide. Because of significant •OH exposure already produced during ozone decomposition, addition of hydrogen peroxide did not significantly increase the yield of •OH exposure. Therefore, these results did not provide a definitive conclusion on relative contribution of ozone and hydroxyl radical to PFAA formation. For brevity, only one graph (Figure 7.12) is shown.

7.4.3 Effects of Molecular Ozone and Hydroxyl Radical

An increase in particular PFAA analytes (e.g., PFPnA and PFOA) was observed with the addition of tBA (Figures 7.13 through 7.15); however, this was not consistent for all PFAAs or precursors. Scavenging of hydroxyl radicals by tBA may have increased the available molecular ozone for reactions with PFAA. In practice, these results imply that wastewater with higher •OH scavenging may also lead to higher PFPnA and PFOA formation. Higher •OH scavenging is typically associated with poorer wastewater quality.

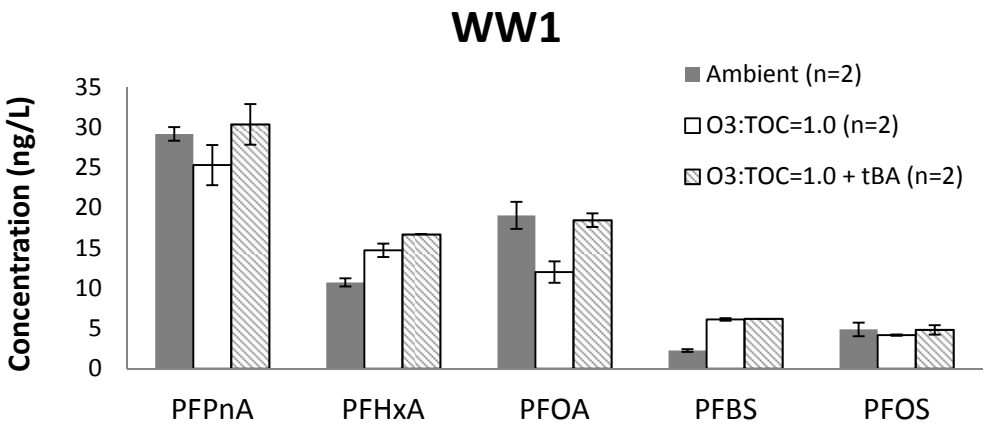

Figure 7.13. PFAA formation for WW1 after ozonation with and without tBA addition at O_3:TOC=1.0.

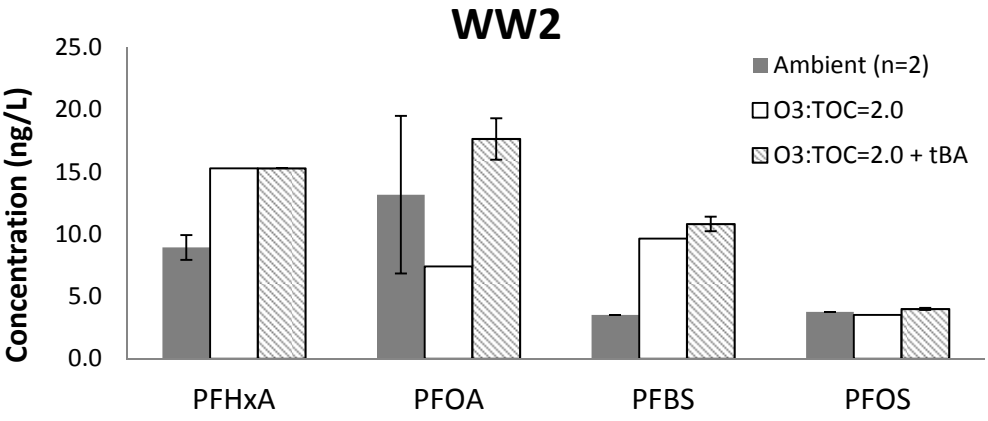

Figure 7.14. PFAA formation for WW2 after ozonation with and without tBA addition at O_3:TOC=2.0.

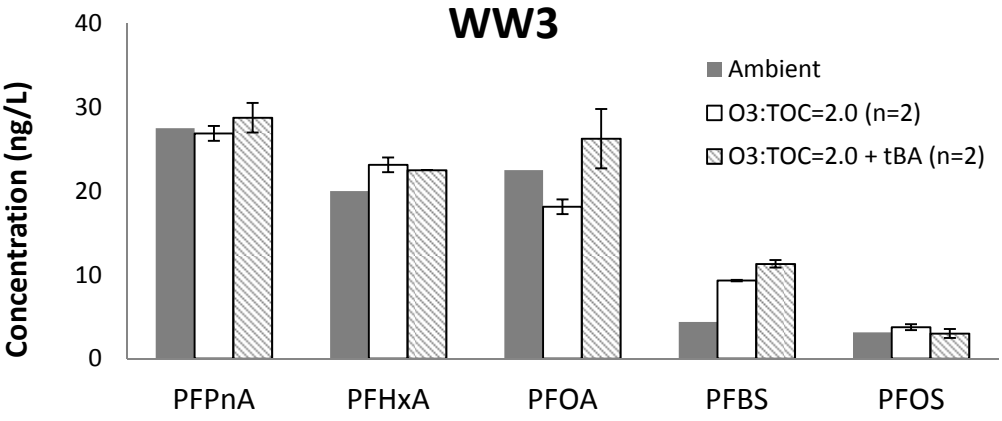

Figure 7.15. PFAA formation for WW3 after ozonation with and without tBA addition at O_3:TOC=2.0.

For radiolysis experiments, there was slight PFAA formation (Figures 7.16 through 7.18). Compared to ozonation experiments, radiolysis resulted in less PFAA formation (Table 7.5). Results from the radiolysis experiments are inconclusive in determining if the responsible oxidant is molecular ozone and not hydroxyl radicals. Considering the minimal PFAA increase for radiolysis test results, AOPs focused on hydroxyl radicals may not be useful for PFAA mitigation.

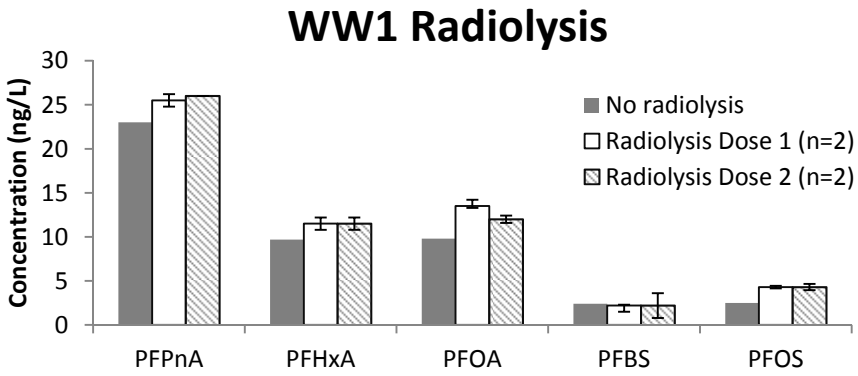

Figure 7.16. PFAA formation for WW1 before and after radiolysis.

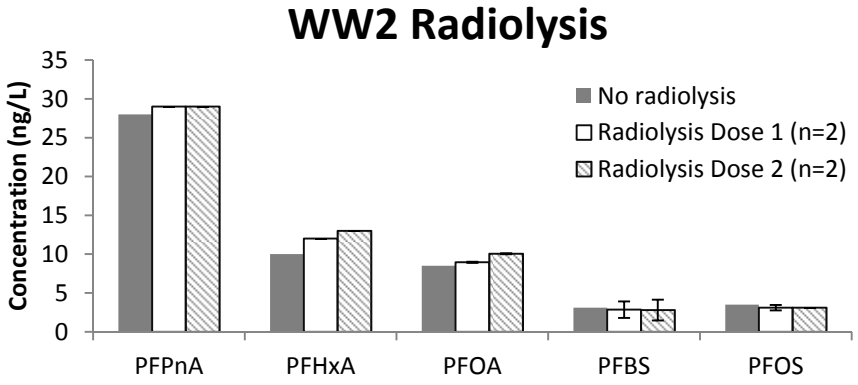

Figure 7.17. PFAA formation for WW2 before and after radiolysis.

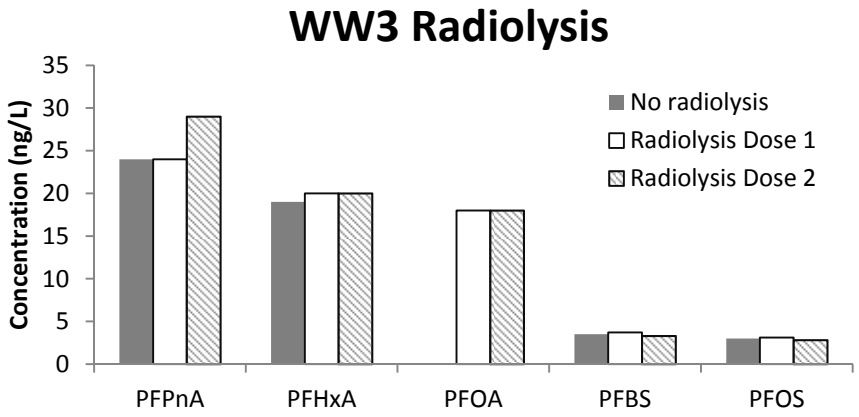

Figure 7.18. PFAA formation for WW3 before and after radiolysis.

7.5 Summary

Several factors affecting PFAA formation were studied and resulted in the following conclusions:

- Several PFAAs increased after secondary treatment. For example, PFHxA increased between 5 and 26 ng/L.
- Some PFAAs are formed after ozonation of secondary treated samples with an O_3:TOC ratio greater than 1.0. The extent of formation and the PFAA that increased varied among wastewaters but commonly included PFHxA, PFBS, PFOA, and PFPnA. Low level increases were observed: PFHxA formed in the range of 1 to 6 ng/L.
- Varying pH had little impact on PFAA formation with ozonation.
- No significant differences in PFAA formation were observed between samples exposed to ozone only and samples exposed to ozone and hydrogen peroxide.
- With the addition of tBA to scavenge hydroxyl radicals during ozonation, some PFAAs increased.
- Slight formation was observed for radiolysis experiments, but results are inconclusive in determining the role of hydroxyl radicals in PFAA formation. The lack of degradation suggests that AOPs focused on hydroxyl radicals will not be useful mitigation strategies.

Table 7.5. Comparison of PFAA Formation Increase for Radiolysis and Ozonation of WW1, WW2, and WW3

WW	PFAA Analyte	Radiolysis Ambient	Radiolysis Dose 1	Formation Increase	Radiolysis Dose 2	Formation Increase
WW1	PFPnA	23	26	*2.5*	26	*3.0*
	PFHxA	9.7	12	*1.8*	12	*1.8*
	PFOA	9.8	14	*3.7*	12	*2.2*
	PFOS	2.5	4.3	*1.8*	4.3	*1.8*
WW2	PFPnA	28	29	*1.0*	29	*1.0*
	PFHxA	10	12	*2.0*	13	*3.0*
	PFOA	8.5	9.0	*0.4*	10	*1.6*
	PFOS	3.5	3.1	*-0.4*	3.1	*-0.4*
WW3	PFPnA	24	24	*0*	29	*5.0*
	PFHxA	19	20	*1.0*	20	*1.0*
	PFOA	--	18	--	18	--
	PFOS	3	3.1	*0.1*	2.8	*-0.2*
WW	**PFAA Analyte**	**Ozone Ambient**	**O_3:TOC=1.0**	**Formation Increase**	**O_3:TOC=2.0**	**Formation Increase**
WW1	PFPnA	21	25	*4.0*	-	-
	PFHxA	11	15	*4.0*	-	-
	PFOA	12	12	*0*	-	-
	PFOS	4.9	4.2	*0.7*	-	-
WW2	PFPnA	34	37	*3.0*	39	*5.0*
	PFHxA	14	16	*2.0*	18	*4.0*
	PFOA	10	12	*2.0*	12	*2.0*
	PFOS	3.3	2.7	*-0.6*	2.9	*-0.4*
WW3	PFPnA	26	-	-	27	*1.0*
	PFHxA	19	-	-	23	*4.0*
	PFOA	19	-	-	18	*-1.0*
	PFOS	2.8	-	-	3.8	*1.0*
	Average Variability		PFPnA=4 ng/L	PFHxA=4 ng/L	PFOA=9 ng/L	PFOS=9 ng/L

Notes: - =data not available; --=data not valid. Refer to Table 3.6 for definitions.

Chapter 8

Mitigation Strategies

8.1 NDMA

As shown in this study and others, NDMA formation occurs after ozonation of treated wastewater. The mitigation of NDMA resulting from this oxidation process can occur by the pretreatment of NDMA precursors, manipulation of the ozone treatment process, or posttreatment of NDMA itself. The presence of biological secondary pretreatment is effective at reducing NDMA precursors; secondary treatment systems that employ partial or full nitrification are more able to reduce their levels than non-nitrified wastewaters.

The degree of NDMA formation during ozonation can be controlled by the applied O_3:TOC dose, where formation is more sensitive for O_3:TOC up to 0.5 for partially and completely nitrified wastewaters. For non-nitrified wastewater, NDMA formation was sensitive up to O_3:TOC of 1.0 and potentially higher. pH can influence NDMA formation from ozonation, but in this study it did not significantly affect NDMA formation between pH 6 and 8. NDMA formation by the ozonation of dimethylsulfamide is catalyzed by bromide (Schmidt and Brauch, 2008; von Gunten et al., 2010), and new precursors from this study also show enhanced NDMA formation with bromide. In other bench-scale experiments performed in this study, where bromide concentration was varied (up to 1000 µg/L), there was no observable effect on the amount of NDMA formed. It is unclear whether the ambient bromide concentration (153 µg/L) was already sufficient to catalyze the maximum NDMA formation or bromide is simply not an important catalyst for this water matrix. Overall, bromide catalysis of NDMA formation may only be a concern for wastewaters with specific precursors affected by bromide.

Krasner (2013) reported that there are limited treatment options for removal of nitrosamines and precursors in drinking water, highlighting the use of riverbank filtration, coagulation, GAC, ozone, polymer control, and UV and sunlight. Chemical AOPs focused on the hydroxyl radical, such as O_3/H_2O_2, are not effective for NDMA destruction (Lee et al., 2007b, Plumlee et al., 2008b, Pisarenko et al, 2012). NDMA removal by postadsorption processes is only moderately effective; NDMA does not adsorb as strongly as other organic compounds (Kommineni et al., 2003). Although GAC can achieve 99% removal (Fleming et al., 1996), the media must be frequently replaced or regenerated, making it not a cost-effective option. RO is able to physically reject NDMA, but only to about 50% because of NDMA's small size (Plumlee et al., 2008b). Yangali-Quintanilla (2010) recommends NF membranes with a low molecular weight cut-off that perform as well as RO but are a lower cost alternative. These processes are not completely effective at targeting NDMA directly, but some of them, such as GAC or NF, could be employed ahead of ozonation to target NDMA precursors that are reactive towards ozone.

Photolysis is a common posttreatment option that is employed, typically after RO, to target NDMA. UV irradiation at 254 nm will degrade NDMA to low ppt levels, but only at around tenfold the dose used to inactivate viruses. Bolton et al. (2002) determined that 510 mJ/cm^2 is needed for a log reduction of NDMA in wastewater using a medium-pressure collimated beam (UV fluence based on 200–300 nm range). Sharpless and Linden (2003) reported 400 to 500 mJ/cm^2 for a 1 log reduction with synthetic river water using either medium- (UV fluence based on 200–300 nm range) or low-pressure lamps; however, the use of high UV doses such as these is a costly treatment.

As observed in this study, NDMA levels are reduced during biological activated sludge treatment, presumably through biodegradation mechanisms. The capability of biodegradation has been confirmed by Sharp et al. (2005), who discovered aerobic biodegradation of NDMA by certain bacteria. It is interesting that in the current study BAC dropped NDMA below the reporting limit at two sites (D-GA and F-QLD) that use this treatment (Figure 8.1). One other study observed the same in a pilot ozone–BAC system (City of Reno, 2010). This indicates that BAC treatment is an effective postmitigation strategy for NDMA. The D-GA and F-QLD sites in Figure 8.1 used BAC that had not been changed out for years, so it is presumed that biodegradation is the main mechanism responsible for NDMA reductions. In addition, ozonation after BAC treatment at these sites did not result in detectable NDMA ("Ozone effluent 2" in Figure 8.1). This indicates that NDMA precursors (reactive towards ozone) did not remain after ozone–BAC treatment, which suggests that posttreatment ozonation can be safely applied. This leads to the possibility of employing BAC before ozonation (no ozone before BAC) to target NDMA precursors. Post-managed aquifer recharge is another alternative mitigation strategy for NDMA removal (Drewes et al., 2006), and reductions have been attributed to biodegradation (Nalinakumari et al., 2010; Zhou et al., 2009).

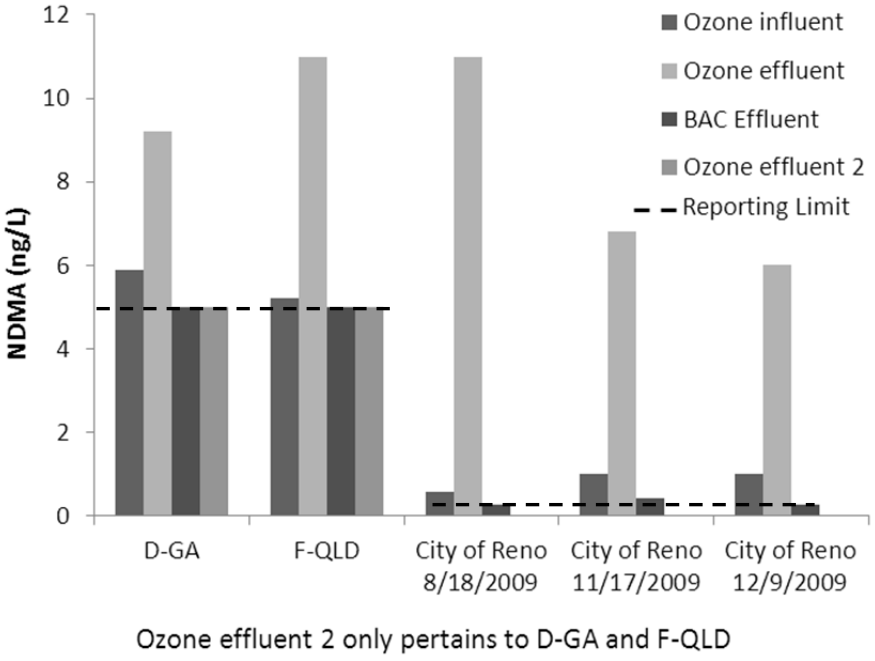

Figure 8.1. Change in NDMA concentration at full-scale wastewater treatment plants D-GA and F-QLD and Reno pilot ozone–BAC system.

8.2 Perfluoroalkyl Acids

As presented in this study, some PFAA levels increase during biological secondary treatment followed by ozone treatment. The shorter chain perfluoroalkyl carboxylic acids (e.g., PFBA, PFPnA, PFHxA, and PFBS) are the PFAAs that are more likely to be formed. Differing CAS treatments (nitrifying to nitrifying/partly denitrifying treatments) do not seem to impact the overall PFAA formation resulting from posttreatment ozonation. There are very few options for posttreatment of PFAAs. At C-TX, E-GA, and F-QLD, post-BAC treatment was unable to reduce PFPnA, PFHxA, PFHpA, PFBS, and PFHxS concentrations, and in some cases the levels were slightly higher after treatment (Table 4.3). These systems used well-established and exhausted BAC filters. Thompson et al. (2011) studied a full-scale wastewater treatment plant and found that shorter chain PFAAs increased following BAC treatment. Other potential posttreatment options that have proven to be ineffective at reducing PFAA levels include coagulation followed by physical separation processes (e.g., sedimentation, UF and MF membranes, dissolved air flotation), chemical oxidation (e.g., AOP: H_2O_2, O_3/UV, O_3/H_2O_2, Fe/H_2O_2), aeration and disinfection (e.g., chlorine, ozone, chlorine dioxide, UV; Dickenson and Higgins, 2013; Quiñones and Snyder, 2009; Schroder and Meesters, 2005). Promising posttreatment physical separation processes include anion exchange (AIX), GAC, NF, and RO.

Sorption techniques remove some PFAAs. GAC will remove PFAA, but the results are dependent on the size of the PFAA, carbon type, remaining capacity, retention time, and how often the carbon is exchanged (Shivakoti et al., 2010; Takagi et al., 2008; Yu et al., 2009b). Limited studies performed to date have demonstrated that AIX and GAC adsorption treatments can remove longer chain PFAAs but are less effective for the shorter chain PFAAs (Dickenson and Higgins, 2013). Yu et al. (2009b) found that powdered activated carbon (PAC) is suitable for PFAA removal and reached sorption equilibrium faster than GAC; however, the use of activated carbon as PAC is limited for the adsorptive removal of shorter chain PFAAs, PFPeA, PFHxA, PFHpA, and PFBS, as this requires activated carbon doses that are too high to be practical (Dudley, 2012). Combining ultrasound with GAC could be a promising technique to increase sorption kinetics by 250 to 900% (Zhao et al., 2011). The same study showed that ion exchange will remove ionic PFAA, such as PFOS and PFOA; however, the large molecular weights, small charged sites, and long nonpolar ends of PFAA molecules slow the sorption kinetics, and it may require a full day to achieve the best removal (Lampert et al., 2007).

Unlike AIX and GAC, current NF and RO membrane technologies are effective for even the smallest PFAA studied, PFBA. Full- (Dickenson and Higgins, 2013) and bench-scale (Steinle-Darling and Reinhard, 2008; Tang et al., 2007) studies have demonstrated the effectiveness of RO treatment for PFAAs. It was observed in the laboratory that NF was able to reject these chemicals, too (Dickenson and Higgins, 2013; Steinle-Darling and Reinhard, 2008). These findings are promising in that NF treatment could be an effective barrier for PFAAs with a range of molecular weights and without the same energy costs associated with RO; however, the treatment should be investigated further at pilot- and full-scale. In addition, it is worth noting that oxidation–reduction technologies, such as vacuum UV at 185 nm, photocatalytic oxidation, photochemical oxidation, photochemical reduction, persulfate radical treatment, thermally induced reduction, and sonochemical pyrolysis, have been shown in other studies to be effective at degrading some PFAAs in water (Cao et al., 2010; Chen and Valentine, 2007; Fujii et al., 2007; Giri et al., 2011; Hori et al., 2005; LaZerte et al., 1953; Lee et al., 2010b; Moriwaki et al., 2005b; Qu et al., 2010; Rayne and Forest, 2009; Wang et al., 2008; Yamamoto et al., 2007). Therefore, it is worth investigating innovative approaches for applying some of these technologies in a cost-effective manner in current drinking water treatment practices.

Chapter 9

Conclusions

This study examined the potential formation of nitrosamines and PFAAs upon ozonation of various treated wastewaters. As shown in full- and pilot-scale systems (Chapter 4) and bench-top studies (Chapter 5), NDMA was the dominant nitrosamine formed during ozonation. Formation was minimal or did not occur for the other targeted nitrosamines, except for isolated formations of NMEA and NDEA. Unknown nitrosamines were formed, however, NDMA accounted for about half of the total nitrosamines after ozone treatment. NMOR was the second most frequently detected nitrosamine in studied wastewaters, but NMOR levels did not change during ozone treatment, suggesting NMOR is neither formed nor transformed during ozone treatment.

Precursors have been identified to yield high NDMA levels (10–80%), like those containing hydrazine (e.g., UDMH, semicarbazides) and sulfamide moieties. The hydrazine compounds have a dimethylamino group that is connected to a nitrogen atom, and the sulfamides have a dimethylamino group and a nitrogen atom that are separated by an -SO_2 group. Similar compounds with a good leaving group like -SO_2 could be potential precursors. This study identified six new significant NDMA precursors: two hydrazones (22–66%), another semicarbazide (64–90%), a thiosemicarbazide (12–14%), and two carbamates (2–15%). For compounds with similar structures, NDMA molar conversion was higher for compounds with an electron donating group and lower for compounds with a greater electron withdrawing effect. It is interesting that these same precursor compounds had low NDMA yield (<1.5%) when they were allowed to react with chloramines alone. In addition, chloramine-reactive precursors, such as secondary and tertiary amine precursors with a dimethylamino group only and no additional nitrogen, can form NDMA upon ozonation, but yields are typically low (<0.1%). These findings suggest that ozone-reacting precursors are distinctly different than other dimethylamino-containing compounds that are more reactive to chloramines. The presence of these ozone-reacting precursors or similar compounds has not been reported in U.S. wastewaters, and therefore more studies are needed.

As shown in full-scale systems (Chapter 4) and bench-top studies (Chapter 7), some PFAAs were formed after ozonation of secondary treated wastewaters. The extent of formation and the PFAAs that formed varied among wastewaters but commonly included PFPnA, PFHxA, PFOA, and PFBS. The most consistently formed PFAA was PFHxA (up to an 11 ng/L increase).

NDMA and PFHxA formation during ozonation of wastewater was dependent on the applied O_3 concentration. For a majority of the treated wastewaters that were evaluated, the NDMA formation was near its maximum at O_3:TOC>0.5. For half of the treated wastewaters, PFHxA reached its maximum formation at O_3:TOC>1.0, whereas for the other wastewaters the maximum was achieved between 0 and 0.5 O_3:TOC. As demonstrated in bench-top wastewater and model compound testing (Chapters 5 and 6), the hydroxyl radical was not significant for NDMA formation, and this suggests that NDMA formation is due to reactions with molecular ozone. Results are inconclusive in determining the relative role of hydroxyl radical and molecular ozone towards PFAA formation. Varying pH (6–8) had little impact on either NDMA or PFAA formation with ozonation. Bromide catalyzed NDMA formation in solutions of a few model precursor compounds, but the majority of precursor compounds showed that

bromide had no enhancing effect on NDMA formation. Surprisingly, higher NDMA formation was observed in ozonated wastewater than ozonated ultrapure water, which contained certain spiked precursor compounds. Wastewater may contain constituents (e.g., common ions, TOC, etc.) that promote NDMA formation.

Biological pretreatment has more of an impact on reducing NDMA precursors than PFAA precursors. The presence of biological secondary pretreatment in addition to primary clarification is effective at reducing NDMA precursors. Secondary treatment systems that employ partial or full nitrification are more able to reduce their levels than non-nitrified wastewaters. On the other hand, several PFAAs such as PFHxA increased (5–26 ng/L), which may be attributable to biological transformation of PFAA precursors. In general, differing CAS pretreatments (nitrifying to nitrifying/partly denitrifying treatments) did not seem to impact resulting PFHxA precursor levels after biological treatment or PFHxA formation resulting from posttreatment ozonation. The results demonstrate that PFAA levels can increase during secondary treatment and subsequent ozone treatment, but PFAA levels are generally less than 40 ng/L, with the exception of one plant (WW5; E-GA). The determination of which PFAAs and their regulatory levels are pursued will bring into context the importance of these occurrence levels and establish whether PFAAs will be an issue.

The posttreatment options for NDMA and PFAA removal vary. UV photolysis and BAC treatment options have been shown to be most effective towards NDMA reduction. UV photolysis has been selected for full-scale applications and proven to be an effective NDMA reduction strategy when NDMA levels are not significantly high. UV treatment relies on an energy-intensive operation requiring high UV dose and high water quality pretreatment (e.g., RO). BAC treatment, a less energy-intensive option, appears to be an effective postmitigation strategy for NDMA, but more research on the factors that govern its removal is necessary. Because of the recalcitrant nature of PFAAs, posttreatment options for PFAA removal rely on physical separation processes such as GAC, AIX, NF, and RO treatment technologies; NF and RO membrane technologies are more effective for the shortest chain PFAAs.

References

Andrzejewski, P.; Kasprzyk-Hordern, B.; and Nawrocki, J. *N*-nitrosodimethylamine (NDMA) formation during ozonation of dimethylamine-containing waters. *Water Res.* **2008,** *42* (4–5), 863–870.

Agency for Toxic Substances and Disease Registry (ATSDR). Toxicological Profile for Perfluoroalkyls. U.S. Department of Health and Human Services, Public Health Service, Atlanta, GA, 2009.

ATSDR. Perfluorochemical Serum Sampling in the Vicinity of Decatur, Alabama, Morgan, Lawrence and Limestone Counties. U.S. Department of Health and Human Services, Public Health Service, Atlanta, GA, 2013.

Becker, A. M.; Gerstmann, S.; Frank, H. Perfluorooctanoic acid and perfluorooctane sulfonate in the sediment of the Roter Main River, Bayreuth, Germany. *Environ. Pollut.* **2008,** *156* (3), 818–820.

Bolton, J. R.; Fitzsimmons, S. R.; Patel, M.; Lem, W.; Gigliotti, J. Experimental determination of the fluence (UV dose) required in the UV photodegradation of NDMA in a treated waste water. *Proc. Am. Wat. Works Assoc. Wat. Qual. Tech. Conf.*, 2002.

Boulanger, B.; Vargo, J. D.; Schnoor, J. L.; Hornbuckle, K. C. Evaluation of perfluorooctane surfactants in a wastewater treatment system and in a commercial surface protection product. *Environ. Sci. Technol.* **2005,** *39* (15), 5524–5530.

Buck, R. C.; Franklin, J.; Berger, U.; Conder, J. M.; Cousins, I. T.; de Voogt, P.; Jensen, A. A.; Kannan, K.; Mabury, S. A.; van Leeuwen, S. P. J. Perfluoroalkyl and polyfluoroalkyl substances in the environment: Terminology, classification, and origins. *Integr. Environ. Assess. Mgmt.* **2011,** *7* (4), 513–541.

Cao, M. H.; Wang, B. B.; Yu, H. S.; Wang, L. L.; Yuan, S. H.; Chen, J. Photochemical decomposition of perfluorooctanoic acid in aqueous periodate with VUV and UV light irradiation. *J. Hazard. Mater.* **2010,** *179* (1–3), 1143–1146.

Chen, H.-W.; Chen, C.-Y.; Wang, G.-S. Performance evaluation of the UV/H_2O_2 process on selected nitrogenous organic compounds: Reductions of organic contents vs. corresponding C-, N-DBPs formations. *Chemosphere* **2011,** *85* (4), 591–597.

Chen, J.; Zhang, P.-y.; Liu, J. Photodegradation of perfluorooctanoic acid by 185 nm vacuum ultraviolet light. *J. Environ. Sci.* **2007,** *19* (4), 387–390.

Chen, W.-H.; Young, T. M. NDMA formation during chlorination and chloramination of aqueous diuron solutions. *Environ. Sci. Technol.* **2008,** *42* (4), 1072–1077.

Chen, W.; Westerhoff, P.; Leenheer, J. A.; Booksh, K. Fluorescence excitation−emission matrix regional integration to quantify spectra for dissolved organic matter. *Environ. Sci. Technol.* **2003,** *37* (24), 5701–5710.

Chen, Z.; Valentine, R. L. Formation of *N*-nitrosodimethylamine (NDMA) from humic substances in natural water. *Environ. Sci. Technol.* **2007,** *41* (17), 6059–6065.

Choi, J.; Valentine, R. L. Formation of *N*-nitrosodimethylamine (NDMA) from reaction of monochloramine: A new disinfection by-product. *Wat. Res.* **2002,** *36* (4), 817–824.

City of Reno. Removing refractory organics from wastewater using MF-O_3-BAC treatment. Draft report prepared by Stantec, 2010.

Clesceri, L. S.; Greenberg, A. E.; Eaton, A. D. *Standard Methods for the Examination of Water and Wastewater*, 20th ed. American Public Health Association: Washington, DC, 1998.

Cushing, R. S.; Mackey, E. D.; Bolton, J. R.; Stefan, M. I. Impact of common water treatment chemicals on UV disinfection. *Proc. Am. Wat. Works Assoc. Ann. Conf.*, 2001.

Dai, N.; Mitch, W. A. Relative importance of *N*-nitrosodimethylamine compared to total N-nitrosamines in drinking waters. *Environ. Sci. Technol.* **2013,** *47* (8), 3648–3656.

Deng, S.; Zhou, Q.; Yu, G.; Huang, J.; Fan, Q. Removal of perfluorooctanoate from surface water by polyaluminium chloride coagulation. *Wat. Res.* **2011,** *45* (4), 1774–1780.

Dickenson, E.; Higgins, C. The removal of perfluoroalkyl and polyfluoroalkyl substances by North American water treatment practices. Water Research Foundation: Denver CO, 2013.

Dinglasan, M. J. A.; Ye, Y.; Edwards, E. A.; Mabury, S. A. Fluorotelomer alcohol biodegradation yields poly- and perfluorinated acids. *Environ. Sci. Technol.* **2004,** *38* (10), 2857–2864.

Drewes, J. E.; Hoppe, C.; Jennings, T. Fate and transport of *N*-nitrosamines under conditions simulating full-scale groundwater recharge operations. *Wat. Environ. Res.* **2006,** *78* (13), 2466–2473.

Dudley, L.-A. M. B. Removal of perfluorinated compounds by powdered activated carbon, superfine powdered activated carbon, and anion exchange resins. M.S. Thesis, North Carolina State University, Raleigh, NC, 2012.

Eggen, T.; Moeder, M.; Arukwe, A. Municipal landfill leachates: A significant source for new and emerging pollutants. *Sci. Total Environ*. **2010,** *408* (21), 5147–5157

Farré, M. J.; Keller, J.; Holling, N.; Poussade, Y.; Gernjak, W. Occurrence of N-nitrosodimethylamine precursors in wastewater treatment plant effluent and their fate during ultrafiltration–reverse osmosis membrane treatment. *Wat. Sci. Technol.* **2011a**, *63* (4), 605–612.

Farré, M. J.; Reungoat, J.; Argaud, F. X.; Rattier, M.; Keller, J.; Gernjak, W. Fate of *N*-nitrosodimethylamine, trihalomethane and haloacetic acid precursors in tertiary treatment including biofiltration. *Wat. Res.* **2011b,** *45* (17), 5695–5704.

Fleming, E. C.; Pennington, J. C.; Wachob, B. G.; Howe, R. A.; Hill, D. O. Removal of *N*-nitrosodimethylamine from waters using physical-chemical techniques. *J. Hazard. Mater.* **1996,** *51* (1–3), 151–164.

Fujii, S.; Polprasert, C.; Tanaka, S.; Lien, N. P. H.; Qiu, Y. New POPs in the water environment: Distribution, bioaccumulation and treatment of perfluorinated compound—A review paper. *J. Wat. Supply: Res. Technol. AQUA* **2007,** *56* (5), 313–326.

Gauthier, S. A.; Mabury, S. A. Aqueous photolysis of 8:2 fluorotelomer alcohol. *Environ. Toxicol. Chem.* **2005**, *24* (8), 1837–1846.

Gerrity, D.; Gamage, S.; Holady, J. C.; Mawhinney, D. B.; Quiñones, O.; Trenholm, R. A.; Snyder, S. A. Pilot-scale evaluation of ozone and biological activated carbon for trace organic contaminant mitigation and disinfection. *Wat. Res.* **2011,** *45* (5), 2155–2165.

Giesy, J. P.; Kannan, K. Global distribution of perfluorooctane sulfonate in wildlife. *Environ. Sci. Technol.* **2001,** *35* (7), 1339–1342.

Giri, R. R.; Ozaki, H.; Okada, T.; Takikita, S.; Taniguchi, S.; Takanami, R. Water matrix effect on UV photodegradation of perfluorooctanoic acid. *Wat. Sci. Technol.* **2011,** *64* (10), 1980–1986.

Gunnison, D.; Zappi, M. E.; Teeter, C.; Pennington, J. C.; Bajpai, R. Attenuation mechanisms of *N*-nitrosodimethylamine at an operating intercept and treat groundwater remediation system. *J. Hazard. Mater.* **2000,** *73* (2), 179–197.

Guo, R.; Sim, W.-J.; Lee, E.-S.; Lee, J.-H.; Oh, J.-E. Evaluation of the fate of perfluoroalkyl compounds in wastewater treatment plants. *Wat. Res.* **2010,** *44* (11), 3476–3486.

Higgins, C. P.; Luthy, R. G. Sorption of perfluorinated surfactants on sediments. *Environ. Sci. Technol.* **2006,** *40* (23), 7251–7256.

Ho, K.-L.; Chung, Y.-C.; Lin, Y.-H.; Tseng, C.-P. Biofiltration of trimethylamine, dimethylamine, and methylamine by immobilized Paracoccus sp. CP2 and Arthrobacter sp. CP1. *Chemosphere* **2008,** *72* (2), 250–256.

Hoehn, E.; Plumlee, M. H.; Reinhard, M. Natural attenuation of downwelling streams for perfluorochemicals and other emerging contaminants. *Water Sci. Technol.* **2007**, *56* (11), 59–64.

Hollender, J.; Zimmermann, S. G.; Koepke, S.; Krauss, M.; McArdell, C. S.; Ort, C.; Singer, H.; von Gunten, U.; Siegrist, H. Elimination of organic micropollutants in a municipal wastewater treatment plant upgraded with a full-scale post-ozonation followed by sand filtration. *Environ. Sci. Technol.* **2009,** *43* (20), 7862–7869.

Hori, H.; Yamamoto, A.; Hayakawa, E.; Taniyasu, S.; Yamashita, N.; Kutsuna, S.; Kiatagawa, H.; Arakawa, R. Efficient decomposition of environmentally persistent perfluorocarboxylic acids by use of persulfate as a photochemical oxidant. *Environ. Sci. Technol.* **2005,** *39* (7), 2383–2388.

Kemper, J. M.; Walse, S. S.; Mitch, W. A. Quaternary amines as nitrosamine precursors: A role for consumer products? *Environ. Sci. Technol.* **2010,** *44* (4), 1224–1231.

Kim, S.-K.; Kannan, K. Perfluorinated acids in air, rain, snow, surface runoff, and lakes: Relative importance of pathways to contamination of urban lakes. *Environ. Sci. Technol.* **2007,** *41* (24), 8328–8334.

Kommineni, S.; Ela, W. P.; Arnold, R. G.; Huling, S. G.; Hester, B. J.; Betterton, E. A. NDMA treatment by sequential GAC adsorption and fenton-driven destruction. *Environ. Eng. Sci.* **2003,** *20* (4), 361–373.

Kosaka, K.; Asami, M.; Konno, Y.; Oya, M.; Kunikane, S. Identification of antiyellowing agents as precursors of *N*-nitrosodimethylamine production on ozonation from sewage treatment plant influent. *Environ. Sci. Technol.* **2009,** *43* (14), 5236–5241.

Krasner, S. W.; Westerhoff, P.; Chen, B.; Rittman, B. E.; Amy, G. Occurrence of disinfection byproducts in United States wastewater treatment plant effluents. *Environ. Sci. Technol.* **2009,** *43* (21), 8320–8325.

Krasner, S. W.; Mitch, W. A.; McCurry, D. L.; Hanigan, D.; Westerhoff, P. Formation, precursors, control, and occurrence of nitrosamines in drinking water: A review. *Wat. Res.* **2013,** *47* (13), 4433–4450.

Krauss, M.; Longree, P.; Dorusch, F.; Ort, C.; Hollender, J. Occurrence and removal of *N*-nitrosamines in wastewater treatment plants. *Wat. Res.* **2009,** *43* (17), 4381–44391.

Krauss, M.; Longree, P.; Van Houtte, E.; Cauwenberghs, J.; Hollender, J. Assessing the fate of nitrosamine precursors in wastewater treatment by physicochemical fractionation. *Environ. Sci. Technol.* **2010,** *44* (20), 7871–7877.

Kruithof, J. C.; Kamp, P. C.; Martijn, B. J. UV/H_2O_2 treatment: A practical solution for organic contaminant control and primary disinfection. *Ozone: Sci. Eng.* **2007,** *29* (4), 273–280.

Kulshrestha, P.; McKinstry, K. C.; Fernandez, B. O.; Feelisch, M.; Mitch, W. A. Application of an optimized total *N*-nitrosamine (TONO) Assay to pools: Placing *N*-nitrosodimethylamine (NDMA) determinations into perspective. *Environ. Sci. Technol.* **2010,** *44* (9), 3369–3375.

Kunacheva, C.; Fujii, S.; Tanaka, S.; Boontanon, S. K.; Poothong, S.; Wongwatthana, T.; Shivakoti, B. R. Perfluorinated compounds contamination in tap water and bottled water in Bangkok, Thailand. *J. Wat. Supply: Res. Technol. AQUA* **2010,** *59* (5), 345–354.

Lampert, D. J.; Frisch, M. A.; Speitel, G. E., Jr. Removal of perfluorooctanoic acid and perfluorooctane sulfonate from wastewater by ion exchange. *Practice Periodical of Hazardous, Toxic, and Radioactive Waste Management* **2007,** *11* (1), 60–68.

LaZerte, J. D.; Hals, L. J.; Reid, T. S.; Smith, G. H. Pyrolyses of the salts of the perfluoro carboxylic acids. *J. Am. Chem. Soc.* **1953,** *75*(18), 4525–4528.

Lee, C.; Schmidt, C.; Yoon, J.; von Gunten, U. Oxidation of *N*-nitrosodimethylamine (NDMA) precursors with ozone and chlorine dioxide: Kinetics and effect on NDMA formation potential. *Environ. Sci. Technol.* **2007a,** *41* (6), 2056–2063.

Lee, C.; Yoon, J.; von Gunten, U. Oxidative degradation of *N*-nitrosodimethylamine by conventional ozonation and the advanced oxidation process ozone/hydrogen peroxide. *Wat. Res.* **2007b,** *41* (3), 581–590.

Lee, H.; Deon, J.; Mabury, S. A. Biodegradation of polyfluoroalkyl phosphates as a source of perfluorinated acids to the environment. *Environ. Sci. Technol.* **2010a,** *44* (9), 3305–3310.

Lee, Y.-C.; Lo, S.-L.; Chiueh, P.-T.; Liou, Y.-H.; Chen, M.-L. Microwave-hydrothermal decomposition of perfluorooctanoic acid in water by iron-activated persulfate oxidation. *Wat. Res.* **2010b,** *44* (3), 886–892.

Lindstrom, A. B.; Strynar, M. J.; Delinsky, A. D.; Nakayama, S. F.; McMillan, L.; Libelo, E. L.; Neill, M.; Thomas, L. Application of WWTP biosolids and resulting perfluorinated compound contamination of surface and well water in Decatur, Alabama, USA. *Environ. Sci. Technol.* **2011,** *45* (19), 8015–8021.

Loewen, M.; Halldorson, T.; Wang, F.; Tomy, G. Fluorotelomer carboxylic acids and PFOS in rainwater from an urban center in Canada. *Environ. Sci. Technol.* **2005,** *39* (9), 2944–2951.

Martijn, B. J.; Fuller, A. L.; Malley, J. P.; Kruithof, J. C. Impact of IX-UF pretreatment on the feasibility of UV/H_2O_2 treatment for degradation of NDMA and 1,4-dioxane. *Ozone: Sci. Eng.* **2010,** *32* (6), 383–390.

Martin, J. W.; Mabury, S. A.; O'Brien, P. J. Metabolic products and pathways of fluorotelomer alcohols in isolated rat hepatocytes. *Chemico-Biological Interactions* **2005,** *155,* 165–180.

Martin, J. W.; Smithwick, M. M.; Braune, B. M.; Hoekstra, P. F.; Muir, D. C. G.; Mabury, S. A. Identification of long-chain perfluorinated acids in biota from the Canadian arctic. *Environ. Sci. Technol.* **2004,** *38* (2), 373–380.

Mitch, W. A.; Gerecke, A. C.; Sedlak, D. L. A *N*-nitrosodimethylamine (NDMA) precursor analysis for chlorination of water and wastewater. *Wat. Res.* **2003a,** *37* (15), 3733–3741.

Mitch, W. A.; Oelker, G. L.; Hawley, E. L.; Deeb, R. A.; Sedlak, D. L. Minimization of NDMA formation during chlorine disinfection of municipal wastewater by application of pre-formed chloramines. *Environ. Eng. Sci.* **2005,** *22* (6), 882–890.

Mitch, W. A.; Sedlak, D. L. Formation of *N*-nitrosodimethylamine (NDMA) from dimethylamine during chlorination. *Environ. Sci. Technol.* **2002,** *36* (4), 588–595.

Mitch, W. A.; Sharp, J. O.; Trussell, R. R.; Valentine, R. L.; Alvarez-Cohen, L.; Sedlak, D. L. *N*-nitrosodimethylamine (NDMA) as a drinking water contaminant: A review. *Environ. Eng. Sci.* **2003b,** *20* (5), 389–404.

Moody, C. A.; Field, J. A. Determination of perfluorocarboxylates in groundwater impacted by fire-fighting activity. *Environ. Sci. Technol.* **1999,** *33* (16), 2800–2806.

Moriwaki, H.; Takagi, Y.; Tanaka, M.; Tsuruho, K.; Okitsu, K.; Maeda, Y. Sonochemical decomposition of perfluorooctane sulfonate and perfluorooctanoic acid. *Environ. Sci. Technol.* **2005a,** *39* (9), 3388–3392.

Moriwaki, H.; Takagi, Y.; Tanaka, M.; Tsuruho, K.; Okitsu, K.; Maeda, Y. Sonochemical decomposition of perfluorooctane sulfonate and perfluorooctanoic acid. *Environ. Sci. Technol.* **2005b,** *39* (9), 3388–3392.

Munoz, F.; von Sonntag, C. The reactions of ozone with tertiary amines including the complexing agents nitrilotriacetic acid (NTA) and ethylenediaminetetraacetic acid (EDTA) in aqueous solution. *J. Chem. Soc., Perkin Transactions 2* **2000,** *0* (10), 2029–2033.

Murakami, M.; Shinohara, H.; Takada, H. Evaluation of wastewater and street runoff as sources of perfluorinated surfactants (PFSs). *Chemosphere* **2009,** *74* (4), 487–493.

Nalinakumari, B.; Cha, W.; Fox, P. Effects of primary substrate concentration on NDMA transport during simulated aquifer recharge. *J. Environ. Eng.* **2010,** *136* (4), 363–370.

Nawrocki, J.; Andrzejewski, P. Nitrosamines and water. *J. Hazard. Mater.* **2011**, *189* (1–2), 1–18.

Ochoa-Herrera, V.; Sierra-Alvarez, R. Removal of perfluorinated surfactants by sorption onto granular activated carbon, zeolite and sludge. *Chemosphere* **2008,** *72* (10), 1588–1593.

Oya, M.; Kosaka, K.; Asami, M.; Kunikane, S. Formation of *N*-nitrosodimethylamine (NDMA) by ozonation of dyes and related compounds. *Chemosphere* **2008,** *73* (11), 1724–1730.

Padhye, L.; Luzinova, Y.; Cho, M.; Mizaikoff, B.; Kim, J.-H.; Huang, C.-H. PolyDADMAC and dimethylamine as precursors of *N*-nitrosodimethylamine during ozonation: Reaction kinetics and mechanisms. *Environ. Sci. Technol.* **2011,** *45* (10), 4353–4359.

Padhye, L.; Wang, P.; Karanfil, T.; Huang, C.-H. Unexpected role of activated carbon in promoting transformation of secondary amines to N-nitrosamines. *Environ. Sci. Technol.* **2010,** *44* (11), 4161–4168.

Padhye, L. P.; Kim, J.-H.; Huang, C.-H. Oxidation of dithiocarbamates to yield N-nitrosamines by water disinfection oxidants. *Wat. Res.* **2013,** *47* (2), 725–736.

Park, S.-H.; Wei, S.; Mizaikoff, B.; Taylor, A. E.; Favero, C. D.; Huang, C.-H. Degradation of amine-based water treatment polymers during chloramination as *N*-nitrosodimethylamine (NDMA) precursors. *Environ. Sci. Technol.* **2009,** *43* (5), 1360–1366.

Pehlivanoglu-Mantas, E.; Hawley, E. L.; Deeb, R. A.; Sedlak, D. L. Formation of *N*-nitrosodimethylamine (NDMA) during chlorine disinfection of wastewater effluents prior to use in irrigation systems. *Wat. Res.* **2006,** *40* (2), 341–347.

Pehlivanoglu-Mantas, E.; Sedlak, D. L. Measurement of dissolved organic nitrogen forms in wastewater effluents: Concentrations, size distribution and NDMA formation potential. *Wat. Res.* **2008,** *42* (14), 3890–3898.

Peller, J.; Wiest, O.; Kamat, P. V. Mechanism of hydroxyl radical–induced breakdown of the herbicide 2,4-Dichlorophenoxyacetic acid (2,4-D). *Chem. Eur. J.* **2003,** *9* (21), 5379–5387.

Pisarenko, A. N.; Stanford, B. D.; Yan, D.; Gerrity, D.; Snyder, S. A. Effects of ozone and ozone/peroxide on trace organic contaminants and NDMA in drinking water and water reuse applications. *Wat. Res.* **2012,** *46* (2), 316–326.

Plumlee, M. H. Occurrence and photochemical fate of emerging contaminants: Nitrosamines and perfluorochemicals. Ph.D. Dissertation, Stanford University, 2008.

Plumlee, M. H.; Larabee, J.; Reinhard, M. Perfluorochemicals in water reuse. *Chemosphere* **2008a,** *72* (10), 1541–1547.

Plumlee, M. H.; López-Mesas, M.; Heidlberger, A.; Ishida, K. P.; Reinhard, M. *N*-nitrosodimethylamine (NDMA) removal by reverse osmosis and UV treatment and analysis via LC-MS/MS. *Wat. Res.* **2008b,** *42* (1–2), 347–355.

Plumlee, M. H.; McNeill, K.; Reinhard, M. Indirect photolysis of perfluorochemicals: Hydroxyl radical–initiated oxidation of N-ethyl perfluorooctane sulfonamido acetate (N-EtFOSAA) and other perfluoroalkanesulfonamides. *Environ. Sci. Technol.* **2009,** *43* (10), 3662–3668.

Qu, Y.; Zhang, C.; Li, F.; Chen, J.; Zhou, Q. Photo-reductive defluorination of perfluorooctanoic acid in water. *Wat. Res.* **2010,** *44* (9), 2939–2947.

Quiñones, O.; Snyder, S. A. Occurrence of perfluoroalkyl carboxylates and sulfonates in drinking water utilities and related waters from the United States. *Environ. Sci. Technol.* **2009,** *43* (24), 9089–9095.

Rakness, K. L.; Wert, E. C.; Elovitz, M.; Mahoney, S. Operator-friendly technique and quality control considerations for indigo colorimetric measurement of ozone residual. *Ozone: Sci. Eng.* **2010,** *32* (1), 33–42.

Rayne, S.; Forest, K. Perfluoroalkyl sulfonic and carboxylic acids: A critical review of physicochemical properties, levels and patterns in waters and wastewaters, and treatment methods. *J. Environ. Sci. Health—Part A: Toxic/Hazardous Substances and Environmental Engineering* **2009,** *44* (12), 1145–1199.

Reungoat, J.; Escher, B. I.; Macova, M.; Keller, J. Biofiltration of wastewater treatment plant effluent: Effective removal of pharmaceuticals and personal care products and reduction of toxicity. *Wat. Res.* **2011,** *45* (9), 2751–2762.

Schmidt, C. K.; Brauch, H.-J. N,N-dimethylsulfamide as precursor for *N*-nitrosodimethylamine (NDMA) formation upon ozonation and its fate during drinking water treatment. *Environ. Sci. Technol.* **2008,** *42* (17), 6340–6346.

Schreiber, I. M.; Mitch, W. A. Occurrence and fate of nitrosamines and nitrosamine precursors in wastewater-impacted surface waters using boron as a conservative tracer. *Environ. Sci. Technol.* **2006,** *40* (10), 3203–3210.

Schroder, H. F.; Meesters, R. J. W. Stability of fluorinated surfactants in advanced oxidation processes—A follow up of degradation products using flow injection-mass spectrometry, liquid chromatography-mass spectrometry and liquid chromatography–multiple stage mass spectrometry. *J. Chromatogr. A* **2005,** *1082,* 110–119.

Schultz, M. M.; Barofsky, D. F.; Field, J. A. Quantitative determination of fluorotelomer sulfonates in groundwater by LC MS/MS. *Environ. Sci. Technol.* **2004,** *38* (6), 1828–1835.

Schultz, M. M.; Higgins, C. P.; Huset, C. A.; Luthy, R. G.; Barofsky, D. F.; Field, J. A. Fluorochemical mass flows in a municipal wastewater treatment facility. *Environ. Sci. Technol.* **2006,** *40* (23), 7350–7357.

Sedlak, D. L.; Deeb, R. A.; Hawley, E. L.; Mitch, W. A.; Durbin, T. D.; Mowbray, S.; Carr, S. Sources and fate of nitrosodimethylamine and its precursors in municipal wastewater treatment plants. *Wat. Environ. Res.* **2005,** *77* (1), 32–39.

Selbes, M.; Kim, D.; Ates, N.; Karanfil, T. The roles of tertiary amine structure, background organic matter and chloramine species on NDMA formation. *Wat. Res.* **2013,** *47* (2), 945–953.

Shah, A. D.; Mitch, W. A. Halonitroalkanes, halonitriles, haloamides, and N-nitrosamines: A critical review of nitrogenous disinfection byproduct formation pathways. *Environ. Sci. Technol.* **2012,** *46* (1), 119–131.

Sharp, J. O.; Wood, T. K.; Alvarez-Cohen, L. Aerobic biodegradation of N-nitrosodimethylamine (NDMA) by axenic bacterial strains. *Biotechnol. Bioeng.* **2005,** *89* (5), 608–618.

Sharpless, C. M.; Linden, K. G. Experimental and model comparisons of low- and medium-pressure Hg lamps for the direct and H_2O_2 assisted UV photodegradation of *N*-nitrosodimethylamine in simulated drinking water. *Environ. Sci. Technol.* **2003,** *37* (9), 1933–1940.

Sharpless, C. M.; Linden, K. G. Interpreting collimated beam ultraviolet photolysis rate data in terms of electrical efficiency of treatment. *J. Environ. Eng. Sci.* **2005,** *4* (SUPPL. 1), S19–S26.

Shaw, S.; Berger, M. L.; Brenner, D.; Tao, L.; Wu, Q.; Kannan, K. Specific accumulation of perfluorochemicals in harbor seals (Phoca vitulina concolor) from the northwest Atlantic. *Chemosphere* **2009,** *74* (8), 1037–1043.

Shen, R.; Andrews, S. A. Demonstration of 20 pharmaceuticals and personal care products (PPCPs) as nitrosamine precursors during chloramine disinfection. *Wat. Res.* **2011,** *45* (2), 944–952.

Shivakoti, B. R.; Fujii, S.; Nozoe, M.; Tanaka, S.; Kunacheva, C. Perfluorinated chemicals (PFCs) in water purification plants (WPPs) with advanced treatment processes. *Wat. Sci.Technol.: Water Supply* **2010,** *10* (1), 87–95.

Shoeib, M.; Harner, T.; Vlahos, P. Perfluorinated chemicals in the arctic atmosphere. *Environ. Sci. Technol.* **2006,** *40* (24), 7577–7583.

Simcik, M. F.; Dorweiler, K. J. Ratio of perfluorochemical concentrations as a tracer of atmospheric deposition to surface waters. *Environ. Sci. Technol.* **2005,** *39* (22), 8678–8683.

Sinclair, E.; Kannan, K. Mass loading and fate of perfluoroalkyl surfactants in wastewater treatment plants. *Environ. Sci. Technol.* **2006,** *40* (5), 1408–1414.

Stahl, L. L.; Snyder, B. D.; Olsen, A. R.; Pitt, J. L. Contaminants in fish tissue from US lakes and reservoirs: A national probabilistic study. *Environmental Monitoring and Assessment* **2009,** *150,* 3–19.

Stanford, B. D.; Pisarenko, A. N.; Holbrook, D. R.; Snyder, S. A. Preozonation effects on the reduction of reverse osmosis membrane fouling in water reuse. *Ozone: Sci. Eng.* **2011,** *33,* 379–388.

Steinle-Darling, E.; Reinhard, M. Nanofiltration for trace organic contaminant removal: Structure, solution, and membrane fouling effects on the rejection of perfluorochemicals. *Environ. Sci. Technol.* **2008,** *42* (14), 5292–5297.

Steinle-Darling, E.; Zedda, M.; Plumlee, M. H.; Ridgway, H. F.; Reinhard, M. Evaluating the impacts of membrane type, coating, fouling, chemical properties and water chemistry on reverse osmosis rejection of seven nitrosoalklyamines, including NDMA. *Wat. Res.* **2007,** *41* (17), 3959–3967.

Takagi, S.; Adachi, F.; Miyano, K.; Koizumi, Y.; Tanaka, H.; Mimura, M.; Watanabe, I.; Tanabe, S.; Kannan, K. Perfluorooctanesulfonate and perfluorooctanoate in raw and treated tap water from Osaka, Japan. *Chemosphere* **2008,** *72* (10), 1409–1412.

Takagi, S.; Adachi, F.; Miyano, K.; Koizumi, Y.; Tanaka, H.; Watanabe, I.; Tanabe, S.; Kannan, K. Fate of perfluorooctanesulfonate and perfluorooctanoate in drinking water treatment processes. *Wat. Res.* **2011,** *45* (13), 3925–3932.

Tang, C. Y.; Fu, Q. S.; Criddle, C. S.; Leckie, J. O. Effect of flux (transmembrane pressure) and membrane properties on fouling and rejection of reverse osmosis and nanofiltration membranes treating perfluorooctane sulfonate containing wastewater. *Environ. Sci. Technol.* **2007,** *41* (6), 2008–2014.

Thompson, J.; Eaglesham, G.; Reungoat, J.; Poussade, Y.; Bartkow, M.; Lawrence, M.; Mueller, J. F. Removal of PFOS, PFOA and other perfluoroalkyl acids at water reclamation plants in South East Queensland Australia. *Chemosphere* **2011,** *82* (1), 9–17.

Toms, L.-M. L.; Calafat, A. M.; Kato, K.; Thompson, J.; Harden, F.; Hobson, P.; Sjodin, A.; Mueller, J. F. Polyfluoroalkyl chemicals in pooled blood serum from infants, children, and adults in Australia. *Environ. Sci. Technol.* **2009,** *43* (11), 4194–4199.

Tsai, Y.-T.; Yu-Chen Lin, A.; Weng, Y.-H.; Li, K.-C. Treatment of perfluorinated chemicals by electro-microfiltration. *Environ. Sci. Technol.* **2010,** *44* (20), 7914–7920.

United States Environmental Protection Agency (US EPA). Technical Fact Sheet—*N*-Nitroso-dimethylamine (NDMA). National Service Center for Environmental Publications, 2012.

Vanderford, B. J.; Rosario-Ortiz, F. L.; Snyder, S. A. Analysis of p-chlorobenzoic acid in water by liquid chromatography–tandem mass spectrometry. *J. Chromatogr. A* **2007,** *1164* (1–2), 219–223.

von Gunten, U.; Salhi, E.; Schmidt, C. K.; Arnold, W. A. Kinetics and mechanisms of *N*-nitrosodimethylamine formation upon ozonation of N,N-dimethylsulfamide-containing waters: Bromide catalysis. *Environ. Sci. Technol.* **2010,** *44* (15), 5762–5768.

Wang, N.; Szostek, B.; Buck, R. C.; Folsom, P. W.; Sulecki, L. M.; Capka, V.; Berti, W. R.; Gannon, J. T. Fluorotelomer alcohol biodegradation—Direct evidence that perfluorinated carbon chains break down. *Environ. Sci. Technol.* **2005,** *39* (19), 7516–7528.

Wang, W.; Ren, S.; Zhang, H.; Yu, J.; An, W.; Hu, J.; Yang, M. Occurrence of nine nitrosamines and secondary amines in source water and drinking water: Potential of secondary amines as nitrosamine precursors. *Wat. Res.* **2011,** *45* (16), 4930–4938.

Wang, Y.; Zhang, P.; Pan, G.; Chen, H. Ferric ion mediated photochemical decomposition of perfluorooctanoic acid (PFOA) by 254 nm UV light. *J. Hazard. Mater.* **2008,** *160* (1), 181–186.

Wert, E. C.; Rosario-Ortiz, F. L.; Snyder, S. A. Effect of ozone exposure on the oxidation of trace organic contaminants in wastewater. *Wat. Res.* **2009,** *43* (4), 1005–1014.

Xu, B.; Chen, Z.; Qi, F.; Ma, J.; Wu, F. Inhibiting the regeneration of *N*-nitrosodimethylamine in drinking water by UV photolysis combined with ozonation. *J. Hazard. Mater.* **2009a,** *168* (1), 108–114.

Xu, B.; Chen Zhonglin, Z.; Qi, F.; Ma, J.; Wu, F. Comparison of *N*-nitrosodiethylamine degradation in water by UV irradiation and UV/O_3: Efficiency, product and mechanism. *J. Hazard. Mater.* **2010,** *179* (1–3), 976–982.

Xu, B.; Chen, Z.; Qi, F.; Shen, J.; Wu, F. Factors influencing the photodegradation of N-nitrosodimethylamine in drinking water. *Frontiers of Environmental Science & Engineering in China* **2009b,** *3* (1), 91–97.

Yamamoto, T.; Noma, Y.; Sakai, S.-i.; Shibata, Y. Photodegradation of perfluorooctane sulfonate by UV irradiation in water and alkaline 2-propanol. *Environ. Sci. Technol.* **2007,** *41* (16), 5660–5665.

Yamashita, N.; Kannan, K.; Taniyasu, S.; Horii, Y.; Petrick, G.; Gamo, T. A global survey of perfluorinated acids in oceans. *Mar. Pollut. Bull.* **2005**, *51* (8-12), 658–668.

Yangali-Quintanilla, V.; Sadmani, A.; McConville, M.; Kennedy, M.; Amy, G. A QSAR model for predicting rejection of emerging contaminants (pharmaceuticals, endocrine disruptors) by nanofiltration membranes. *Water Res.* **2010**, *44* (2), 373–384.

Yoon, S.; Nakada, N.; Tanaka, H. Occurrence and removal of NDMA and NDMA formation potential in wastewater treatment plants. *J. Hazard. Mater.* **2011,** *190* (1–3), 897–902.

Yu, J.; Hu, J.; Tanaka, S.; Fujii, S. Perfluorooctane sulfonate (PFOS) and perfluorooctanoic acid (PFOA) in sewage treatment plants. *Wat. Res.* **2009a,** *43* (9), 2399–2408.

Yu, Q.; Zhang, R.; Deng, S.; Huang, J.; Yu, G. Sorption of perfluorooctane sulfonate and perfluorooctanoate on activated carbons and resin: Kinetic and isotherm study. *Wat. Res.* **2009b,** *43* (4), 1150–1158.

Zhao, B.; Zhang, P. Photocatalytic decomposition of perfluorooctanoic acid with -Ga_2O_3 wide bandgap photocatalyst. *Catal. Commun.* **2009,** *10* (8), 1184–1187.

Zhao, D.; Cheng, J.; Vecitis, C. D.; Hoffmann, M. R. Sorption of perfluorochemicals to granular activated carbon in the presence of ultrasound. *J. Phys. Chem. A* **2011,** *115* (11), 2250–2257.

Zhao, Y.-Y.; Boyd, J. M.; Woodbeck, M.; Andrews, R. C.; Qin, F.; Hrudey, S. E.; Li, X.-F. Formation of *N*-nitrosamines from eleven disinfection treatments of seven different surface waters. *Environ. Sci. Technol.* **2008,** *42* (13), 4857–4862.

Zhou, Q.; Deng, S.; Zhang, Q.; Fan, Q.; Huang, J.; Yu, G. Sorption of perfluorooctane sulfonate and perfluorooctanoate on activated sludge. *Chemosphere* **2010,** *81* (4), 453–458.

Zhou, Q.; McCraven, S.; Garcia, J.; Gasca, M.; Johnson, T. A.; Motzer, W. E. Field evidence of biodegradation of *N*-nitrosodimethylamine (NDMA) in groundwater with incidental and active recycled water recharge. *Wat. Res.* **2009,** *43* (3), 793–805.

Zimmermann, S. G.; Wittenwiler, M.; Hollender, J.; Krauss, M.; Ort, C.; Siegrist, H.; von Gunten, U. Kinetic assessment and modeling of an ozonation step for full-scale municipal wastewater treatment: Micropollutant oxidation, by-product formation and disinfection. *Wat. Res.* **2011,** *45* (2), 605–617.

Appendix

Site Descriptions, Treatment Diagrams, and Data

Utility A-MO

Site description: The average daily flow at this site is approximately 30 million gallons per day, and it removes approximately 70,000 pounds of pollutants from the wastewater per day before it is discharged. After the large particles are removed by bar screen and primary clarifiers, the influent is split to two biological treatment systems (Plant #1 and #2), where the suspended and dissolved organic matters are removed. Following this step, the excess sludge is removed in clarifiers. The remaining suspended solids are removed in polishing filters. Finally, the flows from the two plants combine together for ozone disinfection (25,000 ft^3 O_2/hr at 3% O_3 or 6 mg O_3/L on average).

Process diagram

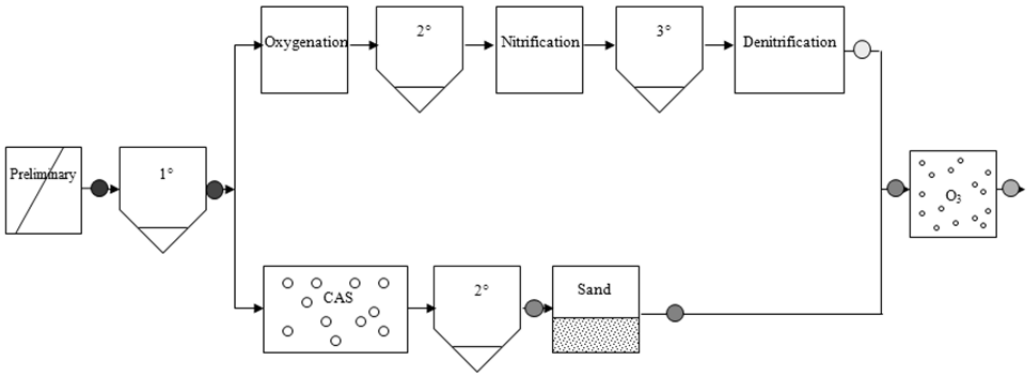

Sampling Locations on Site A-MO

Sample	Description
1	Primary Influent
2	Primary Effluent
3	Secondary Effluent
4	Sand Filter Effluent
5	Denitrification Effluent
6	Combined Ozone Influent
7	Ozone Effluent
8	Field Blank

Water Quality Data for Site A-MO

	Primary Influent	Primary Effluent	Secondary Effluent (Plant 2)	Combined Ozone Influent	Ozone Effluent
TKN (mg/L)	34.1				<0.03
Total Nitrogen (mg/L)		25	10	11	12
BOD (mg/L)					3
TSS (mg/L)	284	200	4		<1
NH_3-N (mg/L)	20.4	20.9	<0.1		<0.1
pH	7.28	7.48	7.67		7.87
Total Phosphorus (mg/L)	3.75				0.45

Note: Data from October 2011

Effluent Organic Matter Characterization Data for Site A-MO

	Primary Influent	Primary Effluent	Secondary Effluent (Plant 2)	Combined Ozone Influent	Ozone Effluent	Field Blank
UV_{254}	0.210	0.231	0.112	0.108	0.0661	<0.00200
UV_{280}	0.155	0.172	0.0844	0.0807	0.0427	<0.00200
TOC (mg/L)	19	44	6.7	5.8	6.1	0.33
TN (mg/L)	15	19	9.3	10	11	<0.20

Note: Data from May 1, 2012

Effluent Organic Matter Characterization Data for Site A-MO

	Primary Influent	Primary Effluent	Secondary Effluent (Plant 2)	Combined Ozone Influent	Ozone Effluent	Field Blank
UV_{254}		0.201	0.134	0.116	0.059	<0.00200
UV_{280}		0.148	0.108	0.0911	0.0387	<0.00200
TOC (mg/L)		45	5.7	4.9	4.8	<0.20
TN (mg/L)		25	10	11	12	<0.20

Note: Data from October 2011

October 10, 2011 Nitrosamines Data for Site A-MO

	Primary Effluent	Secondary Effluent (Plant 2)	Combined Ozone Influent	Ozone Effluent	Field Blank
NDMA	15	11	12	26	<2.5
NMEA	<2.5	<2.5	<2.5	<2.5	<2.5
NDEA	<5.0	<5.0	<5.0	<5.0	<5.0
NDPrA	<10	<10	<10	<10	<10
NMOR	<5.0	12	12	8.8	<5.0
NDBA	<10	<10	<10	<10	<10
NDPhA	16	<10	<10	<10	<10

Note: Nitrosamine concentrations in ng/L

May 1, 2012 Nitrosamines Data for Site A-MO

	Primary Influent	Primary Effluent	Secondary Effluent (Plant 2)	Combined Ozone Influent	Ozone Effluent	Field Blank
NDMA	<25	<25	7.8	6.3	14	<2.5
NMEA	<25	<25	<5.0	<5.0	<5.0	<2.5
NDEA	<50	<50	<10	<10	<10	<5.0
NDPrA	<100	<100	<20	<20	<20	<10
NMOR	65	58	22	23	22	<5.0
NDBA	<100	<100	<20	<20	<20	<10
NDPhA	<100	<100	<20	<20	<20	<10

Note: Nitrosamine concentrations in ng/L

October 2011 PFAS Data for Site A-MO

	Primary Effluent	Secondary Effluent (Plant 2)	Combined Ozone Influent	Ozone Effluent	Field Blank
PFBA	<25	<25	<25	<25	<5.0
PFPnA	<20	15	16	18	<2.0
PFHxA	3.2	15	15	17	<0.50
PFHpA	1.8	2.4	3.2	4.2	<0.50
PFOA	<5.0	14	15	16	<5.0
PFNA	0.84	2.1	2.5	2.9	<0.50
PFDA	0.62	1.3	1.3	3.9	<0.50
PFUnA	<0.50	<0.50	<0.50	<0.50	<0.50
PFDoA	<0.50	<0.50	<0.50	<0.50	<0.50
L-PFBS	2.2	2.5	3.5	5.2	<0.25
L-PFHxS	4.2	3.8	3.7	4.2	<0.25
L-PFOS	2.5	4.1	4.8	9.5	<0.25
L-PFDS	<0.10	<0.10	<0.10	<0.10	<0.10
FOSA	<0.25	<0.25	<0.25	0.44	<0.25
MeFOSAA	<0.25	0.32	<0.25	<0.25	<0.25
EtFOSAA	0.25	<0.25	<0.25	<0.25	<0.25
4:2 FTUCA	<2.0	<2.0	<2.0	<2.0	<2.0
6:2 FTUCA	<2.0	<2.0	<2.0	<2.0	<2.0
8:2 FTUCA	<2.0	<2.0	<2.0	<2.0	<2.0
10:2 FTUCA	<2.0	<2.0	<2.0	<2.0	<2.0
4:2 FtS	<0.50	<0.50	<0.50	<0.50	<0.50
6:2 FtS	10	1.9	1.7	1.6	<0.50
8:2 FtS	<0.50	<0.50	<0.50	<0.50	<0.50

Note: PFAS concentrations in ng/L

May 2012 PFAS Data for Site A-MO

	Primary Influent	Primary Effluent	Secondary Effluent (Plant 2)	Combined Ozone Influent	Ozone Effluent	Field Blank
PFBA	<100	<100	<100	<100	<100	<5.0
PFPnA	<40	<40	18	17	17	<2.0
PFHxA	8.5	8.6	26	24	28	<0.50
PFHpA	3.1	3.3	4.8	5.0	5.1	<0.50
PFOA	5.6	<5.0	20	19	20	<5.0
PFNA	1.5	1.2	2.7	2.9	3.3	<0.50
PFDA	<10	<10	3.7	3.5	3.3	<0.50
PFUnA	<0.50	<0.50	<0.50	<0.50	<0.50	<0.50
PFDoA	<0.25	<0.25	<0.25	<0.25	<0.25	<0.25
L-PFBS	6.8	7.0	7.6	7.0	8.4	<0.25
L-PFHxS	4.5	4.6	4.3	4.7	5.1	<0.25
L-PFOS	8.4	7.6	5.6	6.5	7.4	<0.25
L-PFDS	<0.10	<0.10	<0.10	<0.10	<0.10	<0.10
FOSA	<5.0	<5.0	0.39	0.36	0.38	<0.25
MeFOSAA	<0.25	<0.25	0.30	0.28	<0.25	<0.25
EtFOSAA	0.35	<0.25	<0.25	<0.25	<0.25	<0.25
4:2 FTUCA	<2.0	<2.0	<2.0	<2.0	<2.0	<2.0
6:2 FTUCA	<2.0	<2.0	<2.0	<2.0	<2.0	<2.0
8:2 FTUCA	<2.0	<2.0	<2.0	<2.0	<2.0	<2.0
10:2 FTUCA	<2.0	<2.0	<2.0	<2.0	<2.0	<2.0
4:2 FtS	<0.50	<0.50	<0.50	<0.50	<0.50	<0.50
6:2 FtS	1.4	2.5	1.1	1.6	2.2	<0.50
8:2 FtS	<0.50	<0.50	<0.50	<0.50	<0.50	<0.50

Note: PFAS concentrations in ng/L

Utility B-KY

Site description: The average daily flow at this site is approximately 9.9 million gallons per day. This site was originally constructed with grit removal, primary settling basins, a sludge thickener, and two-stage anaerobic digestion with sludge drying beds. Chlorine was used for disinfection prior to discharge. After a new secondary activated sludge oxidation ditch type wastewater treatment plant was built, the disinfection process was changed to ozone (average 3.3 mg O_3/L).

Process diagram

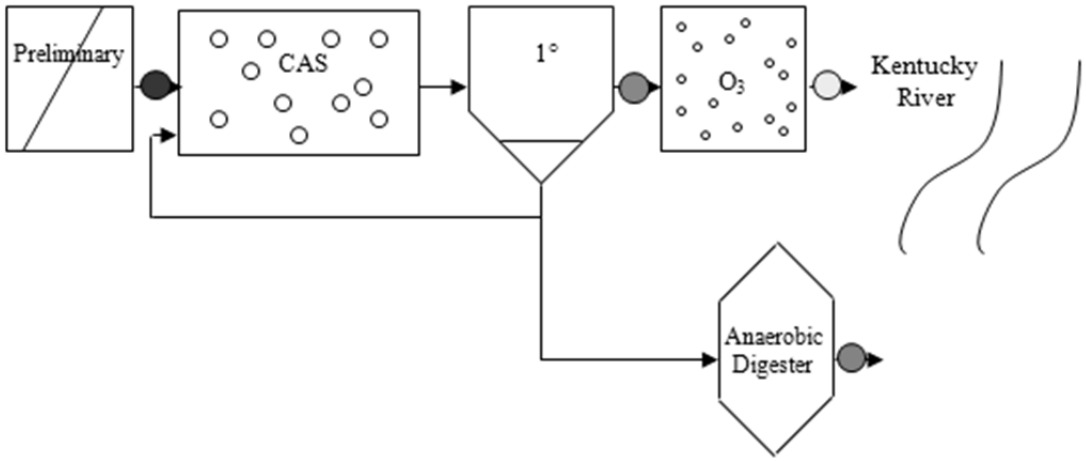

Sampling Locations on Site B-KY

Sample	Description
1	Oxidation Ditch Influent
2	Final Clarifier Effluent
3	Ozone Effluent
4	Digester Supernatant
5	Field Blank

Water Quality Data for Site B-KY

	Plant Influent	Oxidation Ditch Influent	Final Clarifier Effluent	Ozone Effluent	Digester Supernatant
pH	7.0			7.68	
NH_3 (mg/L)	73			0.285	
TSS (mg/L)	297			14.8	
COD (mg/L)	442			30	
Phosphorus (mg/L)	3.52			0.52	
Turbidity (NTU)				3.1	

Note: Data from March 7, 2012

Effluent Organic Matter Characterization Data for Site B-KY

	Oxidation Ditch Influent	Final Clarifier Effluent	Ozone Effluent	Digester Supernatant	Field Blank
UV_{254}	0.195	0.0762	0.0438	0.767	0.00238
UV_{280}	0.140	0.0569	0.0273	0.629	<0.00200
TN (mg/L)	18	4	4.4	14	<0.2
TOC (mg/L)	25	3.6	3.6	30	<0.2

Note: Data from March 7, 2012

Nitrosamines Data for Site B-KY

	Oxidation Ditch Influent	Final Clarifier Effluent	Ozone Effluent	Digester Supernatant	Field Blank
NDMA	25	<5.0	5.2	<5.0	<2.5
NMEA	<25	<5.0	<5.0	<5.0	<2.5
NDEA	<50	<10	<10	<10	<5.0
NDPrA	<100	<20	<20	<20	<10
NMOR	67	21	20	13	<5.0
NDBA	<100	<20	<20	<20	<10
NDPhA	<100	<20	<20	<20	<10

Note: Nitrosamine concentrations in ng/L

PFAS Data for Site B-KY

	Oxidation Ditch Influent	Final Clarifier Effluent	Ozone Effluent	Digester Supernatant	Field Blank
PFBA	<100	<100	<100	<100	<5.0
PFPnA	<40	10	13	160	<2.0
PFHxA	3.5	5.6	9.3	60	<0.50
PFHpA	2.3	1.2	1.8	11	<0.50
PFOA	<5.0	<5.0	8.0	100	<5.0
PFNA	0.67	<0.50	<0.50	2.5	<0.50
PFDA	1.5	<0.50	<0.50	1.7	<0.50
PFUnA	<0.50	<0.50	<0.50	<0.50	<0.50
PFDoA	<5.0	<0.25	<0.25	<5.0	<0.25
L-PFBS	6.2	6.6	8.5	50	<0.25
L-PFHxS	2.9	2.8	3.7	<5.0	<0.25
L-PFOS	5.3	0.82	1.2	2.7	<0.25
L-PFDS	0.11	<0.10	<0.10	<0.10	<0.10
FOSA	<0.25	<0.25	<0.25	<0.25	<0.25
MeFOSAA	<0.25	<0.25	<0.25	<0.25	<0.25
EtFOSAA	<0.25	<0.25	<0.25	<0.25	<0.25
4:2 FTUCA	<2.0	<2.0	<2.0	<40	<2.0
6:2 FTUCA	<2.0	<2.0	<2.0	<2.0	<2.0
8:2 FTUCA	<2.0	<2.0	<2.0	<2.0	<2.0
10:2 FTUCA	<2.0	<2.0	<2.0	<2.0	<2.0
4:2 FtS	1.0	<0.50	<0.50	<0.50	<0.50
6:2 FtS	<0.50	<0.50	<0.50	0.55	<0.50
8:2 FtS	<0.50	<0.50	<0.50	<0.50	<0.50

Note: PFAS concentrations in ng/L

Utility C-TX

Site description: The average daily flow at this site is approximately 10 million gallons per day. Preliminary treatment involves screening, degritting, sedimentation, and flow equalization. Secondary treatment uses a Zimpro™ PACT system with two-stage activated sludge and a powdered activated carbon (PAC) feed. The first stage has aeration and clarification. The second stage is denitrification utilizing methanol as a carbon source. Secondary treatment is followed by lime clarification. The pH is raised to 11 with lime and clarified. Then pH is lowered to 9.3 with carbon dioxide and clarified again. Additional carbon dioxide lowers the pH to 7.3, and then the treated wastewater is gravity filtered with granular activated carbon (GAC). The site uses ozone (1.0–1.3 mg O_3/L) for disinfection. After disinfection, the treated water goes though the biologically activated carbon (BAC) filter before discharge.

Process diagram

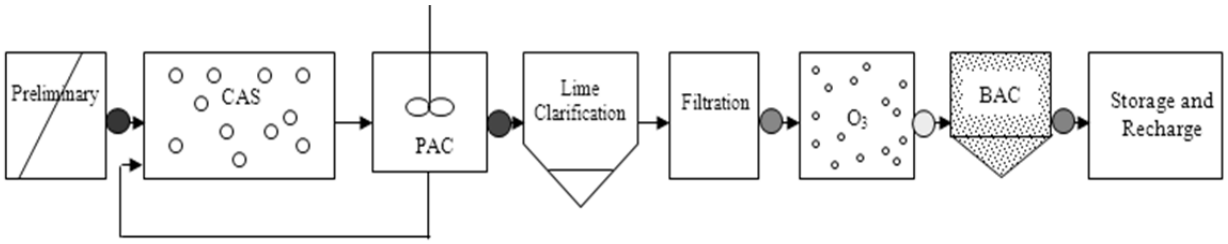

Sampling Locations on Site C-TX

Sample	Description
1	Primary Effluent
2	PACT Effluent
3	Filter Effluent
4	Ozone Effluent
5	BAC Effluent
6	Field Blank

Effluent Organic Matter Characterization Data for Site C-TX

	Primary Effluent	PACT Effluent	Filter Effluent	Ozone Effluent	BAC Effluent	Field Blank
UV_{254}	0.277	0.103	0.0665	0.0401	0.0354	<0.00200
UV_{280}	0.205	0.0803	0.0512	0.0264	0.0238	<0.00200
TN (mg/L)	37	2.6	4.5	4.1	4.0	<0.2
TOC (mg/L)	38	3.6	3.6	3.1	2.3	<0.2

Water Quality and Operation Data for Site C-TX

	PACT Stage 1	PACT Stage 2	BAC
SRT	10 days	36 days	N/A
Age of activated carbon	N/A	N/A	8-12 years

Nitrosamines Data for Site C-TX

	Primary Effluent	PACT Effluent	Filter Effluent	Ozone Effluent	BAC Effluent	Field Blank
NDMA	<25	<5.0	<5.0	<5.0	<5.0	<2.5
NMEA	<25	<5.0	<5.0	6.3	7.6	<2.5
NDEA	<50	<10	<10	<10	<10	<5.0
NDPrA	<100	<20	<20	<20	<20	<10
NMOR	<50	<10	<10	<10	<10	<5.0
NDBA	<100	<20	<20	<20	<20	<10
NDPhA	<100	<20	<20	<20	<20	<10

Note: Nitrosamine concentrations in ng/L

PFAS Data for Site C-TX

	Primary Effluent	PACT Effluent	Filter Effluent	Ozone Effluent	BAC Effluent	Field Blank
PFBA	<100	<5.0	<5.0	<100	<100	<5.0
PFPnA	<2.0	40	43	41	44	<2.0
PFHxA	<0.50	14	14	14	16	<0.50
PFHpA	<0.50	2.0	2	1.8	3.3	<0.50
PFOA	<5.0	15	18	18	24	<5.0
PFNA	0.79	3.1	3.9	3.5	5.3	<0.50
PFDA	<0.50	1.2	1.6	1.4	1.5	<0.50
PFUnA	<0.50	<0.50	<0.50	<0.50	<0.50	<0.50
PFDoA	<0.25	<0.25	<0.25	<0.25	<0.25	<0.25
L-PFBS	<5.0	4.1	6.8	12	17	<0.25
L-PFHxS	<0.25	0.91	1.4	1.3	1.6	<0.25
L-PFOS	<5.0	2.3	3.6	3.3	3.1	<0.25
L-PFDS	<0.10	<0.10	<0.10	<0.10	<0.10	<0.10
FOSA	<5.0	<0.25	<0.25	<0.25	<0.25	<0.25
MeFOSAA	<0.25	<0.25	<0.25	<0.25	<0.25	<0.25
EtFOSAA	<0.25	<0.25	<0.25	<0.25	<0.25	<0.25
8:2 FTUCA	<2.0	<2.0	<2.0	<2.0	<2.0	<2.0
4:2 FtS	1.0	<0.50	<0.50	<0.50	<0.50	<0.50
6:2 FtS	0.94	2.1	2.7	2.2	1.7	<0.50
8:2 FtS	<0.50	<0.50	<0.50	<0.50	<0.50	<0.50

Note: PFAS concentrations in ng/L

Utility D-GA

Site description: The treatment capacity of this site is approximately 42.5 million gallons per day. After passing through the primary sedimentation, activated sludge, and secondary sedimentation, lime is added for clarification. The incoming water is split into two filtration processes: recarbonation with CO_2 followed by dual-media filtration and strainers followed by ultrafiltration (UF). The water from the two filtration steps combine together for ozonation, BAC filtration, and final ozone disinfection. The applied ozone dose is typically 1.5 mg/L.

Process diagram

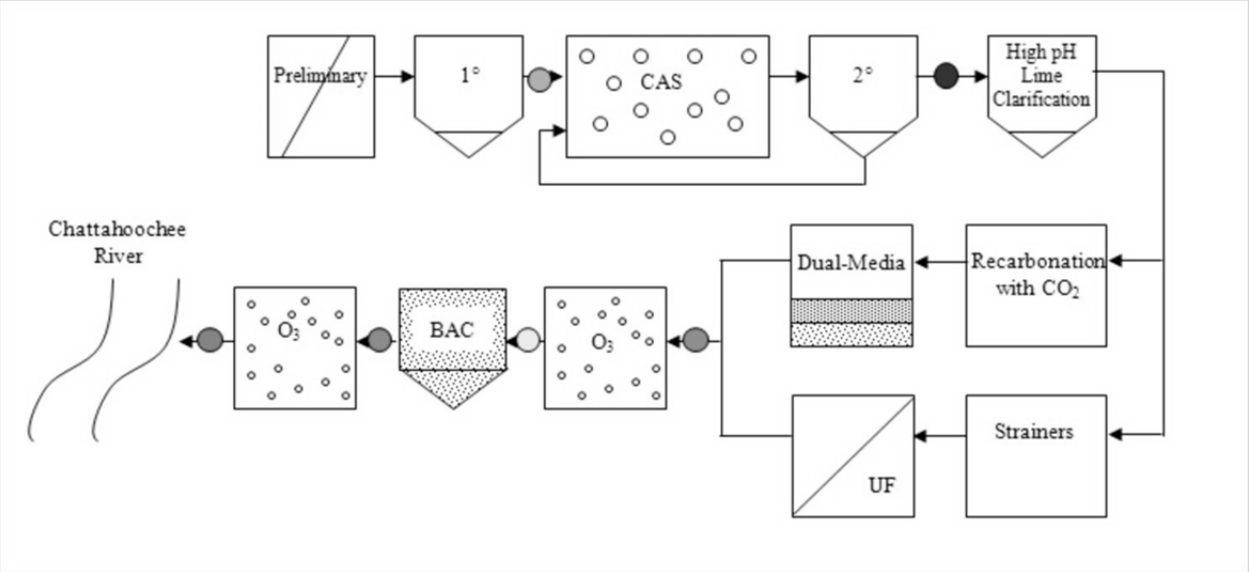

Sampling Locations on Site D-GA

Sample	Description
1	Primary Effluent
2	Secondary Effluent
3	Combined Filter Effluent/Pre-ozone Influent
4	Pre-ozone Effluent
5	BAC Effluent
6	Post-ozone Effluent
7	Field Blank

Effluent Organic Matter Characterization Data for Site D-GA

	Primary Effluent	Secondary Effluent	Combined Filter Effluent/ Pre-Ozone Influent	Pre-Ozone Effluent	BAC Effluent	Post-Ozone Effluent	Field Blank
UV 254	0.372	0.115	0.107	0.0816	0.0704	0.0473	<0.00200
UV 280	0.282	0.0918	0.0839	0.0608	0.0521	0.0322	<0.00200
TOC (mg/L)	42	5.3	5.0	5.0	4.1	3.8	<0.20
TN (mg/L)	44	16	15	15	15	15	<0.20

Water Quality and Operation Data for Site D-GA

Age of activated carbon for BAC	6–8 years

Nitrosamines Data for Site D-GA

	Primary Effluent	Secondary Effluent	Combined Filter Effluent/ Pre-Ozone Influent	Pre-Ozone Effluent	BAC Effluent	Post-Ozone Effluent	Field Blank
NDMA	42	6.8	5.9	9.2	<5.0	<5.0	<5.0
NMEA	<25	<5.0	<5.0	<5.0	<5.0	<5.0	<5.0
NDEA	<50	<10	<10	<10	<10	<10	<10
NDPrA	<100	<20	<20	<20	<20	<20	<20
NMOR	<50	<10	<10	<10	<10	<10	<10
NDBA	<100	<20	<20	<20	<20	<20	<20
NDPhA	<100	<20	<20	<20	<20	<20	<20

Note: Nitrosamine concentrations in ng/L

PFAS Data for Site D-GA

	Primary Effluent	Secondary Effluent	Combined Filter Effluent/ Pre-Ozone Influent	Pre-Ozone Effluent	BAC Effluent	Post-Ozone Effluent	Field Blank
PFBA	<100	<100	7.5	8.3	8.3	28	<5.0
PFPnA	7.4	27	26	27	28	26	<2.0
PFHxA	<10	18	18	22	22	21	<0.50
PFHpA	<10	3.5	4.5	3.9	5.0	4.9	<0.50
PFOA	<100	<100	23	26	33	35	<5.0
PFNA	6.6	6.2	7.1	7.9	8.4	8.6	<0.50
PFDA	2.1	1.8	2.7	3.0	3.1	3.3	<0.50
PFUnA	<10	<10	<0.50	<0.50	<0.50	<0.50	<0.50
PFDoA	<0.25	<0.25	<0.25	<0.25	<0.25	<0.25	<0.25
L-PFBS	4.3	5.6	5.6	8.6	9.6	13	<0.25
L-PFHxS	0.87	0.73	0.81	1.1	1.0	1.1	<0.25
L-PFOS	3.2	1.7	3.8	4.0	3.5	3.7	<0.25
FOSA	<5.0	<0.25	<0.25	<0.25	<0.25	<0.25	<0.25
MeFOSAA	<5.0	<0.25	<0.25	<0.25	<0.25	<0.25	<0.25
EtFOSAA	<5.0	<0.25	<0.25	<0.25	<0.25	<0.25	<0.25
4:2 FTUCA	<2.0	<2.0	<2.0	<2.0	<2.0	<2.0	<2.0
6:2 FTUCA	<2.0	<2.0	<2.0	<2.0	<2.0	<2.0	<2.0
8:2 FTUCA	<2.0	<2.0	<2.0	<2.0	<2.0	<2.0	<2.0
10:2 FTUCA	<2.0	<2.0	<2.0	<2.0	<2.0	<2.0	<2.0
4:2 FtS	<0.50	<0.50	<0.50	<0.50	<0.50	<0.50	<0.50
6:2 FtS	1.4	2.0	2.9	3.3	2.5	<0.50	<0.50
8:2 FtS	<0.50	<0.50	<0.50	<0.50	<0.50	<0.50	<0.50

Note: PFAS concentrations in ng/L

Utility E-GA

Site description: This facility receives wastewater (pH 10.5–11) from a denim mill and has a treatment capacity of 5.5 million gallons per day. Preliminary treatment involves aeration and pH adjustment with sulfuric acid to a range of 7.8 to 8.0. Secondary treatment, which consists of extended aeration, is followed by polymer addition for flocculation. Ozone (1200–1300 lb/day or 28–31 mg/L) is used for color removal and disinfection.

Process diagram

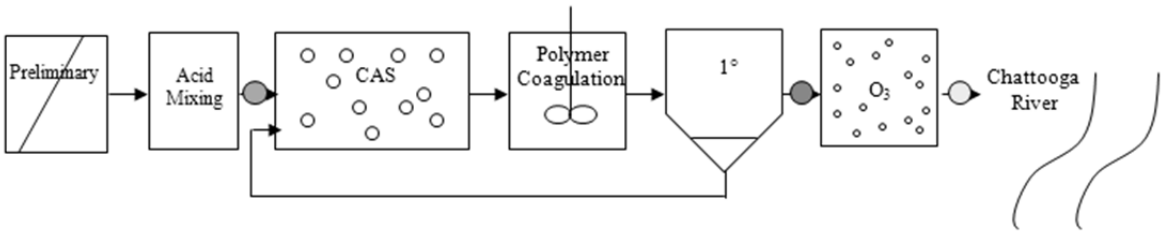

Sampling Locations on Site E-GA

Sample	Description
1	CAS Influent (post-EB and Acid Mixing Tank)
2	Pre-ozonation (postclarifier)
3	Post-ozonation
4	Field Blank

Water Quality Data for Site E-GA

	CAS Influent	Pre-Ozonation	Post-Ozonation	Field Blank
BOD_5 (mg/L)	311		7.54	
TSS (mg/L)	660		6	
Orthophosphate (mg/L)			2.81	
Phosphorus (mg/L)			9.56	
NH_3-N (mg/L)			0.14	
pH			7.53	
DO (mg/L)			16.25	

Note: Data from April 16–17, 2012

Effluent Organic Matter Characterization Data for Site E-GA

	CAS Influent	Pre-Ozonation	Post-Ozonation	Field Blank
UV_{254}	1.35	0.376	0.278	<0.00200
UV_{280}	0.989	0.313	0.208	<0.00200
TN (mg/L)	47	23	21	<0.20
TOC (mg/L)	120	25	28	<0.20

Nitrosamines Data for Site E-GA

	CAS Influent	Pre-Ozonation	Post-Ozonation	Field Blank
NDMA	89	72	85	<2.5
NMEA	<25	<5.0	<5.0	<2.5
NDEA	<50	20	19	<5.0
NDPrA	<100	<20	<20	<10
NMOR	<50	<10	<10	<5.0
NDBA	<100	<20	<20	<10
NDPhA	<100	<20	<20	<10

Note: Nitrosamine concentrations in ng/L

PFAS Data for Site E-GA

	CAS Influent	Pre-Ozonation	Post-Ozonation	Field Blank
PFBA	<100	350	390	<5.0
PFPnA	900	2900	2800	<2.0
PFHxA	590	1100	1100	0.55
PFHpA	310	930	760	<0.50
PFOA	93	220	190	<5.0
PFNA	40	59	51	<0.50
PFDA	35	70	95	<0.50
PFUnA	3.7	5.0	3.9	<0.50
PFDoA	1.8	0.91	0.51	<0.25
L-PFBS	7.1	8.6	5.8	<0.25
L-PFHxS	1.3	5.1	4.3	<0.25
L-PFOS	6.3	22	24	<0.25
L-PFDS	<0.10	<0.10	<0.10	<0.10
FOSA	<5.0	1.2	0.95	<0.25
MeFOSAA	8.2	8.2	8.7	<0.25
EtFOSAA	<0.25	<0.25	<0.25	<0.25
4:2 FTUCA	<2.0	<2.0	<2.0	<2.0
6:2 FTUCA	<2.0	<2.0	<2.0	<2.0
8:2 FTUCA	2.7	<2.0	<2.0	<2.0
10:2 FTUCA	<2.0	<2.0	<2.0	<2.0
4:2 FtS	<0.50	<0.50	<0.50	<0.50
6:2 FtS	<0.50	<0.50	0.5	<0.50
8:2 FtS	3.8	6.1	6.0	<0.50

Note: PFAS concentrations in ng/L

Utility F- QLD

Site description: The site has an average treatment capacity of 8,000 m^3 per day. Three ozonation steps are involved in this treatment process. The first one is pre-ozonation (2 mg/L) after denitrification. The second one is at a relatively low dosage (0.6–08 mgO_3/mg_{DOC}). The pre- and second ozone are separated by dissolved air flotation and sand filtration. The last step is the final disinfection.

Process diagram

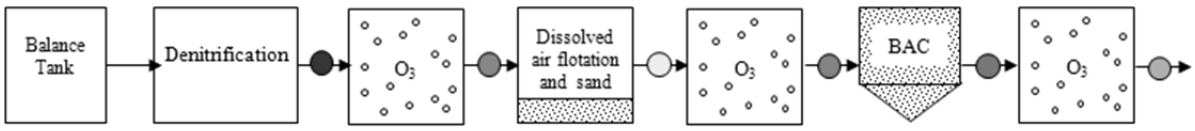

Sampling Locations on Site F-QLD:

Sample	Description
1 (not shown)	Primary Effluent
2 (not shown)	Secondary Effluent
3	Denitrification Effluent
4	Ozone 1 Effluent
5	Flotation/Filtration Effluent
6	Ozone 2 Effluent
7	BAC Effluent
8	Ozone 3 Effluent
9	Field Blank

Water Quality Data for Site F-QLD

Unavailable

Effluent Organic Matter Characterization Data for Site F-QLD

	Primary Eff.	Secondary Eff.	Denit. Eff.	Ozone 1 Eff.	Flotation/ Filtration Eff.	Ozone 2 Eff.	BAC Eff.	Ozone 3 Eff.	Field Blank
UV_{254}	0.587	0.221	0.214	0.204	0.131	0.0882	0.0591	0.0462	<0.00200
UV_{280}	0.463	0.170	0.162	0.155	0.0985	0.0616	0.0416	0.0296	<0.00200
TOC (mg/L)	100	10	9.5	9.8	6.6	6.0	4.1	4.0	<0.20
TN (mg/L)	46	9.5	3.6	3.7	4.0	4.2	4.1	4.2	<0.20

Nitrosamines Data for Site F-QLD

	Primary Eff.	Secondary Eff.	Denit. Eff.	Ozone 1 Eff.	Flotation/ Filtration Eff.	Ozone 2 Eff.	BAC Eff.	Ozone 3 Eff.	Field Blank
NDMA	<25	<5.0	<5.0	5.4	5.2	11	<5.0	<5.0	<25
NMEA	<25	<5.0	<5.0	<5.0	<5.0	<5.0	<5.0	<5.0	<2.5
NDEA	<50	<10	<10	<10	<10	<10	<10	<10	<5.0
NDPrA	<100	<20	<20	<20	<20	<20	<20	<20	<10
NMOR	<50	<10	<10	<10	<10	<10	<10	<10	<5.0
NDBA	<100	<20	<20	<20	<20	<20	<20	<20	<10
NDPhA	<100	<20	<20	<20	<20	<20	<20	<20	<10

Note: Nitrosamine concentrations in ng/L

PFAS Data for Site F-QLD

	Primary Eff.	Secondary Eff.	Denit. Eff.	Ozone 1 Eff.	Flotation/ Filtration Eff.	Ozone 2 Eff.	BAC Eff.	Ozone 3 Eff.	Field Blank
PFBA	<5.0	<5.0	<5.0	<5.0	<5.0	<5.0	6.1	<5.0	<5.0
PFPnA	7.5	6.7	6.2	6.6	7.3	7.3	7.9	8.4	<2.0
PFHxA	20	12	13	12	13	13	17	17	<0.50
PFHpA	8.5	4.9	4.7	4.2	4.5	5	7.2	7.5	<0.50
PFOA	20	17	17	16	15	16	32	32	<5.0
PFNA	1.4	1.1	1.1	1.1	0.8	0.62	1.4	1.6	<0.50
PFDA	0.99	1.6	1.3	1.3	<0.50	<0.50	<0.50	0.99	<0.50
PFUnA	<0.50	<0.50	<0.50	<0.50	<0.50	<0.50	<0.50	<0.50	<0.50
PFDoA	<0.25	<0.25	<0.25	<0.25	<0.25	<0.25	<0.25	<0.25	<0.25
L-PFBS	4.6	2.5	2.1	2.4	2.6	3.5	4.6	5.6	<0.25
L-PFHxS	11	5.6	5.7	5.5	4.8	5.4	6.9	7.8	<0.25
L-PFOS	3.9	3.9	3.7	3.7	1.5	0.83	0.97	1.8	<0.25
L-PFDS	<0.10	<0.10	<0.10	<0.10	<0.10	<0.10	<0.10	<0.10	<0.10
FOSA	<0.25	<0.25	<0.25	<0.25	<0.25	<0.25	<0.25	<0.25	<0.25
MeFOSAA	0.32	<0.25	<0.25	<0.25	<0.25	<0.25	<0.25	<0.25	<0.25
EtFOSAA	<0.25	<0.25	<0.25	<0.25	<0.25	<0.25	<0.25	<0.25	<0.25
4:2 FTUCA	<2.0	<2.0	<2.0	<2.0	<2.0	<2.0	<2.0	<2.0	<2.0
6:2 FTUCA	<2.0	<2.0	<2.0	<2.0	<2.0	<2.0	<2.0	<2.0	<2.0
8:2 FTUCA	<2.0	<2.0	<2.0	<2.0	<2.0	<2.0	<2.0	<2.0	<2.0
10:2 FTUCA	<2.0	<2.0	<2.0	<2.0	<2.0	<2.0	<2.0	<2.0	<2.0
4:2 FtS	<0.50	<0.50	<0.50	<0.50	<0.50	<0.50	<0.50	<0.50	<0.50
6:2 FtS	1.5	<0.50	<0.50	<0.50	<0.50	<0.50	1.1	1.1	<0.50
8:2 FtS	<0.50	<0.50	<0.50	<0.50	<0.50	<0.50	<0.50	<0.50	<0.50

Note: PFAS concentrations in ng/L

Utility H-CA

Site description: This facility has a treatment capacity of 70 million gallons per day and consists of advanced treatment. Incoming water is secondary effluent from a facility employing conventional activated sludge. Advanced treatment steps include microfiltration, reverse osmosis, and UV/H_2O_2 disinfection. Effluent is pumped into a groundwater aquifer.

Process diagram

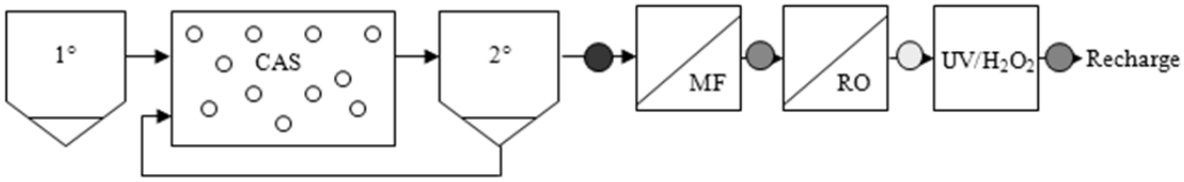

Sampling Locations on Site H-CA

Sample	Description
1 ●	MF Influent
2 ●	MF Effluent
3 ○	RO Permeate
4 ●	UV/H_2O_2 Effluent
5	Field Blank

Water Quality Data for Site H-CA

Unavailable

Effluent Organic Matter Characterization Data for Site H-CA

	MF Influent	MF Effluent	RO Permeate	RO Concentrate	UV/H_2O_2 Effluent	Field Blank
UV_{254}	0.153	0.125		0.696	0.00374	<0.00200
UV_{280}	0.112	0.0872	0.004	0.501	<0.00200	<0.00200
TOC (mg/L)	6.4	6.0	<0.20	33	<0.20	<0.20
Total Nitrogen (mg/L)	11	11	1.1	61	1.2	<0.20

Nitrosamines Data for Site H-CA

	MF Influent	MF Effluent	RO Permeate	RO Concentrate	UV/H_2O_2 Effluent	Field Blank
NDMA	16	42	20	100	<2.5	<2.5
NMEA	<5.0	<5.0	<5.0	<5.0	<5.0	<5.0
NDEA	<5.0	<5.0	<5.0	<5.0	<5.0	<5.0
NDPrA	<10	<10	<10	<10	<10	<10
NMOR	6.9	7.5	<5.0	18	<5.0	<5.0
NPyr	23	34	<10	150	<10	<10
NPip	<5.0	<5.0	<5.0	30	<5.0	<5.0
NDBA	<10	<10	<10	<10	<10	<10
NDPhA	<10	<10	<10	<10	<10	<10

Note: Nitrosamine concentrations in ng/L

PFAS Data for Site H-CA

Unavailable

Utility I-NV

Site description: This site treats an average of 75 million gallons per day, and the maximum capacity is 91 million gallons per day. It uses a conventional treatment process with grit basin, primary sedimentation, trickling filter, secondary sedimentation, activated sludge, filtration, and disinfection. Sodium hypochlorite is used for disinfection at this site.

Process diagram

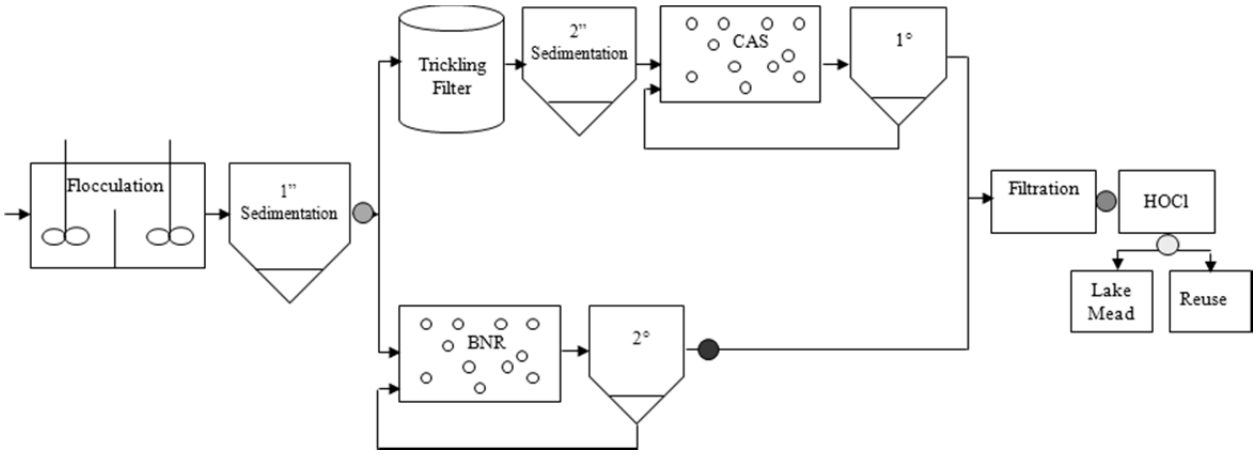

Sampling Locations on Site I-NV

Sample	Description
1	Primary Effluent
2	Secondary Effluent
3	Prechlorination (postfiltration)
4	Post-disinfection
5	Field Blank

Water Quality Data for Site I-NV

	Primary Effluent	Secondary Effluent	Prechlorination (Post-Filtration)	Post-Disinfection
BOD (mg/L)		181	6	<2
TSS (mg/L)		126	3.6	<2
Total Phosphorus (mg/L)		4.17	0.2	0.24
Orthophosphate (mg/L)		2.37	0.1	0.19
Alkalinity (mg/L $CaCO_3$)		252	111	106
NH_4 (mg/L)			0.26	<0.1
TON (mg/L)			14.4	22.2
TKN (mg/L)				1

Note: Data from March 27–28, 2012

Effluent Organic Matter Characterization Data for Site I-NV

	Primary Effluent	Secondary Effluent	Prechlorination (Post-Filtration)	Post-Disinfection	Field Blank
UV_{254}	0.372	0.133	0.134	0.101	<0.00200
UV_{280}	0.292	0.0990	0.102	0.0665	<0.00200
TOC (mg/L)	31	7.7	6.9	6.9	<0.2
TN (mg/L)	34	15	22	20	<0.2

Note: Data from March 28, 2012

Nitrosamines Data for Site I-NV

	Primary Effluent	Secondary Effluent	Prechlorination (Post-Filtration)	Post-Disinfection	Field Blank
NDMA	<25	<5.0	<5.0	<5.0	<2.5
NMEA	<25	<5.0	<5.0	<5.0	<2.5
NDEA	<50	<10	<10	<10	<5.0
NDPrA	<100	<20	<20	<20	<10
NMOR	<50	11	<10	<10	<5.0
NDBA	<100	<20	<20	<20	<10
NDPhA	<100	<20	<20	<20	<10

Note: Nitrosamine concentrations in ng/L

PFAS Data for Site I-NV

	Primary Effluent	Secondary Effluent	Prechlorination (Post-Filtration)	Post-Disinfection	Field Blank
PFBA	<100	<100	<100	<100	<5.0
PFPnA	4.7	27	24	26	<2.0
PFHxA	5.2	20	20	23	<0.50
PFHpA	1.2	2.2	2.7	2.9	<0.50
PFOA	<5.0	12	12	12	<5.0
PFNA	2.9	3.5	3.9	3.9	<0.50
PFDA	1.1	1.3	2.1	1.7	<0.50
PFUnA	<0.50	<0.50	<0.50	<0.50	<0.50
PFDoA	<0.25	<0.25	<0.25	<0.25	<0.25
L-PFBS	6.9	4.5	5.8	5.1	<0.25
L-PFHxS	0.48	0.45	0.69	0.52	<0.25
L-PFOS	7.9	2.3	5.0	4.5	<0.25
L-PFDS	<0.10	<0.10	<0.10	<0.10	<0.10
FOSA	<5.0	<0.25	<0.25	<0.25	<0.25
MeFOSAA	<0.25	<0.25	<0.25	<0.25	<0.25
EtFOSAA	<0.25	<0.25	<0.25	<0.25	<0.25
4:2 FTUCA	<2.0	<2.0	<2.0	<2.0	<2.0
6:2 FTUCA	<2.0	<2.0	<2.0	<2.0	<2.0
8:2 FTUCA	<2.0	<2.0	<2.0	<2.0	<2.0
10:2 FTUCA	<2.0	<2.0	<2.0	<2.0	<2.0
4:2 FtS	<0.50	<0.50	<0.50	<0.50	<0.50
6:2 FtS	<0.50	0.52	0.69	0.56	<0.50
8:2 FtS	<0.50	<0.50	<0.50	<0.50	<0.50

Note: PFAS concentrations in ng/L

Utility J-NV

Site description: This site treats an average of 100 million gallons per day. The wastewater is treated in an advanced purification and disinfection process using two parallel trains and a pilot UF–O_3 system. UV and sodium hypochlorite are used for disinfection at this site.

Process diagram

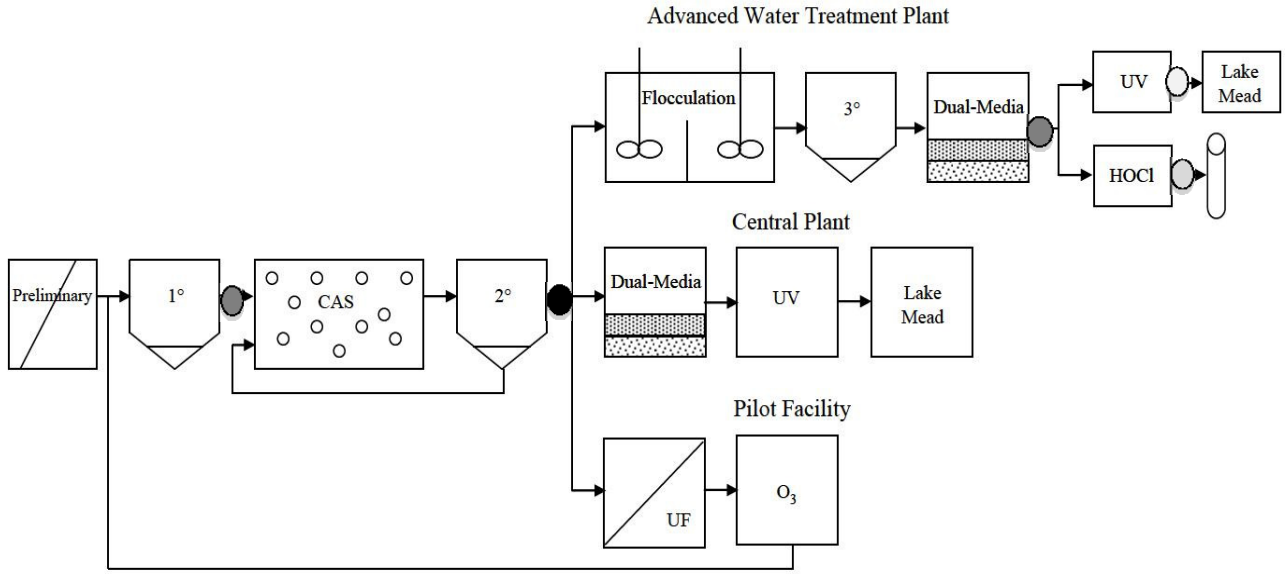

Sampling Locations on Site J-NV

Sample	Description
1	Primary Effluent
2	Secondary Effluent
3	Prechlorination (postfiltration)
4	Post–Chlorine Disinfection
5	Post–UV Disinfection
6	Field Blank

Water Quality Data for Site J-NV

	Primary Effluent	Secondary Effluent	Prechlorination (Post-Filtration)	Post–Chlorine Disinfection	Post–UV Disinfection
TSS (mg/L)	106	9		0	0
BOD (mg/L)	196	2		0	0
Orthophosphate (mg/L)	2.33	0.052		0.016	0.014
Phosphate (mg/L)	4.52	0.37		0.058	0.060
NH4 (mg/L)	26.58	0.05		0	0

Note: Data from March 28, 2012

Effluent Organic Matter Characterization Data for Site J-NV

	Primary Effluent	Secondary Effluent	Prechlorination (Post-Filtration)	Post–Chlorine Disinfection	Post–UV Disinfection	Field Blank
UV_{254}	0.401	0.128	0.118	0.093	0.116	<0.00200
UV_{280}	0.307	0.0972	0.0903	0.0605	0.0895	<0.00200
TN (mg/L)	30	13	13	14	13	<0.2
TOC (mg/L)	59	7	5.8	5.8	5.8	<0.2

Note: Data from March 28, 2012

Nitrosamines Data for Site J-NV

	Primary Effluent	Secondary Effluent	Prechlorination (Post-Filtration)	Post–Chlorine Disinfection	Post–UV Disinfection	Field Blank
NDMA	<25	<5.0	<5.0	<5.0	<5.0	<2.5
NMEA	<25	<5.0	<5.0	<5.0	<5.0	<2.5
NDEA	<50	<10	<10	<10	<10	<5.0
NDPrA	<100	<20	<20	<20	<20	<10
NMOR	<50	11	13	11	<10	<5.0
NDBA	<100	<20	<20	<20	<20	<10
NDPhA	<100	<20	<20	<20	<20	<10

Note: Nitrosamine concentrations in ng/L

PFAS Data for Site J-NV

	Primary Effluent	Secondary Effluent	Prechlorination (Post-Filtration)	Post–Chlorine Disinfection	Post–UV Disinfection	Field Blank
PFBA	<100	<100	<100	<100	<100	<5.0
PFPnA	3.6	16	13	16	13	<2.0
PFHxA	3.2	11	10	13	9.6	<0.50
PFHpA	1.3	1.9	2	2.3	1.9	<0.50
PFOA	<5.0	6.5	7.7	7.4	7.3	<5.0
PFNA	1.7	2.7	4.0	3.6	3.4	<0.50
PFDA	0.55	1.2	1.5	1.7	1.5	<0.50
PFUnA	<0.50	<0.50	<0.50	<0.50	<0.50	<0.50
PFDoA	<0.25	<0.25	<0.25	<0.25	<0.25	<0.25
L-PFBS	2.6	3.8	5.0	6.9	6.0	<0.25
L-PFHxS	0.94	0.93	1.3	1.3	1.3	<0.25
L-PFOS	2.2	2.3	3.7	3.9	4.0	<0.25
L-PFDS	<0.10	<0.10	<0.10	<0.10	<0.10	<0.10
FOSA	<0.25	<0.25	<0.25	<0.25	<0.25	<0.25
MeFOSAA	<0.25	<0.25	<0.25	<0.25	<0.25	<0.25
EtFOSAA	<0.25	<0.25	<0.25	<0.25	<0.25	<0.25
4:2 FTUCA	<2.0	<2.0	<2.0	<2.0	<2.0	<2.0
6:2 FTUCA	<2.0	<2.0	<2.0	<2.0	<2.0	<2.0
8:2 FTUCA	<2.0	<2.0	<2.0	<2.0	<2.0	<2.0
10:2 FTUCA	<2.0	<2.0	<2.0	<2.0	<2.0	<2.0
4:2 FtS	<0.50	<0.50	<0.50	<0.50	<0.50	<0.50
6:2 FtS	1.0	2.0	2.1	2.3	1.4	<0.50
8:2 FtS	<0.50	<0.50	<0.50	<0.50	<0.50	<0.50

Note: PFAS concentrations in ng/L




WATEREUSE

1199 North Fairfax Street, Suite 410
Alexandria, VA 22314 USA
703.548.0880
703,548.5085 (fax)
foundation@watereuse.org
www.WateReuse.org